

UTILIZATION OF RECYCLED PLASTICS AS BINDER MODIFIERS FOR USE IN
HOT-MIX ASPHALT PAVEMENT

by

Sina Varamini

Submitted in partial fulfilment of the requirements
for the degree of Master of Applied Science

at

Dalhousie University
Halifax, Nova Scotia
December 2013

© Copyright by Sina Varamini, 2013

*To my family – Mohammad, Fatemeh, Saeed, and Sahba
whose unconditional love gives me all my motivation and inspiration.*

To my beloved sister, Solmaz. Rest in peace.

TABLE OF CONTENTS

LIST OF TABLES	v
LIST OF FIGURES	vi
ABSTRACT	ix
LIST OF ABBREVIATIONS AND SYMBOLS USED	x
ACKNOWLEDGEMENTS	xiii
CHAPTER 1: INTRODUCTION	1
1.1. Background	1
1.2. Research Hypothesis	3
1.3. Research Objectives and Motivations	3
1.4. Methodology	4
1.5. Thesis Organization	5
CHAPTER 2: LITERATURE REVIEW	7
2.1. Background	7
2.2. Effect of Modified Binders on Flexible Pavement Performance	9
2.2.1. Permanent Deformation	9
2.2.1. Fatigue and Thermal Cracking	13
2.2.2. Moisture Damage and Aging	18
2.3. Types of Asphalt Modifiers	20
2.3.1. Polymers	21
2.3.2. Hydrocarbons and Extenders	22
2.4. Characterization and Performance Evaluation of Modified Binders	23
2.4.1. Superpave™ Performance Grading	23
2.4.2. Multiple-Stress Creep Recovery (MSCR) Performance Grading	38
2.5. Additional Tests for Modified Binders	42
2.6. Summary	43
CHAPTER 3: RESEARCH METHODOLOGY	44
3.1. Experimental Materials	45

3.1.1.	Asphalt Binders.....	45
3.1.2.	Aggregate Blend	46
3.2.	Asphalt Binders Characterization	49
3.2.1.	Workability	50
3.2.2.	Aging.....	52
3.2.3.	Permanent Deformation	54
3.2.4.	Fatigue and Thermal Cracking.....	56
3.2.5.	Additional Empirical Tests	58
3.3.	Mixture Design	63
3.3.1.	Mixture Volumetric Analysis	64
3.3.2.	Marshall Method of Mixture Design	65
3.3.3.	Superpave™ Gyratory Compactor	70
3.4.	Asphalt mixture characterization	72
3.4.1.	Rutting Susceptibility.....	72
3.4.2.	Tensile Strength	73
3.4.3.	Moisture Susceptibility	74
CHAPTER 4:	RESULTS AND DISCUSSION.....	77
3.5.	Effect of Modification on Workability	80
3.6.	Effect of Modification on Permanent Deformation	81
3.7.	Effect of Modification on Fatigue and Thermal Cracking.....	93
3.8.	Effect of Modification on Moisture Susceptibility	97
3.9.	Effect of Modification on Additional Empirical Tests	100
CHAPTER 5:	CONCLUSIONS AND RECOMMENDATIONS	104
5.1.	Conclusions.....	104
5.2.	Recommendations for Future Work.....	105
REFERENCES	106
APPENDIX A	Test Results	113

LIST OF TABLES

Table 2-1	Traffic level designations for MSCR performance grading	38
Table 2-2	Comparison of “grade-bumping” chart and MSCR performance grading ...	39
Table 2-3	List of most commonly used traditional tests for MBs.....	42
Table 3-1	Material Control variables for Binders	45
Table 3-2	Physical properties of aggregate blend	49
Table 4-1	Hot-Mix Asphalt (HMA) mixture physical properties	79
Table 4-2	Mixing and compaction temperature range for all MBs.....	80
Table 4-3	Summary of Asphalt Pavement Analyzer (APA) test results	86
Table 4-4	Hot Mix Asphalt Rutting Susceptibility Rankings	90
Table 4-5	AASHTO MP 19-10 Performance-Grading (PG) of MBs	92
Table 4-6	Moisture susceptibility test results.....	98
Table 4-7	Softening point and separation test results.....	100

LIST OF FIGURES

Figure 1-1	Overall research methodology	5
Figure 2-1	Asphalt binder refining process	7
Figure 2-2	Performance Grades (PG) available for paving industry	8
Figure 2-3	Typical flexible pavement structure	9
Figure 2-4	Severely rutted road, photo taken at Duke St., Bedford Nova Scotia,.....	10
Figure 2-5	Shear loading behaviour of asphalt mixture	11
Figure 2-6	Principal causes of Asphalt layer rutting	11
Figure 2-7	Visco-Elastic behaviour of asphalt binder	12
Figure 2-8	Contrasting asphalt binder contribution to mixture shear strength	13
Figure 2-9	Development of a pothole	14
Figure 2-10	Early stages of fatigue cracking formation, photo taken at Old Sambro Rd,	15
Figure 2-11	Bottom-up (i), and top-down (ii) fatigue cracking	16
Figure 2-12	Consistently spaced thermal transverse cracking, photo taken at Bayers.	17
Figure 2-13	Effects of aging on viscosity	20
Figure 2-14	Most commonly used stationary polymer blending system	21
Figure 2-15	Kraton® D-type Styrene-Butadiene-Styrene (SBS) pellets.....	22
Figure 2-16	Sulfur pellets	23
Figure 2-17	PG selection for different reliabilities	24
Figure 2-18	Superpave™ grade-bumping chart	25
Figure 2-19	Combination of Superpave™ PG system rheological tests with aging	27
Figure 2-20	Rotational viscometer test setup top view (i), and side view (ii).....	28
Figure 2-21	An example of ASTM viscosity-temperature curve	29
Figure 2-22	Comparison of Newtonian and non-Newtonian fluids	29
Figure 2-23	Dynamic Shear Rheometer operation and resulting graphs	31
Figure 2-24	Concept used in driving Superpave™ rutting parameter of $G^*/\sin(\delta)$	32
Figure 2-25	Schematic of Bending Beam Rheometer	34
Figure 2-26	Related graphs of measuring creep stiffness (S) and creep rate (m-value)	35
Figure 2-27	Summary of the Superpave™ PG system and requirements	37
Figure 2-28	Sample of calculation for MSCR test parameters	40

Figure 2-29	MSCR PG system summary	41
Figure 2-30	Schematics of the target change in rheological and failure properties	43
Figure 3-1	Experimental flow chart.....	44
Figure 3-2	Mixing apparatus used to produce MBs	46
Figure 3-3	Aggregate blend gradation chart.....	48
Figure 3-4	Aggregate blend gradation deviation from the continuous maximum.....	48
Figure 3-5	Modified binders characterization flow chart.....	50
Figure 3-6	Rotational Viscometer, sample chamber and spindle.....	51
Figure 3-7	Rolling Thin-Film Oven (RTFO).....	52
Figure 3-8	Pressure Aging Vessel (PAV).....	53
Figure 3-9	Dynamic Shear Rheometer (DSR).....	54
Figure 3-10	DSR cycle of oscillation	55
Figure 3-11	MSCR creep-recovery response	55
Figure 3-12	Bending Beam Rheometer (BBR) mold assembly	57
Figure 3-13	BBR apparatus	57
Figure 3-14	Filled and trimmed ER molds.....	59
Figure 3-15	ER molds mounting, elongation and recovery.....	59
Figure 3-16	Penetration test apparatus	60
Figure 3-17	Separation tubes	61
Figure 3-18	Ring and Ball (R&B) softening point test.....	62
Figure 3-19	Solubility test	63
Figure 3-20	Mixture design and characterization flow chart.....	64
Figure 3-21	Volumetric properties of an asphalt mixture	65
Figure 3-22	Marshall compaction apparatus	66
Figure 3-23	Vacuum apparatus for determination of G_{mm}	67
Figure 3-24	Apparatus used to determine weight of compacted specimen in water	68
Figure 3-25	Marshall Stability-Flow tester.....	69
Figure 3-26	Superpave™ Gyrotory Compactor	71
Figure 3-27	A sample plot of SGC trial specimen compaction characteristic	72
Figure 3-28	The APA test apparatus	72
Figure 3-29	A sample the APA test result	73

Figure 3-30	IDT test apparatus and load configuration.....	74
Figure 3-31	AASHTO T 283-11 conditioning cycles	75
Figure 4-1	Optimization of trial blends of LDPE and PS to produce final binders....	77
Figure 4-2	Superpave™ Performance Grade (PG) of Modified Binders (MBs).....	78
Figure 4-3	Plots required for Marshall mixture design	79
Figure 4-4	Comparison of rutting parameter of $G^*/\sin(\delta)$ for all binders at different	81
Figure 4-5	Comparison of rutting performance for unaged binders based on.....	82
Figure 4-6	RTFO Mass loss percentage for all MB	83
Figure 4-7	Values of $ G^*/\sin(\delta)$ at 64°C for all unaged and RTFO aged MBs.....	84
Figure 4-8	APA results for mixtures containing LDPE RPM	85
Figure 4-9	APA results for mixtures containing PS RPM.....	86
Figure 4-10	Cross sections of APA specimens after 8,000 load repetitions at 64°C containing: A (SBS-control binder), B (PS+[A]), C (LDPE+[A]+[B]), and D (Base PG 58-28).....	87
Figure 4-11	Relationship Between unaged $G^*/\sin(\delta)$ at 64°C and Mixture Rut Depth	88
Figure 4-12	Relationship Between RTFO $G^*/\sin(\delta)$ at 64°C and Mixture Rut Depth.	88
Figure 4-13	Relationship Between Non-Recoverable Creep Compliance, J_{nr} (3.2 kPa), ..	89
Figure 4-14	Results of the accumulated strain under MSCR testing at maximum	91
Figure 4-15	Relationship between mixture rut depth and cost of MB per Tonne	93
Figure 4-16	Fatigue parameter of $G^*\sin(\delta)$ at intermediate pavement temperature of	94
Figure 4-17	Indirect Tensile Strength (IDT) of Modified Mixtures (MM) at testing ..	95
Figure 4-18	Relationship between mixture IDT and cost of MB per Tonne.....	95
Figure 4-19	Creep stiffness $S(60)$ at minimum pavement temperature of -18°C.....	96
Figure 4-20	Creep rate $m(60)$ at minimum pavement temperature of -18°C	97
Figure 4-21	Moisture susceptibility test visual inspection	99
Figure 4-22	Relationship between ER % at 10°C and rutting susceptibility.....	101
Figure 4-23	Relationship between MSCR percent recovery at 3.2 kPa at 58°C and..	102
Figure 4-24	Penetration values of modified binder at testing temperature of 25°C ...	103

ABSTRACT

Atlantic Canadian highways are vulnerable to impacts of climate change, including more frequent cycles of both wetting and drying, and freezing and thawing. These climate impacts coupled with continued increases in truck traffic can cause more severe and premature permanent deformation at high service temperature, fatigue and thermal cracking at low service temperatures, surface wear resistance, and ageing of the pavement. Such negative impacts can be mitigated with changes to the binder. However, replacing a local binder with a different imported binder can increase construction costs and cause supply problems. Alternatively, modifying agents can be used to adjust binder properties as required, but can also cause an increase in construction costs mainly due to their high cost and the need for highly specialized production techniques. The objective of this research project was to investigate the feasibility of utilizing underutilized household and packaging recycled plastics, that are generated in Atlantic Canada, as more cost effective alternatives or as co-modifiers to displace the amount of virgin modifiers used in hot mix asphalt application.

The research study entailed analyzing physical characteristics of an array of modified binders and hot mix asphalt mixtures containing recycled low-density polyethylene, recycled polystyrene and the typical engineered virgin modifier (styrene-butadiene-styrene). The analysis included tests used commonly in pavement engineering to evaluate binders and asphalt mixtures. Results of this study suggests that these recycled plastics can be successfully utilized in asphalt binder as modifiers to enhance the functional properties of the mixture and reduce construction costs, thus creating an engineered value-added application of these underutilized resources as opposed to a disposal mechanism.

LIST OF ABBREVIATIONS AND SYMBOLS USED

AASHTO	American Association of State Highway and Transportation Officials
APA	Asphalt Pavement Analyzer
ASTM	American Society for Testing and Materials
BBR	Bending Beam Rheometer
CII	Centre for Innovation in Infrastructure
D	Maximum particle size
d	Selected sieve size
D	diameter
DCF	Dirty Crusher Fine
DSR	Dynamic Shear Rheometer
ER	Elastic Recovery
ESAL	Equivalent Single Axle Loads
ESAL	80 kN equivalent single-axle load
FHWA	Federal Highway Administration
GLC	General Liquids Canada Ltd.
g	Gram, 10^{-3} kg
$G^*\sin(\delta)$	Superpave™ fatigue parameter
G^*	Complex modulus
G_{mb}	Bulk specific gravity of compacted specimen
G_{mb}	Bulk specific gravity of compacted specimen and
$G_{mb@N100}$	Bulk specific gravity of compacted trial specimen at 100 gyrations
$G_{mb@Nx}$	Estimated bulk specific gravity of compacted specimen at x gyrations
G_{mm}	Theoretical maximum specific gravity
G_{mm}	Theoretical maximum specific gravity of loose trial mixture
G_{mm}	Theoretical maximum specific gravity of loose mixture
G_{sb}	Bulk specific gravity of the compacted mix
$h_{@N100}$	Final height of trial specimen compacted at 100 gyrations
$h_{@Nx}$	Height of specimen throughout the compaction at x gyrations
HDPE	High Density Poly-Ethylene
HMA	Hot Mix Asphalt application of a pavement
Hz	Hertz
IDT	Indirect Tensile Strength
IPS	Industrial Post-Graduate Scholarship
ISO	International Standard Organization
J_{nr}	Non-recoverable compliance
kg	Kilogram
km	Kilometre, 10^3 m
kN	Kilonewton, 10^3 N
kPa	KiloPascal, kN/m^2
LDPE	Low Density Poly-Ethylene
M	Mass of specimen
MB	Modified Binder
mm	Millimetre, 10^{-3} m
mN	MilliNewton, 10^{-3} N

MPa	MegaPascal, N/mm ²
MSCR	Multiple Stress Creep Recovery
MTD	Maximum relative theoretical density
N	Newton
N	Grading coefficient
NCHRP	National Cooperative Highway Research Program
NSERC	Natural Science and Engineering Research Council of Canada
°C	Degrees Celsius
P	Percentage by mass of material passing sieve size “d”
$P_{CMD}(d_2)$	Percent passing, continuous maximum density gradation, for sieve size d_2
P_b	The asphalt content by weight of total mix
PAV	Pressurized Aging Vessel
PE	Poly-Ethylene
PG	Performance Grade
PP	Poly-Propylene
PS	Poly-styrene
RPM	Recycled Plastic Modifiers
rpm	Revolution per minute
RRFB	Resource Recovery Fund Board Inc.
RTFO	Rolling Thin-Film Oven
RV	Rotational Viscometer
S_t	IDT strength
S_{t1}	Average tensile strength of the dry subset
S_{t2}	Average tensile strength of the conditioned subset
SBS	Styrene-Butadiene-Styrene
SGC	The Superpave™ Gyrotory Compactor
SHRP	Strategic Highway Research Program
Superpave™	Superior Performing Asphalt Pavements
T	Temperature
t	Thickness
TSR	Tensile strength ratio
UTR	Useful Temperature Range
WCF	Washed Crusher Fine
$L, b, \text{ and } h$	Dimension of asphalt beam tested for the BBR test
P	Applied load
$P(d_1)$	Percent passing sieve d_1
$S(t)$	Creep stiffness at time of t
TSR	Tensile strength ratio
VTM_x	Estimated air voids in compacted mixture at x gyrations
VFA	Voids filled with asphalt
VMA	Volume of voids in mineral aggregate
VTM	Air voids in compacted mixture
W	Work dissipated
c	Cohesion
γ	Shear strain
δ	Phase angle

$\delta(t)$	Deflection at time of t
η	Viscosity
σ	Normal stress
%R	Percent recovery
%PMD	Percent passing for maximum density gradation
ϵ	Strain
d_1	One sieve size larger than d_2
σ	Stress
\emptyset	Angle of internal friction
τ	Shear stress

ACKNOWLEDGEMENTS

I would like to gratefully express my appreciation towards my supervisor, Dr. N. Ali, for his invaluable supports and assistance not only through my graduate degree, also through my Bachelor's degree at the Department of Civil and Resource Engineering at Dalhousie University.

My gratitude goes to my supervisory committee member, Dr. C. Barnes, whose enthusiasm towards research and lasting encouragement has been truly inspiring. I should acknowledge the countless hours spent by Dr. C. Barnes discussing, and reviewing my research proposal and work, and Dr. G. Jarjoura, for taking the time to review my thesis.

Of course, this project would not have been possible without the financial support of the Natural Science and Engineering Research Council of Canada (NSERC) and General Liquids Canada Ltd. (GLC), a division of The Municipal Group of Companies. I would also like to thank everyone from GLC who helped me to accomplish this goal; some of them by answering my questions or teaching me different aspects of the industry, some others simply by making the work environment friendly. I would also like to thank all my friends for their moral support.

Last but not least, I would like to gratefully thank my family, particularly my parents, Mohammed and Fatemeh, for their unconditional love, support, and unwavering belief in me. Without their support, I would not be the person I am today.

CHAPTER 1: INTRODUCTION

1.1. Background

The Canadian pavement industry has generally adopted the Superpave™ asphalt binder specification system of classifying bituminous asphalt binders¹ since late 1990's in an effort to better match the physical binder properties to the desired level of resistance to rutting, fatigue and low temperature cracking, subjected to local climate and environmental conditions. The design reliability level and average 7-day maximum and minimum pavement service temperatures for a locality indicate the Performance Grade (PG) that is required to provide adequate pavement performance using the Superpave™ mixture design approach. However, the conventional asphalt binder properties often does not meet the traffic requirements of most Hot Mix Asphalt (HMA) concrete projects in the area, specifically heavily loaded applications.

To some extent, local experience, the availability, and cost of binders have played an important role in determining which binders are actually specified in practice. PG 58-28 binder has been locally produced at several regional refineries in Atlantic Canada, making it the least expensive and historically accepted choice for most hot mix asphalt concrete projects in the area. In certain cases, specialty binders (i.e. PG 64-28) have been imported but are typically available at a premium cost, providing disincentive for their use. Aside from importing costly higher PG binders, modifying agents can be used to adjust asphalt binder properties and PG classification as required. However, binder modification technique is currently not being used in Atlantic Canada at its potential, due to the need for highly specialized production techniques and the high cost of the modifiers.

¹ The term *asphalt binder* or *asphalt cement* is mostly used in North America. Outside North America, especially Europe, the term *asphalt* is used to describe the asphalt concrete mixtures and the term terms *bitumen* and *asphaltic bitumen* are used in place of asphalt binder.

In addition to aforementioned issues, transportation infrastructure in Atlantic Canada is also vulnerable to climate change impacts, including more frequent freeze-thaw cycles in colder regions combined with more wetting and drying cycles, changes to precipitation regimes, and increases in temperature extremes [1]. Researchers at the University of Waterloo in collaboration with Environment Canada used global climate models to examine sites located throughout Canada including Atlantic Canada to investigate the vulnerability of Canadian pavement infrastructure to these negative impacts [2]. The study concluded that climate change impacts coupled with traffic growth can cause a decline in pavement service life in terms of more severe and premature rutting (asphalt, base, and sub-base layers) at high service temperature, and both longitudinal and alligator cracking at intermediate service temperatures. It has also been stated that transverse cracking may become less of a problem, allowing decisions to focus on high temperature Performance Grade (PG) rather than low temperature PG [3] [4]. The negative impacts of such changes could be mitigated with adjustments to the asphalt mixes such as changing the binder Performance Grade (PG) [3] [5]. However, replacing a local binder with a different imported PG can increase construction costs and cause supply problems.

Household and packaging recycled plastics may provide an inexpensive alternative source of virgin polymers that could be utilized for binder modification. Some of these polymers exhibit suitable general characteristics that may be beneficial in improving the high and/or low temperature rating of the PG 58-28 binder. These underutilized plastics are abundant within the waste stream, creating a strong incentive for their incorporation into a premium pavement material. As stated in the most recent report prepared for Resource Recovery Fund Board Inc. (RRFB) [6], approximately 72 tonnes of different recyclable grades of plastics were discarded in Nova Scotia in 2006, while grades of Low Density Poly-Ethylene (LDPE) and Poly-styrene (PS) were identified to be among the grades that are less commonly recycled or are difficult to market [7]. The quantity of discarded plastics is reported to increase by at least 35 percent by 2016 [6].

Usage of waste or recycled plastics in asphalt binder is not a new idea. There are studies and patents dating back to 1980 [8], which have demonstrated successful utilization of recycled plastic grade of Poly-Ethylene (PE) in HMA for enhancing the high in-service temperature stiffness of the mixture and reducing construction costs. There are more recent efforts of utilizing grades such as low and high density Poly-Ethylene (LDPE and HDPE) for enhancing the stiffness of the mixture and reducing construction costs. However, some studies highlighted the tendency of Recycled Plastic Modifiers (RPM) to separate from asphalt binders and exhibit a high level of variability in physical properties, creating a significant drawback to their use [9] [10] [11] [12].

1.2. Research Hypothesis

It was hypothesized that Recycled Plastic Modifiers (RPM) may behave similarly to engineered modifiers such as Styrene-Butadiene-Styrene (SBS) as an effective means of increasing the contribution of binders to the high in-service temperature stiffness of the mixture (i.e. rutting resistance) of HMA, while limiting the increase in cost of the modified binder. The effect of the recycled plastics on other properties of mixture such as fatigue and thermal cracking was hypothesized marginal. The tendency of RPMs to separate from asphalt binder was also hypothesized, but such tendency was assumed to decrease by addition of cross-linking agent, and oil softener, as well as co-blending with SBS polymer.

1.3. Research Objectives and Motivations

The intent of this research study was to investigate the feasibility of utilizing recycled plastics as binder modifiers in HMA while maintaining performance levels that are achieved using engineered modifiers such as Styrene-Butadiene-Styrene (SBS). The grades of plastics studied in this research were selected based on those available in Nova Scotia that are less commonly recycled or are difficult to market, such as LDPE and PS [7]. This research was established as a three-way partnership between General Liquids Canada Ltd. (GLC), the Natural Science and Engineering Research Council of Canada (NSERC), and Centre for Innovation in Infrastructure (CII) at Dalhousie University as part of the Industrial Post-Graduate Scholarship (IPS) program [13].

General Liquids Canada Ltd. (GLC), a division of The Municipal Group of Companies, brought considerable testing capacity and expertise to this research project. GLC's interest in this research study was part of their overall objective of bringing new technology and products to the Atlantic region that result in longer lasting pavements and competitive products that can be used by numerous existing pavement contractors [14].

GLC is an ISO 9001 (Quality), and 14001 (Environment) accredited facility located in Bedford, Nova Scotia, capable of supplying different grades of bitumen-based products as well as blending and processing of different binders and polymers. GLC's facility is a key element to ensure that what was being evaluated in this research project will be mass produced, readily commercialized, and then be exported, leveraging GLC's rail, ship and trucking capabilities, to the rest of Canada as well as to the US and Europe with similar climates and conditions.

In addition to GLC's interest, this research study was also part of overall objectives of CII at Dalhousie University. Established in 1983 as the Nova Scotia CAD/CAM Centre, the center's current research interests are focused on development of higher performance materials and structural systems particular to the Canadian environment to address the critical needs of Canada's aging and deteriorating public infrastructure. CII is an industry-oriented research center in collaboration with the Faculty of Engineering and with strong affiliations with the Department of Civil and Resource Engineering at Dalhousie University [15].

1.4.Methodology

This research study investigated the effects of LDPE and PS grades of recycled plastics as binder modifiers on the physical properties of base asphalt binder (i.e. PG 58-28) as well as the mechanical properties of HMA mixture produced using the prototype modified binders. Such experimental work entailed performing standardized material testing in accordance with the American Association of State Highway and Transportation Officials (AASHTO) and the American Society for Testing and Materials (ASTM) in the overall research methodology shown in Figure 1-1. More details of each

module is presented in chapters three and four of this thesis, while details on module four is not included in this thesis for competitive reasons and possible patentability.

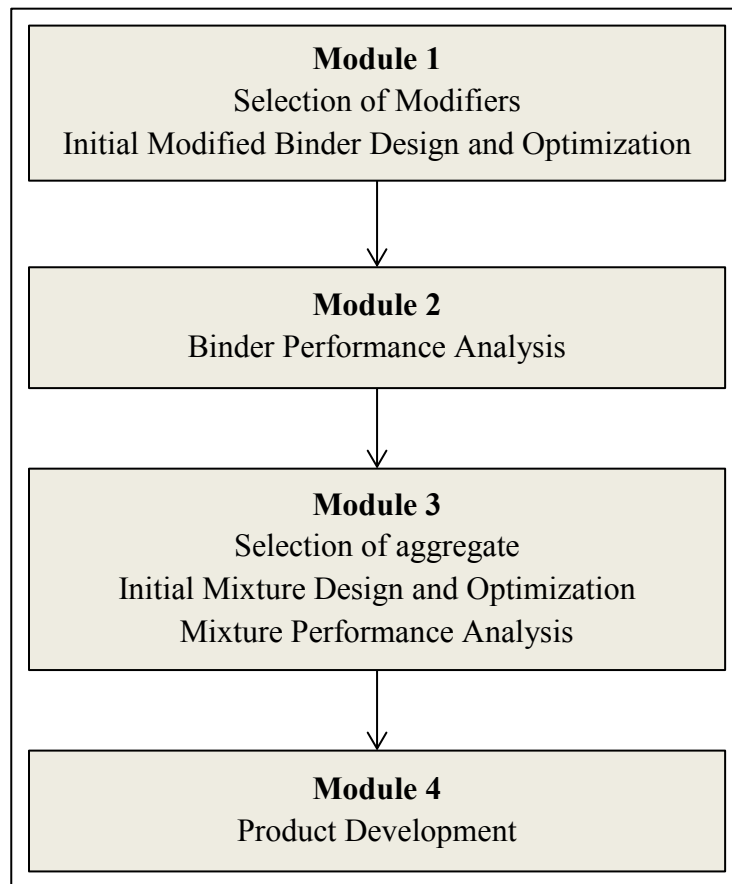


Figure 1-1 Overall research methodology

1.5.Thesis Organization

This thesis is organized into five chapters with contents as follows:

Chapter 1: Introduction – This introductory chapter highlights the background of necessity of Binder Modification for Hot-Mix Asphalt (HMA) pavement. This chapter also provides the scope and overall objectives of this research project.

Chapter 2: Literature Review – A comprehensive literature review into asphalt binder modification is provided in this chapter. This review includes information on the possible effects of modifiers on the physical properties of asphalt binder and mechanical

properties of HMA, selection of modifiers, characterization of modified binders, and effect of modifiers on production and field construction of HMA concrete.

Chapter 3: Materials and Methods – This chapter details the laboratory testing employed to complete the research objectives of this thesis.

Chapter 4: Results and Discussions – Results of modules one through three of the research program are presented in this chapter.

Chapter 5: Conclusions and Recommendations - In this chapter conclusions and recommendations deduced from the research study is offered.

CHAPTER 2: LITERATURE REVIEW

The purpose of this chapter is to provide comprehensive details on current state of knowledge on concepts and approaches related to asphalt binder modification pertain to Hot-Mix Asphalt (HMA) application of flexible pavements.

2.1. Background

Binder modification technique is used as an alternative when conventional asphalt binder produced at refineries does not meet climate, traffic, and pavement structure requirements. Conventional asphalt binders currently used in pavement applications are co-products of refining crude petroleum (crude oil) to produce gasoline, diesel fuel, and many other petroleum products. During the refining process (shown in Figure 2-1), fuels and lubricants are removed from crude oil leaving a thick and heavy residuum product that can be further processed in various ways to meet limited set of specifications for paving-grade asphalt binders [16].

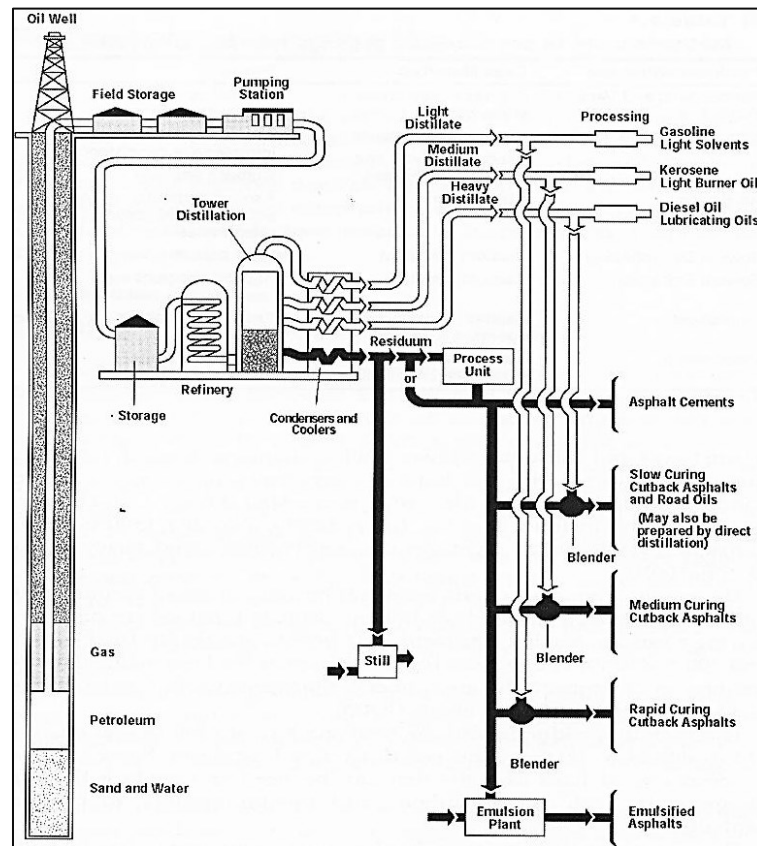


Figure 2-1 Asphalt binder refining process [16]

In North America, Superpave™ is the most commonly used specification system of classifying conventional asphalt binders as well as modified binders. In the specification, an array of rheological tests is employed to match physical properties of an asphalt binder to a Performance Grade (PG) intended for a climatic and environmental condition. The binder grade is specified by two numbers, for example “PG 58-28”. The first number, 58, represents an average 7-day maximum pavement service temperature (in degrees Celsius, °C) at which the binder is intended to perform adequately to resist rutting. The second number, minus 28°C, represents the minimum pavement temperature at which the binder is intended to resist thermal cracking. Figure 2-2 shows different combinations of PG temperatures available in North America.

		Lower Specification Temperature, °C						
Upper Specification Temperature, °C	PG 82	-10	-16	-22	-28	-34		
	PG 76	-10	-16	-22	-28	-34		
	PG 70	-10	-16	-22	-28	-34	-40	
	PG 64	-10	-16	-22	-28	-34	-40	
	PG 58		-16	-22	-28	-34	-40	
	PG 52	-10	-16	-22	-28	-34	-40	-46
	PG 46					-34	-40	-46

Figure 2-2 Performance Grades (PG) available for paving industry [17]

As shown above, a diagonal line ,connecting PG 82-10 to PG 46-46, allocates grades that have upper and lower pavement service temperatures with a difference of not more than 86°C. Such grades can be produced at refineries, while other grades appeared in the shaded area can be only produced by modification due to limitations in refining practices. The difference between upper and lower service temperatures is referred to as Useful Temperature Range (UTR). A Modified Binder (MB) often has a $UTR \geq 92$ °C. UTR is used to measure the degree of required modification as well as the cost of modification. As UTR increase, the cost need for modification and cost increase accordingly [17].

2.2.Effect of Modified Binders on Flexible Pavement Performance

The flexible pavement (Figure 2-3) is a type of pavement structure that composed of asphalt-bound layers distributing stress caused by traffic loads downward to the underlying soil foundation in an acceptable level of stress at different seasonal environmental conditions. To play this functional role, also referred to as serviceability, pavement's asphalt-bound layer must be smooth and skid resistant. However, a number of distresses contribute to reducing the serviceability and cause deterioration of asphalt-bound layer [18]. Permanent deformation, fatigue cracking, low-temperature cracking, moisture damage, and aging can be contributing distresses.

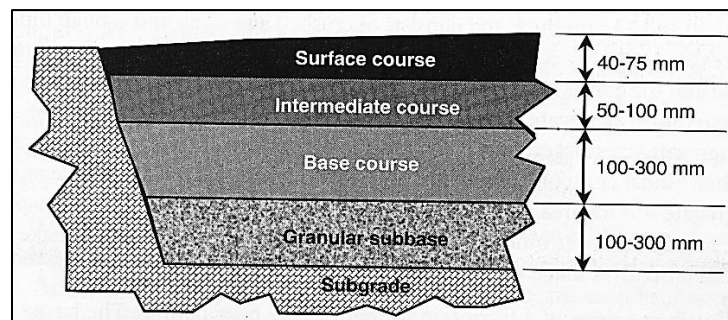


Figure 2-3 Typical flexible pavement structure [19]

There are various surface types of asphalt-bound layer including hot mix asphalt, warm mix asphalt, and cold mix asphalt depending on temperature of mixing and construction. Hot Mix Asphalt (HMA) is the most common surface type used for medium to high traffic volume roads. This type of asphalt mixture is referred to as HMA mainly because of an elevated temperature range of 135 to 160°C used prior to mixture mixing at production plant. The HMA mixture usually consists of 94 to 96 percent of mineral aggregates and 4 to 6 percent of asphalt binder by weight of the mixture. The thickness of HMA layer is typically in a range of 40 to 75 mm depending on the level of the traffic [19].

2.1.1. Permanent Deformation

Permanent deformation (also referred to as rutting) is the most common type of asphalt-bound layer distress, which manifests itself as accumulated longitudinal dispersions or grooves of wheel paths because of repetitive traffic-loading coupled with environmental

effects (as shown in Figure 2-4). While rutting is a functional concern affecting serviceability, it could also cause serious safety concerns in both dry and wet road conditions. In dry conditions, rutting affects the lateral maneuverability of vehicles causing steering problems. On the other hand, in wet conditions, rutted wheel paths can prevent cross drainage of water during rains, leading to accumulation of water in the ruts and causing vehicular hydroplaning². Generally, a rut depth of more than 10 mm is considered a significant safety hazard [19].



Figure 2-4 Severely rutted road, photo taken at Duke St., Bedford Nova Scotia, October 23rd 2013.

At early stages of pavement service-life, some negligible amount of rutting occurs in HMA surface-layer due to continued densification under repetitive traffic-loading. The densification gradually causes a reduction in air voids, leading to a decrease in the mixture's volume. After mixture reaches a limit that volume does not change anymore, plastic deformation (or also referred to as plastic flow) starts to occur. During plastic deformation, a shear plane (as shown in Figure 2-5) starts to develop [20]. When the shear strength of the mixture becomes less than applied shear stress by a wheel load, the

² Although rutting is not the main cause of hydroplaning, other factors such as vehicle speed, tire condition, and pavement drainage should be also considered as contributing factors to hydroplaning [74].

mixture starts to deform permanently from the wheel path to the small upheavals beside the wheel paths [21].

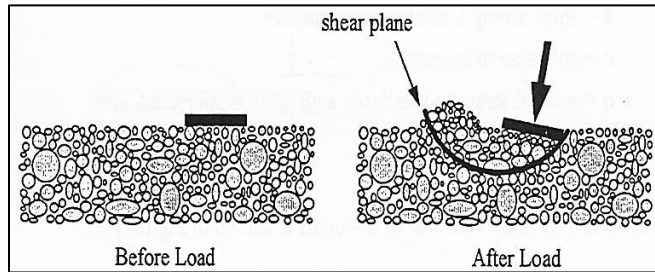


Figure 2-5 Shear loading behaviour of asphalt mixture [22]

As stated by McGennis et al. [22], rutting can be caused by many causes (e.g., underlying HMA weakened by moisture damage, abrasion, traffic densification), but has two principal causes; firstly, too much repeated stress being applied to the native soil, subgrade, or base below the asphalt layer, and secondly, accumulated deformation in the asphalt layer.

Both principal rutting causes are shown in Figure 2-6. While this thesis does not attempt to address the issue of rutting from weak subgrade as it is often considered as a structural failure rather than a material problem [22], a brief explanation of the factors lead to rutting will be presented.

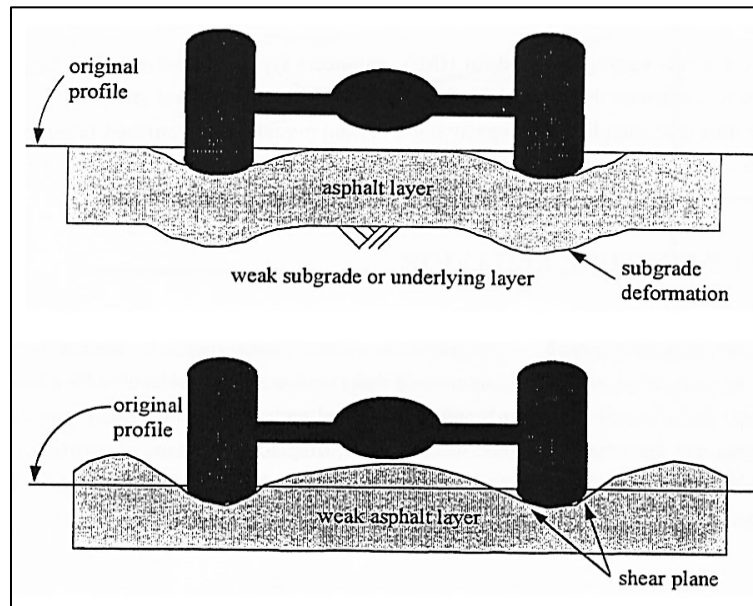


Figure 2-6 Principal causes of Asphalt layer rutting [22]

The shear strength of a mixture is affected significantly by asphalt binder physical properties. As shown in Figure 2-7, Asphalt binder is a visco-elastic material behaving as viscous cementitious liquid at higher temperatures, leathery/rubbery semi-solid at intermediate temperature, and very stiff and brittle at lower temperatures. Such behaviour also depends on rate of loading. At higher temperature with slower rate of loading, the asphalt binder becomes relatively softer. In contrast, the asphalt binder becomes stiffer at lower temperature and faster rate of loading [22].

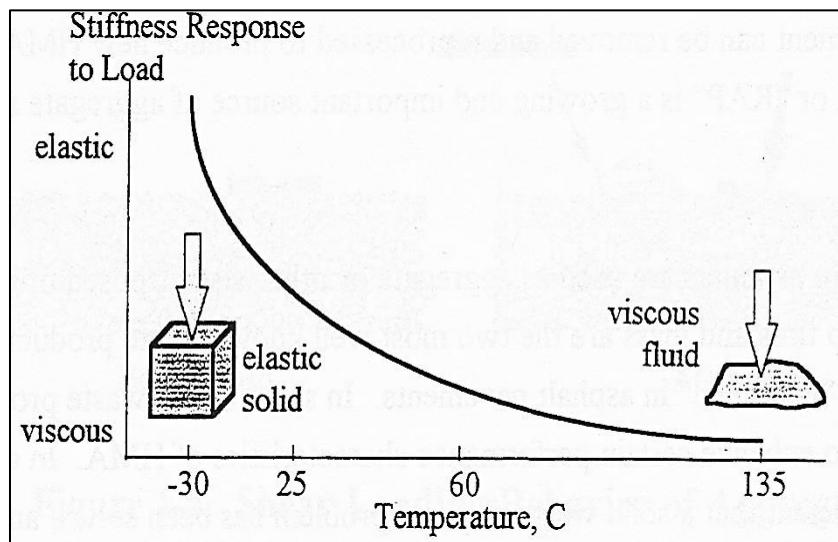


Figure 2-7 Visco-Elastic behaviour of asphalt binder [22]

The rutting mostly occurs in summer times when high pavement service temperatures are evident. Although aggregate angularity and shape play an important role in rutting resistance, the stiffness of asphalt binder is a contributing factor [22]. The contribution of asphalt binder can be captured using Mohr-Coulomb theory as follow:

$$\tau = c + \sigma \tan \phi \quad 2-1$$

where:

- τ = shear strength of asphalt mixture,
- c = cohesion of mixture,
- σ = normal stress to which the mixture is subjected, and
- ϕ = angle of internal friction.

In Equation 2-1, the cohesion term (c) is considered the contribution of asphalt binder to the overall mixture's shear strength, thus rutting resistance [22]. The contribution of the cohesion term is better illustrated in Figure 2-8. As stated by McGennis et al. [22]: *“Because rutting is an accumulation of very small permanent deformations, one way to ensure that asphalt cement provides its “fair share” of shear strength is to use an asphalt cement that is not only stiffer but also behaves more like an elastic solid at high pavement temperatures”*

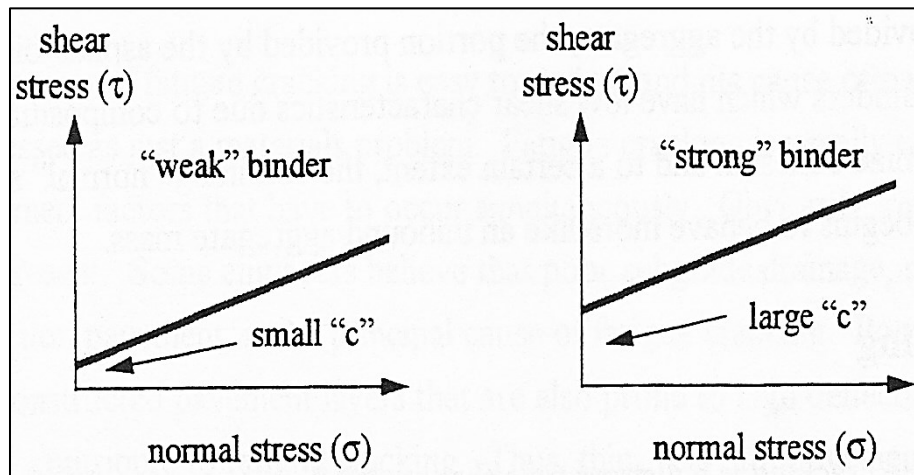


Figure 2-8 Contrasting asphalt binder contribution to mixture shear strength [22]

One of the prime roles of binder modifiers is to increase the resistance of asphalt binder to rutting during summer months especially in areas of slow or standing traffic (i.e. intersections and bus stations). Fulfilling this role requires modifiers to reduce the resulted permanent strain, which can be achieved by either or both of two methods; increase the high-temperature stiffness of the asphalt binder or/and increasing the elasticity of the asphalt binder [18].

2.1.1 Fatigue and Thermal Cracking

Similar to rutting, fatigue cracking is caused progressively by a large number of repetitive traffic-loading stressing a pavement to the limit of its life. However, fatigue cracking tends to form at intermediate (i.e. moderate) pavement service temperature. Because asphalt binder acts more stiff and brittle at moderate service temperatures compare to relatively higher service temperature, it tends to cracks rather than deform [19].

In the early stages of formation, fatigue cracks start to form as intermittent longitudinal wheel path cracks which then start to join and cause even more cracks forming a dense pattern similar to alligator's skin appearance [19]. McGennis et al. [22] recognized such stage (Figure 2-10) as an indication that pavement has received the designed number of load applications and requires rehabilitation. However, most of small municipalities neglect such indicative measures (often due to budget cuts and deferred rehabilitation) and let the pavement to continue carrying the traffic loads. As a result of such negligence, the localized alligator cracks start to allow more water to and brine to seep into the underlying granular base, leading to further dislodgment and removal partial of surface layer under action of traffic or snow removal operations. Figure 2-9 illustrates such steps which can lead to development of pothole. While Potholes are functional concern and sign of exceeded pavement's design life, they also lead to safety hazard for road users.

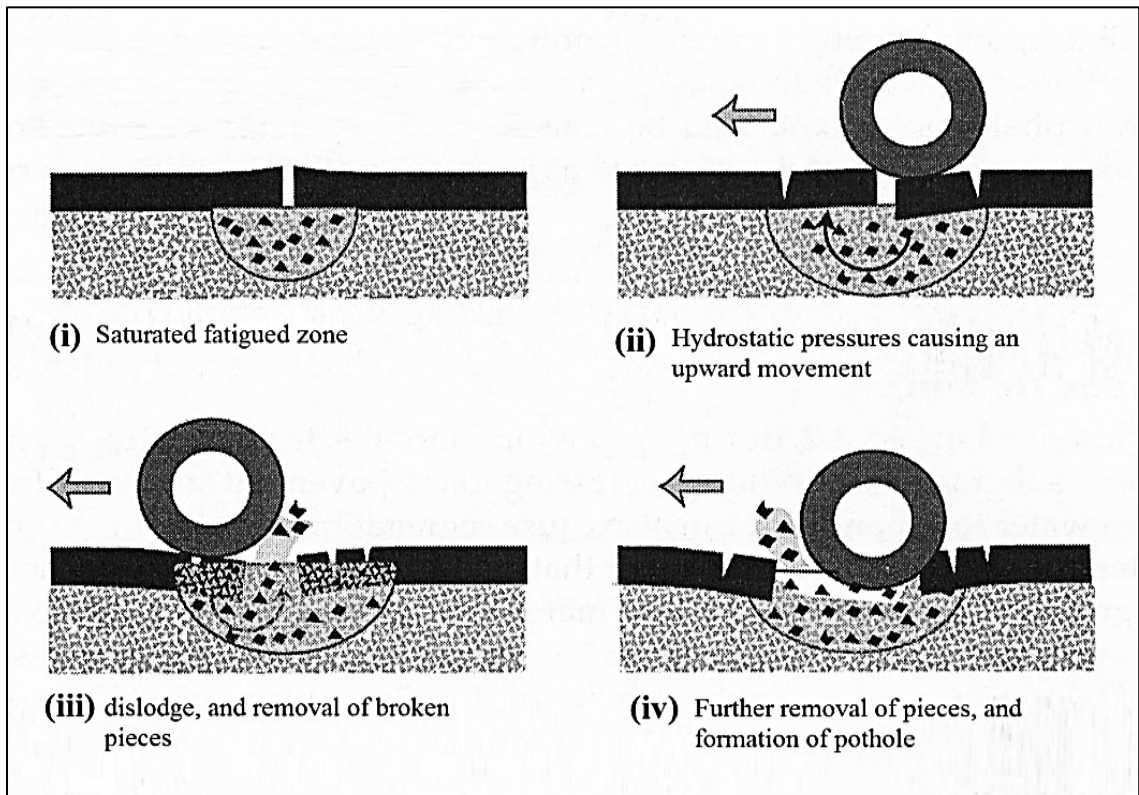


Figure 2-9 Development of a pothole (modified from [20])



Figure 2-10 Early stages of fatigue cracking formation, photo taken at Old Sambro Rd, Halifax NS, October 29, 2013

Considering the fatigue cracking as the progression of a pavement's design strategy, fatigue cracking often occur sooner than the design life. Regarding the formation of fatigue cracking, National Cooperative Highway Research Program³ (NCHRP) [19] stated that: *“Traditionally, pavement engineers believed that fatigue cracks first formed on the underside of the HMA layers, and gradually grew toward pavement surface. It has become clear during the past 10 years that pavements are also subject to top-down fatigue cracking, where the cracks begin at or near the pavement surface and grow downward, typically along the edges of the wheel paths”*. Figure 2-11 illustrates both top-down, and bottom-up fatigue cracking.

³ NCHRP is a cooperative research program administrated by the Transportation Research Board (TRB) and sponsored by the American Association of State Highway and Transportation Officials (AASHTO), in cooperation with the Federal Highway Administration (FHWA). Created in 1962, the program is still in-effect to conduct research in acute problem areas that affect highway planning, design, construction, operation, and maintenance in the United States as well as North America [75].

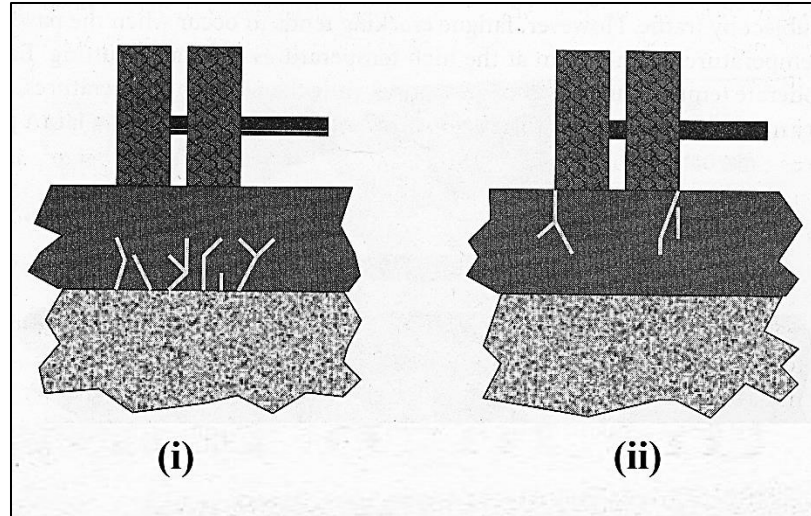


Figure 2-11 Bottom-up (i), and top-down (ii) fatigue cracking [19]

Roberts et al. [23] stated the inadequate pavement drainage as one of the main causes of premature fatigue failure. Because underlying layers are weakened by the excess moisture in underlying layers, the HMA layers experience higher tensile strains that are more than the strength of the mixture. Dore et al. [24] recognized the drainage factor as the primary factor of fatigue cracking in relatively colder regions, and further discussed the combination of drainage factor and stiffness of the surface HMA layer, stating that: *“most of the fatigue cracking in Quebec, Canada, occurs during the spring when underlying deflections are relatively larger, but also the HMA layer is still cold and consequently more brittle”*.

In a manual for design of HMA prepared by NCHRP [19], the stiffness of the surface layer binder is also stated as a contributing factor to fatigue resistance. This relationship is further stated to be dependent on the pavement structure: for HMA layers with thickness of less than three inches (76 mm), increasing the high temperature binder stiffness is stated to decrease the resistance to both bottom-up and top-down fatigue cracks. On the other hand, increasing the high temperature stiffness is stated to increase the resistance to bottom-up fatigue cracking for HMA layers thicker than or equal to five inches (127 mm).

Thus, to enhance fatigue cracking resistance by using modified binder (MB), modifiers should be selected that they behave like soft elastic material during intermediate (moderate) pavement service temperatures. Fulfilling this role requires modifiers to reduce the stiffness of the asphalt binder, thus soften the asphalt binder to deform without exhibiting larger stresses. Meanwhile, modifiers are required to impart elasticity to the binder helping to recover to its original condition without dissipating energy in any form [25].

Unlike fatigue cracking and rutting, thermal cracking is caused by adverse environmental conditions rather than traffic loading. Thermal cracking displays itself as consistently spaced transverse cracks perpendicular to the traffic direction (Figure 2-12).



Figure 2-12 Consistently spaced thermal transverse cracking, photo taken at Bayers Rd. toward Highway 102 North, Halifax, Nova Scotia, October 27th 2013

NCHRP [19] stated that: *“the low-temperature thermal cracking performance of asphalt pavements is almost completely controlled by the environmental conditions and the low temperature properties of the asphalt binder”*. Bahia et al. [25] suggested that thermal cooling cycle shrinkage in an asphalt bound layer restrained by friction with the underlying layers can cause a tensile stress development. It is further suggested that such developed stress in the asphalt-bound layer should be relaxed by ability of asphalt binder to flow readily and have less elasticity in its response, which if not relaxed, the cracking will be resulted. Modifiers play an important role in enhancing thermal cracking resistance. Some modifiers tend to soften the asphalt binder at lower pavement service temperatures, causing less thermal cracks [25].

2.1.2 Moisture Damage and Aging

Moisture damage (or also referred to as “stripping”) is one of the major modes of distresses in pavements, resulting in the loss of cohesive strength between asphalt binder and the aggregates in the mixture. Barnes et al. [26] stated that: *“Stripping occurs when the binder detaches from the aggregates in the presence of water, becomes displaced from the aggregate by water and/or a water droplet emulsion develops within the binder. The phenomenon occurs because an aggregate may have a greater affinity for moisture than for a particular asphalt binder”*. To provide a remedy for bond improvement between aggregate particles and asphalt binder, certain types of liquid chemicals are used to promote adhesion between the asphalt binder and aggregate surface. These chemical modifiers are referred to as anti-stripping agents, which blended with the asphalt binder before mixing with aggregate [16].

As discussed earlier, asphalt binder, as a visco-elastic material, behave differently depending on service temperature as well as rate of loading. Such behaviour can be altered further during hot-mixing with aggregate at the production plant as well as deterioration due to traffic and environmental loadings during pavement’s in-service stage. This alteration is referred to as binder aging, and is believed to be related significantly to pavement performance [27].

Research on identifying the factors contributing to the binder aging can be dated as early as mid-50's, when Vallerga et al. [28] and Finn et al. [29] identified oxidation, loss of loss of volatiles, polymerization, thixotropy, syneresis, and separation as possible contributing factors the aging phenomena during mixing and in-service stages. Later, more contributing factors were identified by Traxler [30]. In addition to such asphalt-specific related aging factors, other factors including the effect of climatic conditions, mixture type, aggregate gradation, and air voids content and distribution in mixture are also stated to be effective factors in the age hardening of asphalt binder [31]. Although all aforementioned are contributing factors to the binder aging, Johansson [32] identified the oxidation, volatilization, exudation, and physical hardening as principal asphalt-specific factors of the binder aging:

- Oxidation aging is an irreversible chemical reaction between the asphalt binder components and the atmospheric oxygen. Oxidation rate depends greatly on the chemical composition of the asphalt cement and temperature. Oxidation can occur during mixing, construction and in-service stages;
- Volatilization occurs predominantly during mixing of the binder with aggregate particles at the plant, when the binder (formed as a thin film covering aggregate particle's surface areas) losses some volatile components due to exposition to heat;
- Exudation is an irreversible composition change in an asphalt binder due to contact with aggregate particles, when oils from the asphalt binder are exuded into the aggregate particles;
- Physical hardening is a reversible process of the binder's molecular reorientation, while does not alter the chemical composition of the binder. Physical hardening is belied to significantly change rheological properties of asphalt binder.

An example of the effect of previously mentioned aging factors on the binder physical properties is shown in Figure 2-13. As shown, viscosity of the binder (as a measure of physical property) is significantly affected during the plant mixing. The aging effects continue at slower rate during in-service stages.

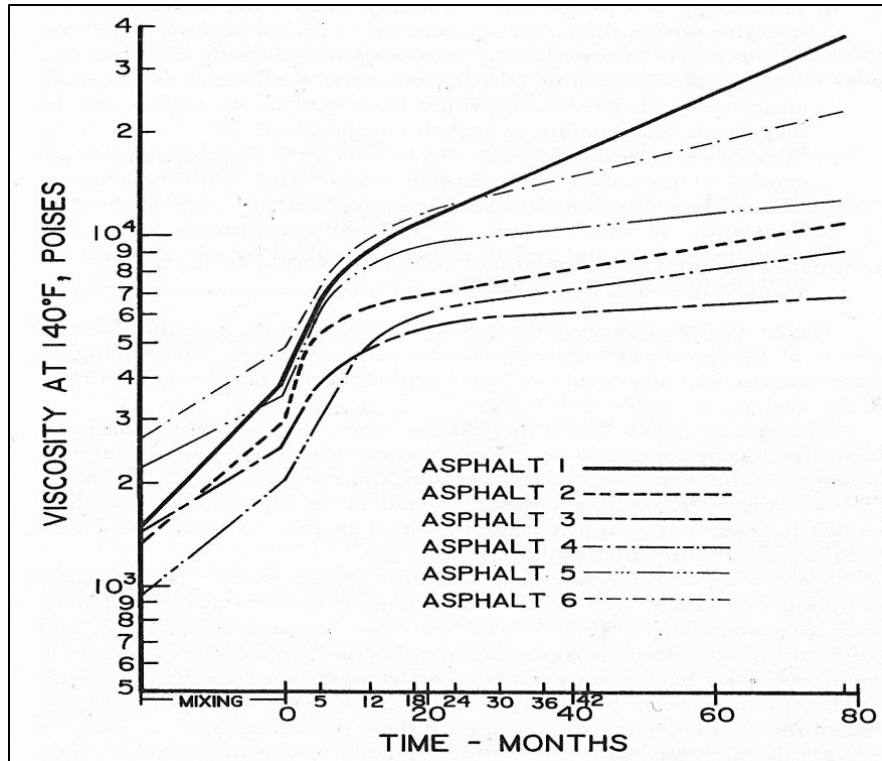


Figure 2-13 Effects of aging on viscosity [33]

Binder modification often results in excessive oxidative aging, thereby increasing the viscosity and stiffness of the binder excessively. This could result in earlier than expected thermal and fatigue cracking.

2.3.Types of Asphalt Modifiers

Binder modification can be performed in a number of production methods by using various modifiers. In the most recent survey conducted by Bahia et al. in the NCHRP 9-10 project [18], a total of 55 modifiers were identified which can be classified into 17 generic classes based on the nature of the modifier and its effect on the pavement distress modes previously explained in section 2.2 of this chapter. While only the types of modifiers that are interest of the GLC Ltd. (sponsoring company) will be reviewed in the following sections, these modifiers were also identified in the survey report conducted by NCHRP 9-10 project [18], among the most widely known and used in practice modifiers. These modifiers are widely known to be cost effective, easy to market, and easy to blend with asphalt binder.

2.3.1. Polymers

Polymers used to modify asphalt binder are broadly classified into polyolefins and styrenic polymers. Polyolefins polymers are produced by polymerization of molecules containing simple double bond or olefin (i.e. ethylene or propylene). Most common examples of polyolefins are PE, Poly-Propylene (PP), and Ethylene Vinyl Acetate (EVA). On the other hand, styrenic polymers are produced by co-polymerization of Poly-Styrene with other small molecules, most commonly butadiene [16]. In General, polymer can be classified further into plastomers (often referred to as “*plastics*”) and elastomers, depending on their behaviour when stretched with sufficient force.

Elastomers are among the most commonly used polymer modifiers in paving industry, especially Styrene-Butadiene-Styrene (SBS). As a block co-polymer, can be easily utilized into the HMA by blending system shown in Figure 2-14. Such blending system is located either at asphalt terminal or refineries, where asphalt binder can be modified and transported to the HMA facility subsequently.

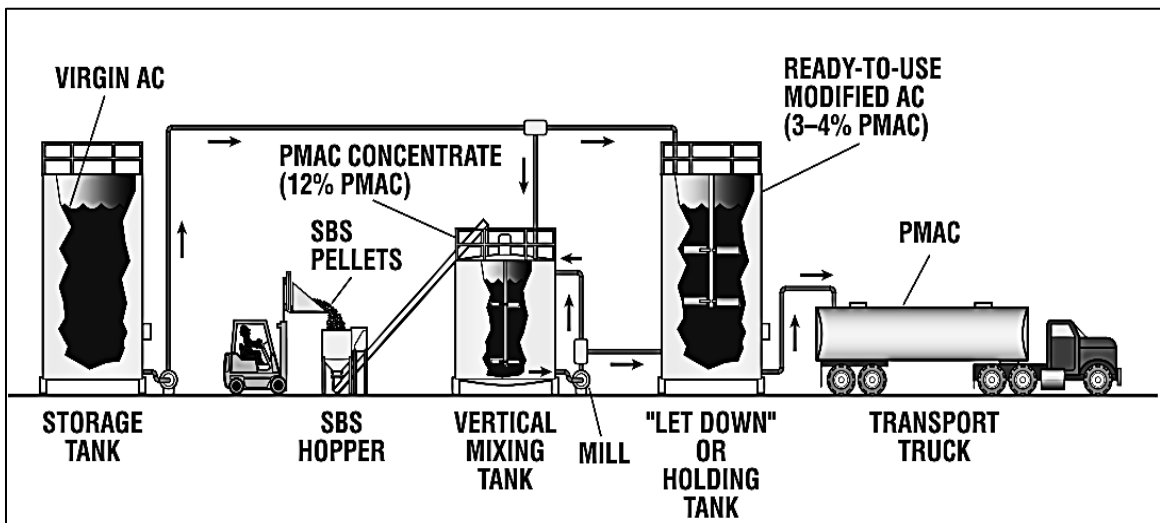


Figure 2-14 Most commonly used stationary polymer blending system [34]

SBS polymer is believed by many agencies to help mitigating permanent deformation, fatigue and thermal cracking [35]. Most commonly, SBS polymers are produced in form of pellets for ease of processing and blending. Figure 2-15 shows SBS pellets used for this research study, which is commercialized under brand name of Kraton® D-type.



Figure 2-15 Kraton® D-type Styrene-Butadiene-Styrene (SBS) pellets

Compare to elastomers, plastomers exhibit less elasticity under an equivalent load. Plastomers are believed to improve the permanent deformation resistance, while fatigue and thermal cracking resistance might decrease due to increased intermediate and low-temperature stiffness relatively [36]. However, mixed-polymer modification technique (i.e. blending plastomers and elastomers) is stated by Asphalt Institute [16] as an effective method to enhance intermediate and low-temperature characteristics of such modifiers. Most commonly used plastomers to modify asphalt binder are LDPE, EVA [37].

2.3.2. Hydrocarbons and Extenders

Hydrocarbon modifiers are broadly classified into hardeners and softeners. Such modifiers are used particularly to reduce or increase viscosity of the asphalt binder in mixture. The most common example of hydrocarbon modifier is aromatic oils. Aromatic oils are reported to improve low temperature cracking by decreasing the low-temperature stiffness [37]. Aromatic oils are used in a form of liquid, which can be added either to the “mixing tank” or “let-down tank” (as shown in Figure 2-14) after addition of polymers.

Extenders are modifiers used to improve the permanent deformation resistance. Sulfur is the most commonly used modifier among extenders. Although sulfur can be used as a modifier alone, it may be used in combination with other polymer modifiers.

The intention of co-blending sulfur with other polymer modifiers is reported to result in a better chemical bond between the polymer molecules, creating a continuous network of molecules that can exhibit relatively more elastic response [16]. The technique of using sulfur to enhance chemical bonding is referred to as “cross-linking”. The cross-linking technique is also reported to decrease the separation tendency in the modified binder [38]. Sulfur can be used in a form of pellets (Figure 2-16), which can be added through the hopper (as shown in Figure 2-14) after addition of SBS.



Figure 2-16 Sulfur pellets

2.4.Characterization and Performance Evaluation of Modified Binders

2.4.1. Superpave™ Performance Grading

The Superpave™ (*Superior Performing Asphalt Pavements*) is a final product of the Strategic Highway Research Program (SHRP)⁴ initiated by the the United States Department of Transportation Federal Highway Administration (FHWA) during the late 1980s. The Superpave™ is a system of mixture design for HMA based upon mechanistic concepts, which includes an asphalt-grading system called Performance Grading (PG) with intention of linking the physical properties of asphalt binder (both modified and unmodified) to three specific types of HMA pavement distresses: rutting, fatigue cracking, and thermal cracking [22].

⁴ In direct response to the SHRP, The Canadian Strategic Highway Research Program (C-SHRP) was launched in 1987 by the Council of Deputy Ministers Responsible for Transportation and Highway Safety to extract benefits of the Superpave™ concepts. As a result, the Superpave™ concepts gained acceptance and PG grades become accepted in Canadian pavement industry [76].

The pavement temperatures used for performance grades are determined by converting historical air temperatures into maximum pavement temperature at depth of 20mm below the surface and minimum pavement temperature at the surface of pavement. The conversion is performed as per algorithms given in AASHTO M 323-13 [39]. A computerized method of AASHTO M323 is also available in a form of software (named as “*LTPPBind*”) provided by the FHWA, in which more than 6500 weather stations data from the United States and Canada are compiled.

The design reliability level is also incorporated in the process of selecting pavement service temperatures. Reliability is defined as the percent probability that the average 7-day maximum and minimum pavement temperature will not exceed the corresponding PG temperatures in a single year. The design reliability level is calculated according to a standard deviation that describes the every year variation in the average. Figure 2-17 illustrates a sample of calculation for determination of PG based on different reliability levels.

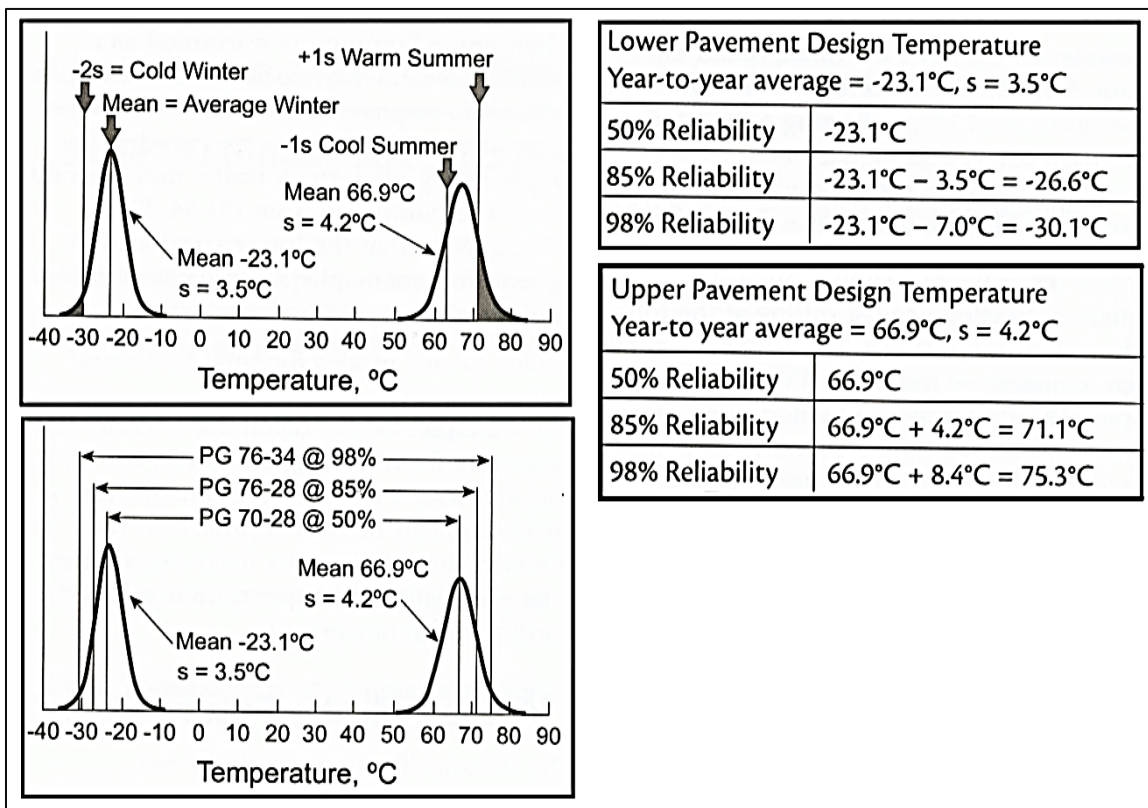


Figure 2-17 PG selection for different reliabilities [17]

The PG grades selected by Superpave™ system apply for typical highway loading conditions. In case of standing or slow traffic, Superpave™ requires an additional shift in the selected high PG grade to avoid permanent deformation. Also, an additional shift is required for high volume of design Equivalent Single Axle Loads (ESAL⁵). This practice of adjusting high PG grade for traffic loading and speed is referred to as “grade-bumping” [40]. Figure 2-18 summarizes Superpave’s grade-bumping chart.

Design ESALs ¹ (million)	Adjustment to Binder PG Grade ⁵		
	Standing ²	Slow ³	Standard ⁴
< 0.3	_(6)		
0.3 to < 3	2	1	
3 to < 10	2	1	
10 to < 30	2	1	_(6)
≥ 30	2	1	1

1. Design ESALs are the anticipated project traffic level expected on the design lane over a 20 year period. Regardless of the actual design life of the roadway determine the design ESALs for 20 years and choose the appropriate N_{design} level.
2. Standing Traffic - where the average traffic speed is less than 20 km/h.
3. Slow Traffic - where the average traffic speed ranges from 20 to 70 km/h.
4. Standard Traffic - where the average traffic speed is greater than 70 km/h.
5. Increase the high temperature grade by the number of grade equivalents indicated (one grade equivalent to 6°C). Do not adjust the low temperature grade.
6. Consideration should be given to increasing the high temperature grade by one grade equivalent.

Practically, performance graded binders stiffer than PG 82-XX should be avoided. In cases where the required adjustment to the high temperature binder grade would result in a grade higher than a PG 82, consideration should be given to specifying a PG 82-XX and increasing the design ESALs by one level (e.g., 10 to < 30 million increased to ≥ 30 million).

Figure 2-18 Superpave™ grade-bumping chart [21]

In addition to climatic conditions, the Superpave™ PG system also accounts for the effects of asphalt binder aging by adopting two procedures simulating two stages of binder’s life. The first stage simulates the short-term aging of the binder due to heat and air exposure during mixing at the HMA plant, transportation, and placement. The second stage simulates the long-term aging of asphalt binders that occurs by UV exposure, oxidization, and hardening of asphalt binder after several years of service.

⁵ An *ESAL* is a unit used in designing transportation infrastructures, which accounts for an 80 kN (18,000 lb) four-tired dual axle truck.

The short-term aging can be performed in accordance with AASHTO T240-09, “Effect of Heat and Air on a Moving Film of Asphalt Binder (Rolling Thin-Film Oven Test) [41]. In this test, aging is simulated by blowing a hot jet of air into cylindrical glass bottles filled with 35 grams of asphalt binder. The glass bottles are attached horizontally into a vertically rotating frame (also called “carriage”). The frame rotates at speed of 15 revolutions per minute (rpm) causing the sample to flow along the walls of glass bottle. During each rotation, taking few seconds, air is blown once into each glass bottle. This action continues for 75 minutes in an oven with a constant operating temperature of 163°C. Bottles are then removed, and the aged asphalt sample is poured into thin cans for further testing and long-term aging. As part of the RTFO procedure, mass of volatiles loss from the asphalt binder can be also determined.

To simulate long-term aging, a Pressure-Aging Vessel (PAV) can be used in accordance with AASHTO R 28-12, “Accelerated Aging of Asphalt Binder Using a Pressurized Aging Vessel (PAV)” [42]. In this test method, RTFO residue is poured on a stainless steel pans which are then placed vertically in a sealed pressure vessel. The aging conditioning is then performed by 20 hours of constant pressure of 2.10 MPa. Depending on the climate where the binder is intended to be used, conditioning temperature during testing can be either 90, 100, or 110°C. The residue from this test is used for additional rheology tests explained in following sections.

Figure 2-19 illustrates the way that the aging tests are used in combination with PG rheological tests to control pavement distress modes as described in AASHTO M 320-10, “Standard Specification for Performance-Graded Asphalt Binder” [40]. All rheological tests such as Rotational Viscometer (RV), Dynamic Shear Rheometer (DSR), Direct Tension Test (DTT), and Bending Beam Rheometer (BBR) are described in further details in the following sections.

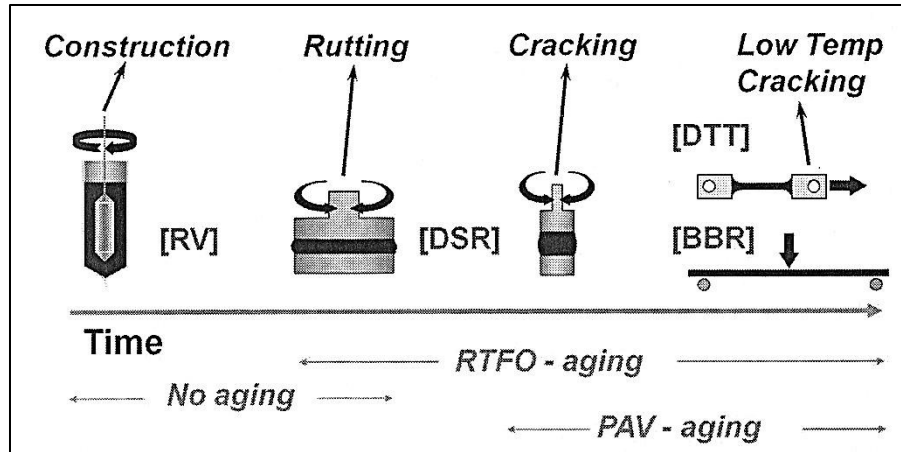


Figure 2-19 Combination of Superpave™ PG system rheological tests with aging conditions [16]

2.4.1.1. Workability

In Superpave™ PG specification, workability is defined as viscosity parameter of the asphalt binder corresponding to stages involving high temperature pumping, mixing with the aggregate at the hot-plant, and field compaction [16]. Although such behaviour of the binder is not directly related to pavement distress modes, it can affect the coating of the aggregate as well as the ability to compact the mixture in the field.

To ensure binder workability, the Superpave™ PG system specifies using a Rotational Viscometer (RV) (also referred to as “*Brookfield Viscometer*”) to measure the viscosity of the binder under constant rate of strain in accordance with AASHTO T 316-11, “Viscosity Determination of Asphalt Binder Using Rotational Viscometer” [43].

In this test method, RV applies a twisting or rotational shearing load by using a cylindrical spindle submerged into a specific amount of asphalt binder (Figure 2-20-ii). As the spindle starts to rotate, the asphalt binder, sandwiched between the wall of chamber and the surface of the spindle, turns into a series of many concentric layers (numbered through 1 to 6 in Figure 2-20-i) rotating relative to each other. During the rotation of asphalt-concentric layers, weak bond between molecules are continuously broken and regained which causes a resistance to shearing action. Such resistance is referred to as viscosity, which can be estimated by using Equation 2-2.

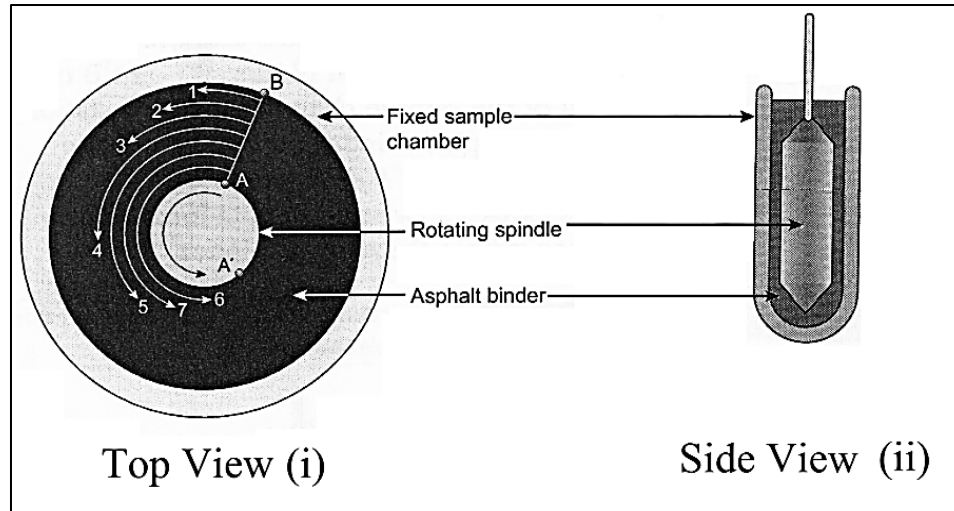


Figure 2-20 Rotational viscometer test setup top view (i), and side view (ii) (Modified from [17])

$$\eta = \frac{\tau}{\dot{\gamma}} \quad 2-2$$

where:

η = viscosity,
 τ = shear stress, and
 $\dot{\gamma}$ = shear strain rate,

The Superpave™ PG system specifies an upper limit of 3.0 Pa.S for the viscosity value measured at 135°C as criterion for the proper pumping and handling at the hot-plant. The PG system specifies viscosity values of 0.17 ± 0.02 , and 0.28 ± 0.03 Pa.s to approximate the shear rates that occur during hot-plant mixing and field compaction respectively [40]. To determine such equiviscous⁶ mixing and compaction temperatures, an ASTM viscosity-temperature plot is used to find temperature ranges corresponding to the specified viscosity values. The ASTM plot can be obtained as per ASTM D 2493, “Standard Viscosity-Temperature Chart for Asphalts” [44]. Figure 2-21 illustrates a viscosity-temperature curve for one of binders studied for this study.

⁶ *Equiviscous* temperatures are binder specific temperatures at which a common viscosity is reached [17].

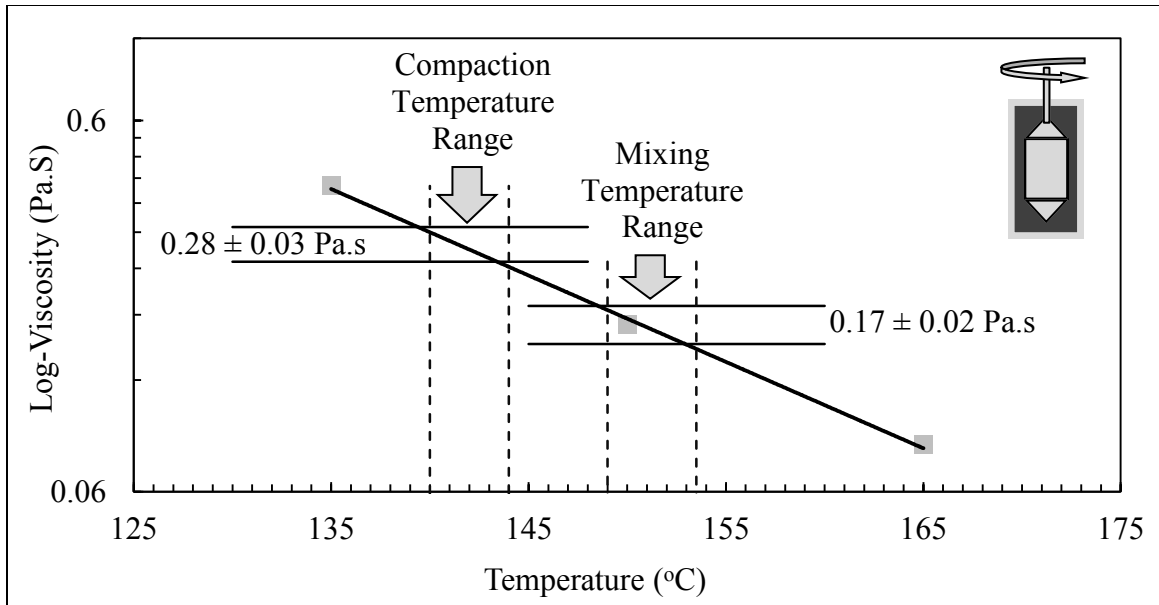


Figure 2-21 An example of ASTM viscosity-temperature curve

Since the ASTM plot is used only for Newtonian binders (unmodified binders), the AASHTO T 316-11 suggests some modified binders might exhibit nonlinear viscosity curve due to non-Newtonian behaviour [43]. The viscosity of Newtonian fluids (i.e. asphalt binder) is constant regardless of shear rate, whereas the viscosity for non-Newtonian fluids is not constant (as shown in Figure 2-22) [16]. As stated by West et al. [45], determination equiviscous temperatures by using ASTM plot might results in excessive mixing and compaction temperatures that might cause emission issues and degradation of the binder's properties.

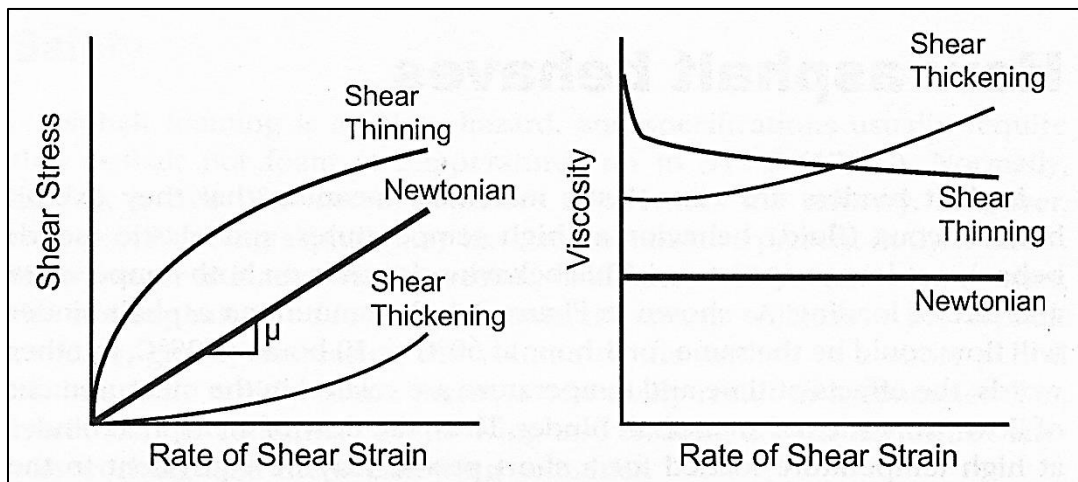


Figure 2-22 Comparison of Newtonian and non-Newtonian fluids [16]

2.4.1.2. Permanent Deformation

In Superpave™ PG specification, permanent deformation is considered as a stress-controlled cyclic loading phenomenon, which during each cycle of reversible loading, a certain amount of work is being done to deform the HMA surface layer. A portion of this work is recoverable due to elastic rebound of the surface and remaining is dissipated energy in form of permanent deformation and heat. For viscoelastic materials, the amount of dissipated energy per loading cycle can be determined by using Equation 2-3.

$$W_c = \pi \cdot \sigma_0^2 \cdot \left(\frac{1}{G^*/\sin\delta} \right) \quad 2-3$$

where:

- W_c = work dissipated per loading cycle,
- σ_0 = stress applied during the loading cycle,
- G^* = complex modulus, and
- δ = phase angle.

The parameter $G^*/\sin(\delta)$ in Equation 2-3 is selected to evaluate permanent deformation damage resistance. This parameter is a combination of the total resistance to deformation (G^*) and relative non-elasticity of the binder ($\sin(\delta)$). Increasing the $G^*/\sin(\delta)$ parameter causes the binder to behave stiffer and more elastic, and thus more resistant to permanent deformation.

To relate the $G^*/\sin(\delta)$ parameter to permanent deformation, the Superpave™ specifies this parameter to be measured at maximum pavement temperature at a frequency of 10 radians per second (1.59 Hz). Such loading frequency is selected to simulate the average frequency of a stress wave in the typical HMA surface layer caused by a vehicle travelling at speed of standard (more than 70 km/hr).

The $G^*/\sin(\delta)$ parameter is determined by using a Dynamic Shear Rheometer (DSR) in accordance with AASHTO T 315-12, “Determining the Rheological Properties of Asphalt Binder Using a Dynamic Shear Rheometer (DSR) [46]. In this test, a certain amount of sample is sandwiched between a fixed plate and an oscillating plate. When torque is applied, as shown in Figure 2-23, the oscillating plate traversed from points

shown in Figure 2-23 (i) to complete one cycle of oscillation. During the operation of DSR, the resulting strain (as shown in Figure 2-23 (ii)) is recorded and then used to determine the G^* by using Equation 2-4.

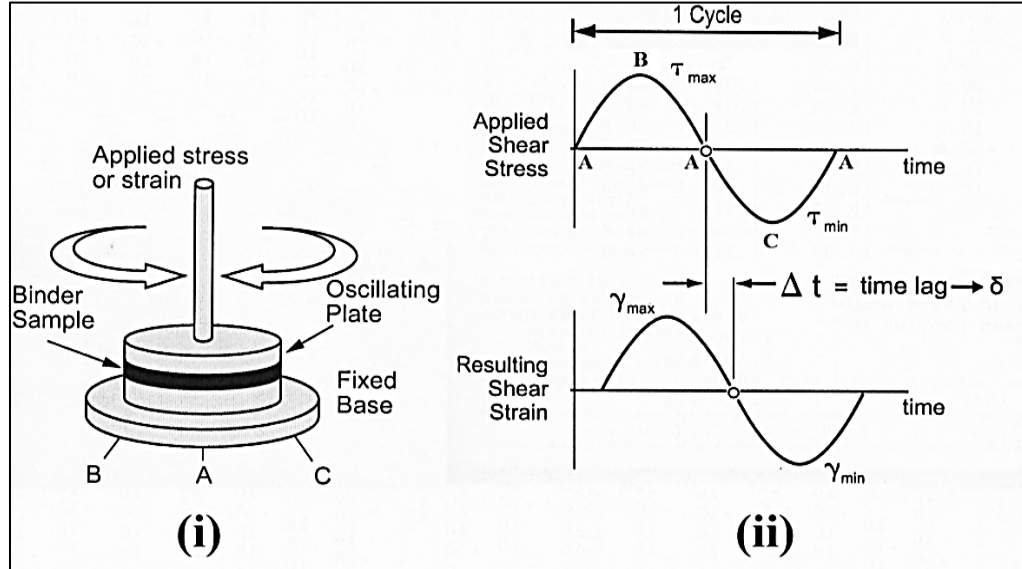


Figure 2-23 Dynamic Shear Rheometer operation and resulting graphs [16]

$$G^* = \frac{\tau_{max} - \tau_{min}}{\gamma_{max} - \gamma_{min}} \quad 2-4$$

where:

- G^* = the complex modulus,
- τ = shear stress, and
- γ = shear strain.

As mentioned earlier, one of the main objectives of the Superpave™ PG system was linking the asphalt binder physical properties to permanent deformation resistance of HMA layer. However, there are two main concerns about the applicability of $G^*/\sin(\delta)$ specification. The first concern is that during the SHRP research majority of studied asphalt binders were unmodified ranging between a PG 64-28, a PG 45-34 with one PG 70-22. Secondly, most of extreme grades such as PG 76-22, and PG 58-40 that are being used today for construction of high-volume pavements in warm or cold regions did not exist at the time of the research [47]. Additionally, different researchers have found the $G^*/\sin(\delta)$ parameter to be inadequate in describing the rutting performance of certain modified binders [48].

To solve concerns about applicability of Superpave™ PG specification to all range of asphalt binders, NCHRP initiated a comprehensive research project [18], “Superpave™ Protocols for Modified Asphalt Binders”. As part of this project, $G^*/\sin(\delta)$ parameter was found to be inadequate in predicting mixture rutting of some type of modified binders. As stated by Bahia [47], during the cyclic reversible loading only total work dissipated is possible to be estimated (as shown in Figure 2-24 (i)). However, permanent deformation is a repeated mechanism with sinusoidal loading pulse (Figure 2-24 (ii)) which does not include cyclic reversible loading required to force back pavement material to zero deformation [47].

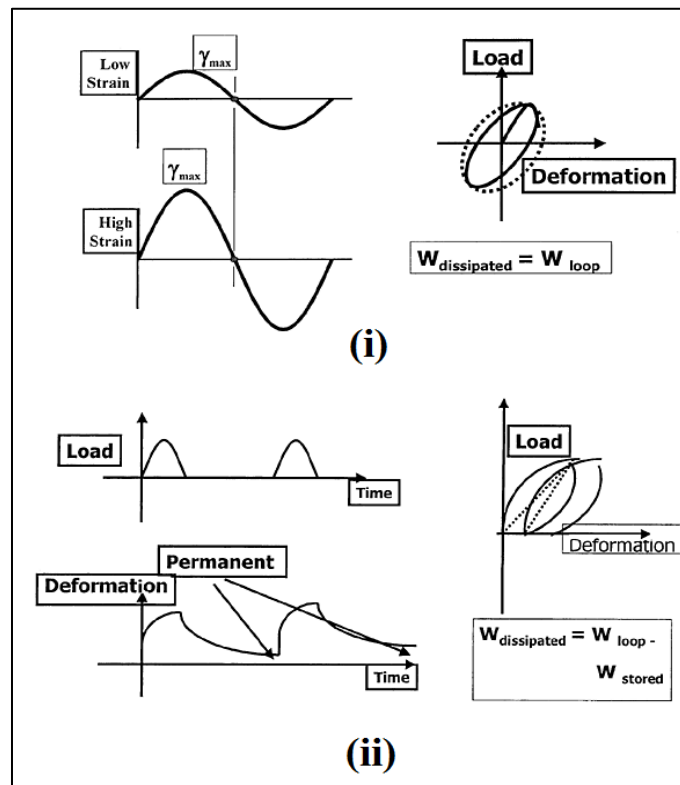


Figure 2-24 Concept used in driving Superpave™ rutting parameter of $G^*/\sin(\delta)$ (i) and proposed concept for rutting parameter (ii) [47]

As illustrated in Figure 2-24 (ii), the pavement layer is not forced back to zero deformation but would recover some deformation due to elasticity of the layer's material. In this case, unrecoverable portion is dissipated in permanent deformation which is believed to be the main contributor to the permanent deformation behaviour of HMA layer and any other asphalt mixtures [47].

Recognizing the fundamental problem with the cyclic reversible loading, many researchers have tried to develop and propose test methods including Repeated Shear Constant Height (RSCH), Repeated Creep and Recovery (RCR), Zero Shear Viscosity (ZSV), and Multiple Stress Creep Recovery (MSCR). MSCR is the test method that has proposed as a better test to evaluate binder's contribution in rutting resistance of asphalt mixtures. This test method is explained more in details in section 2.4.2 of this thesis.

2.4.1.3. Fatigue and Thermal Cracking

In Superpave™ PG specification, fatigue cracking is assumed to be more prevalent in thin pavements, which is considered as a strain-controlled cyclic loading phenomenon [27]. The dissipated work per loading cycle at constant strain is determined by using Equation 2-5.

$$W_c = \pi \cdot \epsilon_0^2 \cdot (G^* \times \sin\delta) \quad 2-5$$

where:

- W_c = work dissipated per loading cycle,
- ϵ_0 = strain applied during the load cycle,
- G^* = complex modulus, and
- δ = phase angle.

The parameter $G^*\sin(\delta)$ in Equation 2-5 is selected to evaluate fatigue cracking resistance. This parameter is a combination of the total resistance to cracking (G^*) and relative non-elasticity of the binder ($\sin(\delta)$). Decreasing the G^* and/or $\sin(\delta)$ causes the binder to behave less stiff, and thus able to deform without storing large stresses [27].

To relate the $G^*\sin(\delta)$ parameter to fatigue cracking resistance, the Superpave™ specifies this parameter to be measured at intermediate pavement temperature at a frequency of 10 radians per second (1.59 Hz). Superpave™ also specifies aging requirement as well as an upper limit for $G^*\sin(\delta)$ parameter to ensure that the binder has adequate stiffness to resist fatigue cracking. Similar to rutting parameter determination, the $G^*\sin(\delta)$ parameter is also determined by using a Dynamic Shear Rheometer (DSR). The $G^*\sin(\delta)$ parameter is determined for PAV-aged binders. PAV aging is performed to ensure that

the most critical in-service condition is considered as asphalt binders tend to stiffen and aged during pavement's life [25].

In the Superpave™ specification, the thermal susceptibility of an asphalt binder is evaluated by creep response (creep stiffness) and relaxation (creep rate) of a binder to a constant applied load. For this purpose, a Bending Beam Rheometer (BBR) is used to apply a constant load to a small binder beam at lowest pavement service temperature. Figure 2-25 illustrates the schematic of BBR operation.

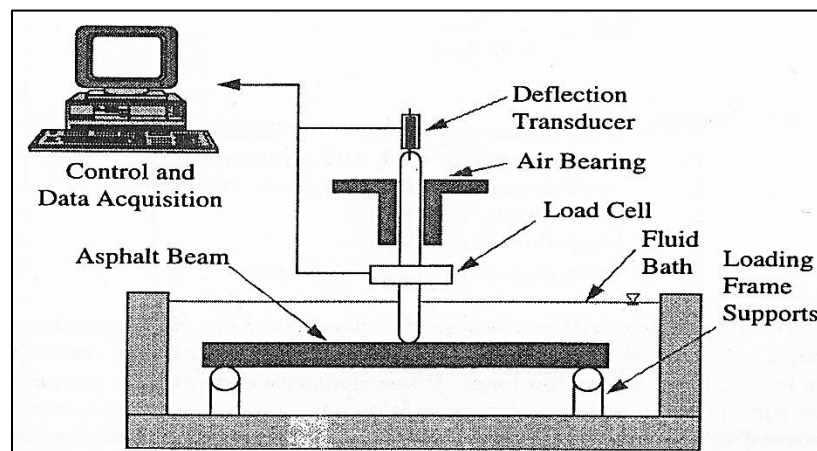


Figure 2-25 Schematic of Bending Beam Rheometer [49]

As stated by Bahia et al. [49], both the beam dimensions and load applying techniques are resemblance of ASTM D 790, “Standard Test Methods for Flexural Properties of Unreinforced and Reinforced Plastics and Electrical Insulating Materials” [50]. By using this standard, the elementary Bernoulli-Euler theory of bending prismatic beams is applicable, thus the creep response is calculated by using Equation 2-6.

$$S(t) = \frac{PL^3}{4bh \delta(t)} \quad 2-6$$

where:

- $S(t)$ = creep stiffness at time of t seconds,
- P = applied constant load,
- $\delta(t)$ = deflection at time of t seconds, and
- $L, b, \text{ and } h$ = dimension of asphalt beam.

In Equation 2-6, a constant creep load of 100 grams (980 mN) is applied to an asphalt binder beam specimen measuring 125 mm in length, 6.35 mm in width, and 12.7 mm in height for 240 seconds. As shown in Figure 2-26, deflection of the beam is continuously measured during the test. To relate the creep stiffness to thermal cracking resistance of a binder, the Superpave™ specifies an upper limit of 300 MPa for the creep stiffness measured at 60 seconds ($S(60)$), and a lower limit of 0.300 for creep rate (m -value).

Superpave™ also specifies PAV-aging requirement for measurement of the mentioned parameters since aging stiffen the binder and lower the m -value, representing the worst case situation. The $S(60)$ is determined by using Equation 2-6, while the m -value is the slope of the logarithmic stiffness versus logarithmic time curve at time of 60 seconds (as shown in Figure 2-26).

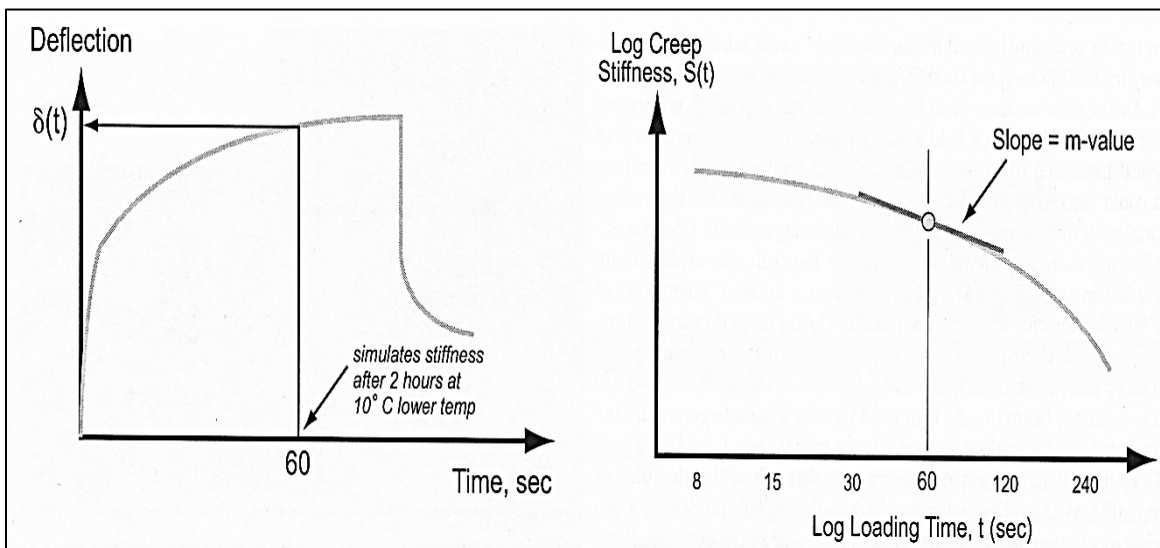


Figure 2-26 Related graphs of measuring creep stiffness (S) and creep rate (m -value) [16]

McGennis et al. [22] stated that binders with relatively lower values of creep stiffness will exhibit fewer amounts of thermal cracks in cold weather. Likewise, higher value of m -value shows the ability of binder to absorb stress in the event of temperature drop and exhibit lesser cracking tendency.

It should be noted that the testing temperature for the BBR test is 10°C higher than the lowest pavement service temperature for loading time of 60 seconds. Bahia et al. [49] stated that such offset was verified, at the time of Superpave™ development, to be sufficient to equate the S(60) to the asphalt binder stiffness at two hours loading time in the field at lowest pavement service temperature.

2.4.1.4. Moisture Damage and aging

Although moisture damage is a major distress mode, the Superpave™ does not provide particular specification on binder properties. Bahia et al. [49] stated that the moisture damage, at the time of the Superpave™ specification development, was concluded to be as a result of the aggregate particles and asphalt interaction, and thus cannot be appropriately addressed by binder properties. However, the moisture damage (or susceptibility) can be quantified by test method designed specifically to evaluate the bond between the binder and aggregate particles in form of the mixture.

Recognizing the significant effect of aging on pavement distress modes, the Superpave™ PG system specifies two aging procedures (as explained in 2.4.1):

- *RTFO* to simulate the short-term aging of the binder due to heat and air exposure during mixing at the HMA plant, transportation, and placement; and
- *PAV* to simulate the long-term aging of asphalt binders that occurs by UV exposure, oxidization, and hardening of asphalt binder after several years of service.

2.4.1.5. Superpave™ Specification Summary

Figure 2-27 summarises the Superpave™ PG specifications as described in AASHTO M 320-10 [40].

Performance Grade	PG 46				PG 52				PG 58				PG 64									
	34	40	46	<46	10	16	22	28	34	40	46	16	22	28	34	40	10	16	22	28	34	40
Average 7-day max pavement design temp, °C ^a	> -34	> -40	> -46	<46	> -10	> -16	> -22	> -28	> -34	> -40	> -46	> -16	> -22	> -28	> -34	> -40	> -10	> -16	> -22	> -28	> -34	> -40
Min pavement design temperature, °C ^b	> -34	> -40	> -46	<46	> -10	> -16	> -22	> -28	> -34	> -40	> -46	> -16	> -22	> -28	> -34	> -40	> -10	> -16	> -22	> -28	> -34	> -40
Flash point temp, T 48, min °C	230																					
Viscosity, T 316, ^c max 3 Pa s, test temp, °C	135																					
Dynamic shear, T 315: ^d G* sinδ, ^e min 1.00 kPa test temp @ 10 rad/s, °C	46				52				58				64									
Mass change, f, max, percent	1.00																					
Dynamic shear, T 315: ^d G* sinδ, ^e min 2.20 kPa test temp @ 10 rad/s, °C	46				52				58				64									
PAV aging temperature, °C ^f	90				90				100				100									
Dynamic shear, T 315: ^d G* sinδ, ^e max 5000 kPa test temp @ 10 rad/s, °C	10	7	4	25	22	19	16	13	10	7	25	22	19	16	13	10	31	28	25	22	19	16
Creep stiffness, T 313: ^g S, max 300 MPa m-value, min 0.300 test temp @ 60 s, °C	-24	-30	-36	0	-6	-12	-18	-24	-30	-36	-6	-12	-18	-24	-30	-36	0	-6	-12	-18	-24	-30
Direct tension, T 314: ^g Failure strain, min 1.0% test temp @ 1.0 mm/min, °C	-24	-30	-36	0	-6	-12	-18	-24	-30	-36	-6	-12	-18	-24	-30	-36	0	-6	-12	-18	-24	-30

Original Binder

Rolling Thin-Film Oven Residue (T 240)

Pressurized Aging Vessel Residue (R 28)

^a Pavement temperatures are estimated from air temperatures using an algorithm contained in the LTPP Bind program, may be provided by the specifying agency, or by following the procedures as outlined in M 323 and R 35.

^b This requirement may be waived at the discretion of the specifying agency if the supplier warrants that the asphalt binder can be adequately pumped and mixed at temperatures that meet all applicable safety standards.

^c For quality control of unmodified asphalt binder production, measurement of the viscosity of the original asphalt binder may be used to supplement dynamic shear measurements of G* sinδ at test temperatures where the asphalt is a Newtonian fluid.

^d G* sinδ = high temperature stiffness and C* sinδ = intermediate temperature stiffness.

^e The mass change shall be less than 1.00 percent for either a positive (mass gain) or a negative (mass loss) change.

^f The PAV aging temperature is based on simulated climatic conditions and is one of three temperatures, 90°C, 100°C, or 110°C. Normally the PAV aging temperature is 100°C for PG 58-xx and above. However, in desert climates, the PAV aging temperature for PG 70-xx and above may be specified as 110°C.

^g If the creep stiffness is below 300 MPa, the direct tension test is not required. If the creep stiffness is between 300 and 600 MPa, the direct tension failure strain requirement can be used in lieu of the creep stiffness requirement. The m-value requirement must be satisfied in both cases.

Figure 2-27 Summary of the Superpave™ PG system and requirements [40]

2.4.2. Multiple-Stress Creep Recovery (MSCR) Performance Grading

Recognizing the inadequacy of Superpave™ $|G^*|/\sin(\delta)$ rutting parameter in predicting the rutting performance of some modified asphalt binders, an alternative standard specification was developed to use the non-recoverable compliance (J_{nr}) to performance grade binders as part of AASHTO MP 19-10, “Performance-Graded Asphalt Binder Using Multiple Stress Creep Recovery (MSCR) Test” [51]. It should be noted that testing for high temperature evaluation of binders is replaced in the AASHTO MP 19-10, while fatigue cracking, thermal cracking, workability, and aging testing are still similar the Superpave™ PG system.

As part of the MSCR PG grading, the required environmental PG and design reliability level are still selected as per Superpave™ PG system algorithm, while “grade-bumping” approach is eliminated by applying adjustments to the J_{nr} criteria to reflect different traffic levels [51]. Such adjustment is reflected through using traffic grade prefixes such as Standard (“S”), Heavy (“H”), Very heavy (“V”), and Extreme heavy (“E”) with corresponding traffic to the J_{nr} criteria is performed by traffic level designations corresponding for different ESALs levels and speeds listed in Table 2-1. For a better understanding of the new traffic criteria, Table 2-2 shows such traffic designations incorporated into the previously presented “grade-bumping” chart (Figure 2-18).

Table 2-1 Traffic level designations for MSCR performance grading [51]

Traffic Level Designation	Description
Standard (“S”)	ESALs of less than 10 million <i>and</i> standard traffic with speed of more 70 km/hr
Heavy (“H”)	ESALs of 10 to 30 million <i>or</i> slow moving traffic with speed of 20 to 70 km/hr
Very heavy (“V”)	ESALs of more than 30 million <i>or</i> standing traffic with speed of less than 20 km/hr
Extreme heavy (“E”)	ESALs of more than 30 million <i>and</i> standing traffic with speed of less than 20 km/hr

Table 2-2 Comparison of “grade-bumping” chart and MSCR performance grading traffic designations

Design ESALs (million)	Adjustment to Binder Superpave™ PG grade (MSCR Traffic designation)		
	Traffic Load Rate		
	Standing (<20 km/hr)	Slow (20 to 70 km/hr)	Standard (>70 km/hr)
<0.3	- (S)	- (S)	- (S)
0.3 to <3	2 (H)	1 (S)	- (S)
3 to <10	2 (V)	1 (H)	- (H)
10 to <30	2 (E)	1 (V)	- (V)
≥30	2 (E)	1 (E)	1 (E)

The non-recoverable compliance (J_{nr}) is measured in accordance with AASHTO TP 70-12, “The Multiple Stress Creep Recovery (MSCR) Test of Asphalt Binder Using a Dynamic Shear Rheometer (DSR)” [52]. The MSCR is the following development of Repeated Creep and Recovery (RCR) test, which was developed and recommended as an alternative to the Superpave™ $|G^*|/\sin(\delta)$ parameter during the NCHRP 9-10 project [18]. RCR was recommended to be performed by a DSR at shear stresses rang of 30, and 300 Pa for 100 cycles of 1 second loading time followed by immediate unloading time of 9 seconds [18]. However, further study of RCR by D'Angelo et al. [48] showed that the using RCR requires an extensive amount of time. This study led to the development of the MSCR test as a better alternative to both RCR test as well as the Superpave™ $|G^*|/\sin(\delta)$ parameter in capturing essential contribution of asphalt binder in rutting resistance [53]. Although the MSCR test has been accepted by many agencies as the best rutting performance evaluation, it is still an evolving test in need of continuing improvements. A recent study performed by Bahia et al. [54] is one of the few studies attempting to impart improvements to the MSCR test in terms of variability, stress sensitivity, and traffic level.

The MSCR test uses the creep and recovery test concept similar to the RCR test, except different loading conditions. The test uses 10 cycles of 1-second creep load and subsequent 9-second recovery at two stress levels of 0.1 and 3.2 kPa to calculate parameter of J_{nr} as well as percent recovery (%R). Figure 2-28 illustrates a sample calculation method for parameters J_{nr} and %R, for a binder response at stress level 0.1

kPa. It should be noted that the MSCR test recommends use of RTFO aged to capture the possible effects of binder aging at mixing and construction [51].

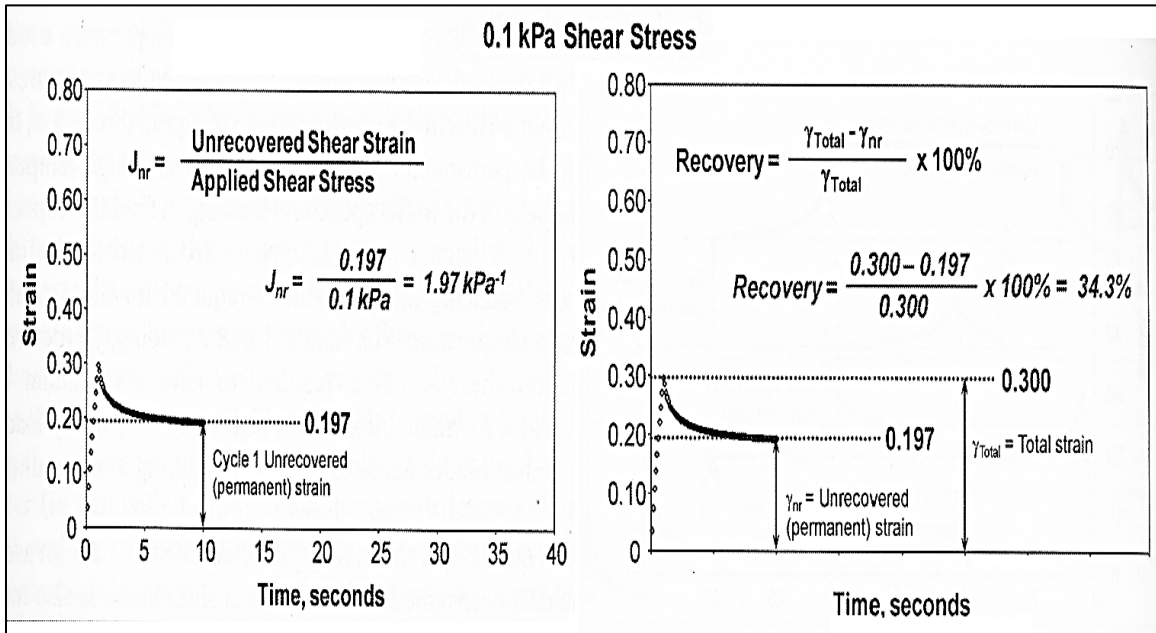


Figure 2-28 Sample of calculation for MSCR test parameters [16]

As mentioned previously, the AASHTO MP 19-10 recommends J_{nr} criteria corresponding to different traffic loading rates and levels ranging from standard to extreme heavy, while the criteria values are recommended as the average of J_{nr} for 10 cycles at each stress level. The MSCR test also recommends an upper limit for the difference between the average J_{nr} values at stress levels of 0.1 kPa and 3.2 kPa. The difference is calculated by using Equation 2-7. The J_{nr} difference limit is recommended by the MSCR test to ensure that the under testing modified binder is not sensitive to the stress levels of 0.1 kPa and 3.2 kPa.

$$J_{nr,diff.(\%)} = 100 \left(\frac{J_{nr,3.2} - J_{nr,0.1}}{J_{nr,3.2}} \right) \quad 2-7$$

where:

$J_{nr,3.2}$ = The average non-recoverable compliance measured at 3.2 kPa shear stress level (kPa^{-1}), and

$J_{nr,0.1}$ = The average non-recoverable compliance measured at 0.1 kPa shear stress level (kPa^{-1}).

Although the fatigue cracking parameter of $G^* \sin(\delta)$ is same for both Superpave™ PG system and AASHTO MP 19-10, the criterion changes to an upper limit of 6000 kPa for any traffic level designations other than standard (“S”). Figure 2-29 PG requirements corresponding to different traffic level designations as part of the MSCR PG specifications as described in AASHTO MP 19-10 [51].

Performance Grade	PG 46			PG 52						PG 58					
	34	40	46	10	16	22	28	34	40	46	16	22	28	34	40
Average 7-day max pavement design temp, °C ^b	<46			<52						<58					
Min pavement design temp, °C ^b	>-34	>-40	>-6	>-10	>-6	>-22	>-28	>-34	>-40	>-46	>-16	>-22	>-28	>-34	>-40
Original Binder															
Flash point temp, T 48, min °C	230														
Viscosity, T 316: ^c max 3 Pa·s, test temp, °C	135														
Dynamic shear, T 315: ^d $G^*/\sin\delta$, min 1.00 kPa ^e test temp @ 10 rad/s, °C	46			52						58					
Rolling Thin-Film Oven Residue (T 240)															
Mass change, max, percent ^f	1.00														
MSCR, TP 70: Standard Traffic “S” Grade $J_{N3.2}$, max 4.0 kPa ⁻¹ J_{Ndiff} , max 75% test temp, °C	46			52						58					
MSCR, TP 70: Heavy Traffic “H” Grade $J_{N3.2}$, max 2.0 kPa ⁻¹ J_{Ndiff} , max 75% test temp, °C	46			52						58					
MSCR, TP 70: Very Heavy Traffic “V” Grade $J_{N3.2}$, max 1.0 kPa ⁻¹ J_{Ndiff} , max 75% test temp, °C	46			52						58					
MSCR, TP 70: Extremely Heavy Traffic “E” Grade $J_{N3.2}$, max 0.5 kPa ⁻¹ J_{Ndiff} , max 75% test temp, °C	46			52						58					
Pressurized Aging Vessel Residue (R 28)															
PAV aging temp, °C ^g	90			90						100					
Dynamic shear, T 315: “S” Grade $G^* \sin\delta$, max 5000 kPa ^e test temp @ 10 rad/s, °C	10	7	4	25	22	19	16	13	10	7	25	22	19	16	13
Dynamic shear, T 315: “H”, “V”, “E” Grades $G^* \sin\delta$, max 6000 kPa ^e test temp @ 10 rad/s, °C	10	7	4	25	22	19	16	13	10	7	25	22	19	16	13
Creep stiffness, T 313: ^h S , max 300 MPa m -value, min 0.300 test temp @ 60 s, °C	-24	-30	-36	0	-6	-12	-18	-24	-30	-36	-6	-12	-18	-24	-30
Direct tension, T 314: ^h Failure strain, min 1.0% test temp @ 1.0 mm/min, °C	-24	-30	-36	0	-6	-12	-18	-24	-30	-36	-6	-12	-18	-24	-30

^a MSCR testing on RTFO residue should be performed at the PG grade based on the environmental high pavement temperature. Grade bumping is accomplished by requiring a lower J_N value while testing at the environmental temperature.

^b Pavement temperatures are estimated from air temperatures using an algorithm contained in the LTPP Bind program, may be provided by the specifying agency, or by following the procedures as outlined in M 323 and R 35, excluding the provisions for “grade bumping”.

^c This requirement may be waived at the discretion of the specifying agency if the supplier warrants that the asphalt binder can be adequately pumped and mixed at temperatures that meet all applicable safety standards.

^d For quality control of unmodified asphalt binder production, measurement of the viscosity of the original asphalt binder may be used to supplement dynamic shear measurements of $G^*/\sin\delta$ at test temperatures where the asphalt is a Newtonian fluid.

^e $G^*/\sin\delta$ = high temperature stiffness and $G^* \sin\delta$ = intermediate temperature stiffness.

^f The mass change shall be less than 1.00 percent for either a positive (mass gain) or a negative (mass loss) change.

^g The PAV aging temperature is based on simulated climatic conditions and is one of three temperatures, 90°C, 100°C, or 110°C. Normally the PAV aging temperature is 100°C for PG 58-xx and above. However, in desert climates, the PAV aging temperature for PG 70-xx and above may be specified as 110°C.

^h If the creep stiffness is below 300 MPa, the direct tension test is not required. If the creep stiffness is between 300 and 600 MPa, the direct tension failure strain requirement can be used in lieu of the creep stiffness requirement.

Figure 2-29 MSCR PG system summary [51]

2.5. Additional Tests for Modified Binders

Prior to development of the Superpave™ PG system, traditional or index rheological properties were used to characterize asphalt binders as well as modified binders. Some of these properties are still being used by many transportation agencies as complement to the PG system. Table 2-3 includes a list of the most widely used traditional tests.

Table 2-3 List of most commonly used traditional tests for MBs [55]

Test	Standard	Purpose
Softening Point (R&B)	AASHTO T 53	An index of consistency at high temperatures. This test is still used to measure instability of MBs.
Penetration	AASHTO T 49	An index of consistency at intermediate temperature.
Forced Ductility	ASTM D 2042	An Index of tensile strength and energy required for complete failure.
Elastic Recovery	AASHTO T 301	An index of the capability of modified binder for elastic recovery.
Toughness and Tenacity	ASTM D 5801	An index of energy to failure used to detect modifiers and assess their contribution to toughness.
Solubility	AASHTO T 44	An index of measuring purity of MBs.
Separation test	ASTM D 7173	An index of measuring the degree of separation in MBs.

As stated by Bahia et al. [25], the main issue with the aforementioned tests (often referred to as “empirical tests”) is their independency as they use different loading modes, rates, and temperatures. Despite such independency, many researchers have tried to combine these tests to better estimate fundamental rheological properties of asphalt binder, hence pavement performance by using various types of nomographs. Bahia et al. [25] recognized such studies misleading and more empirical in nature mainly due to suffering in several instances from exceptions, statistical insignificance, and size of sample or types of asphalts studied.

2.6. Summary

By using the primary recommendations and conclusions presented in the literature review, it is proven that a modifier can be selected to improve rheological properties of the base asphalt (“typical asphalt”) to match requirements defined by resistance to one or more pavement distresses. In terms of matching requirements, Figure 2-30 (i) is the best illustration of an ideal effect of binder modification on pavement performance. Such modification can enhance the rutting performance by increasing the stiffness at higher pavement service temperature, while decreasing the stiffness at relatively lower temperatures to avoid excessive fatigue and thermal cracking. It is also important that binder modification result in lower stiffness at mixing and construction temperatures to reduce the energy consumption during production and construction. Finally, as shown in Figure 2-30 (ii), the increase in ductility and elasticity after modification is also important as binders would tolerate higher rate stresses and strains before failure, hence a better resistance to different modes of pavement distresses.

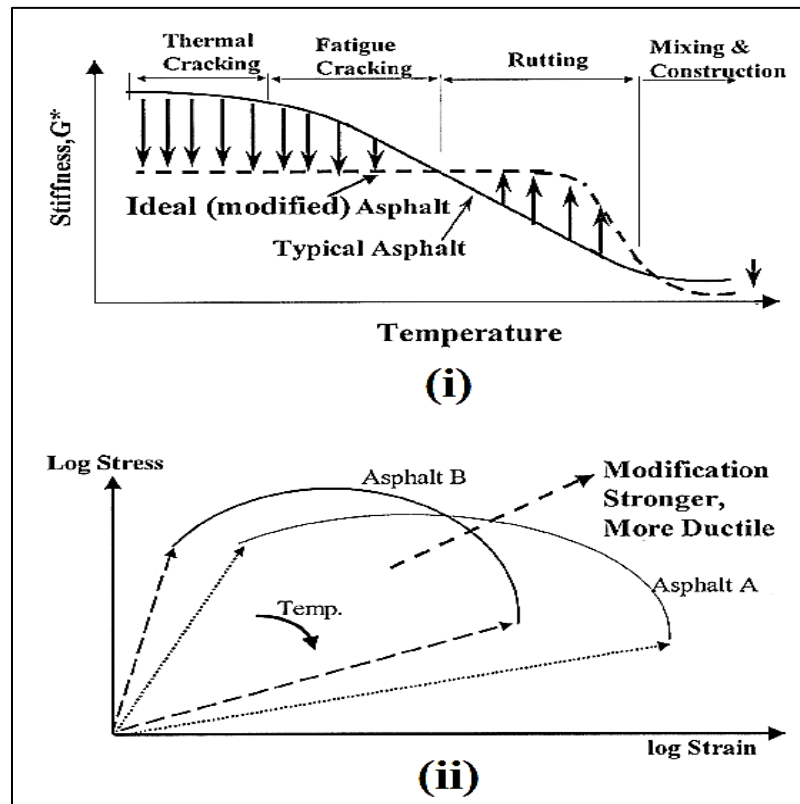


Figure 2-30 Schematics of the target change in rheological and failure properties expected from modification [47]

CHAPTER 3: RESEARCH METHODOLOGY

The intent of this research study was to investigate the feasibility of utilizing recycled plastics as binder modifiers in HMA while maintaining performance levels that are achieved using engineered modifiers such as Kraton® D-type Styrene-Butadiene-Styrene (SBS). The grades of plastics studied in this research were selected based on those available in Nova Scotia that are less commonly recycled or are difficult to market, such as Low Density Poly-Ethylene (LDPE) and Poly-styrene (PS) [7]. The research program included tests used commonly in pavement engineering to evaluate Modified Binders (MBs). All tests were selected based on AASHTO and ASTM standards divided into three modules. Module 1 was to design proprietary binder prototypes exhibiting similar high and low performance grades as PG 64-28. Module 2 was to performance grade MBs in accordance with both Superpave™ and MSCR PG systems. Finally, module 3 was to produce and evaluate asphalt mixtures. Figure 3-1 provides a flow chart of all modules.

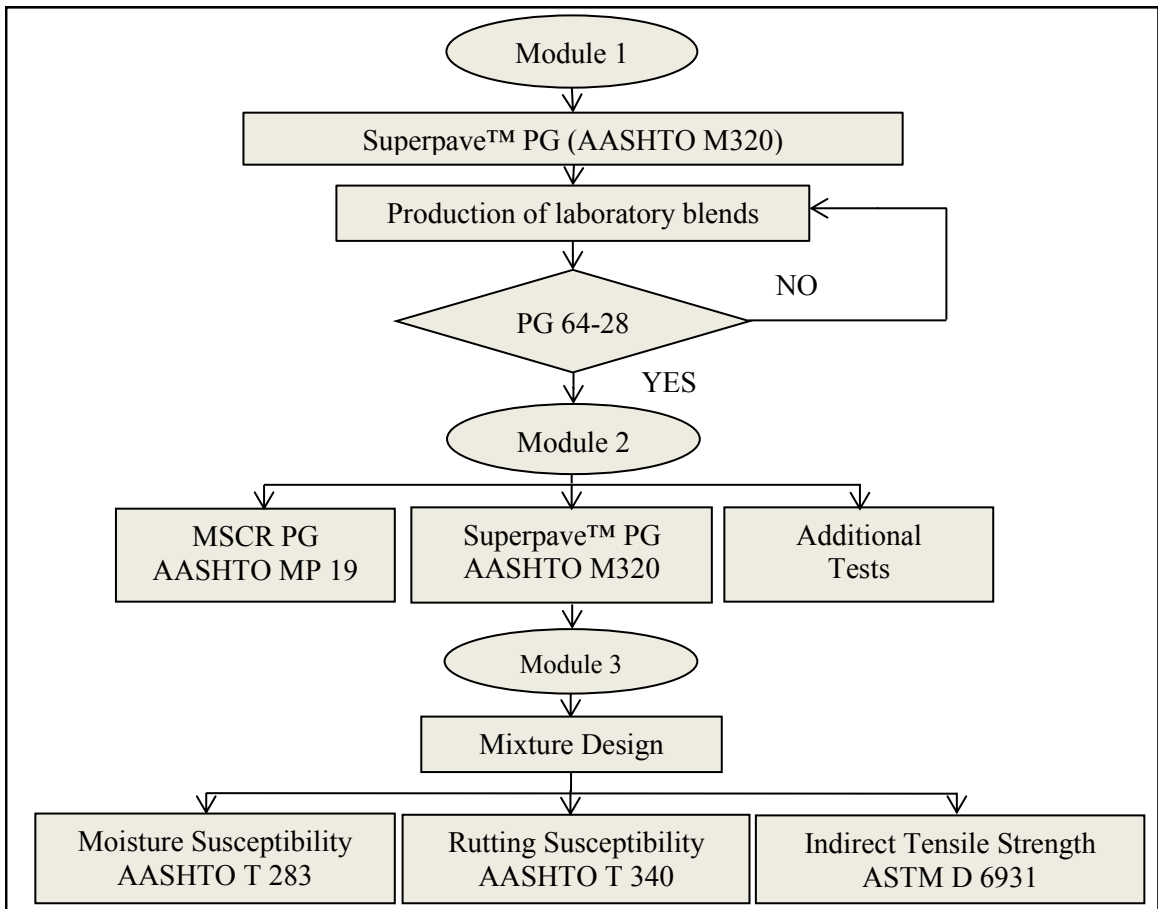


Figure 3-1 Experimental flow chart

3.1.Experimental Materials

3.1.1. Asphalt Binders

For modules 1 and 2, different modified binders were produced to exhibit performance grades similar to PG 64-28. All MBs for this module were produced following a consistent approach by using a single-source PG 58-28 base asphalt binder in combination with two types of modifiers, and two types of additives at different levels of control, as listed in Table 3-1. The recycled plastics were also co-blended with virgin SBS with and without usage of cross-linking agent to displace the amount used for the control binder.

Table 3-1 Material Control variables for Binders

Variable	Level	Description
Base Binder	1	PG 58-28
Control Binder	1	Virgin Styrene-Butadiene-Styrene (SBS)
Type of Recycled Plastic Modifier (RPM)	2	Recycled Low Density Poly-Ethylene (LDPE) Recycled Poly-Styrene (PS)
Additive A (Cross-Linking Agent)	2	With or without
Additive B (Aromatic Oil Softener)	2	With or without
Replication	2	In case of more than 5% deviation between replicates, a third replicate was required.

To achieve consistency in production of each binder, RPMs with similar particle size were used. The amount of modifiers/additives was determined based on the final weight of the binder. For each binder, modifiers and additives were added to the base asphalt binder at a constant rate. Modification was performed at a constant mixing intensity and temperature for all binders by means of mixing apparatus shown in Figure 3-2, which was used at GLC laboratory.

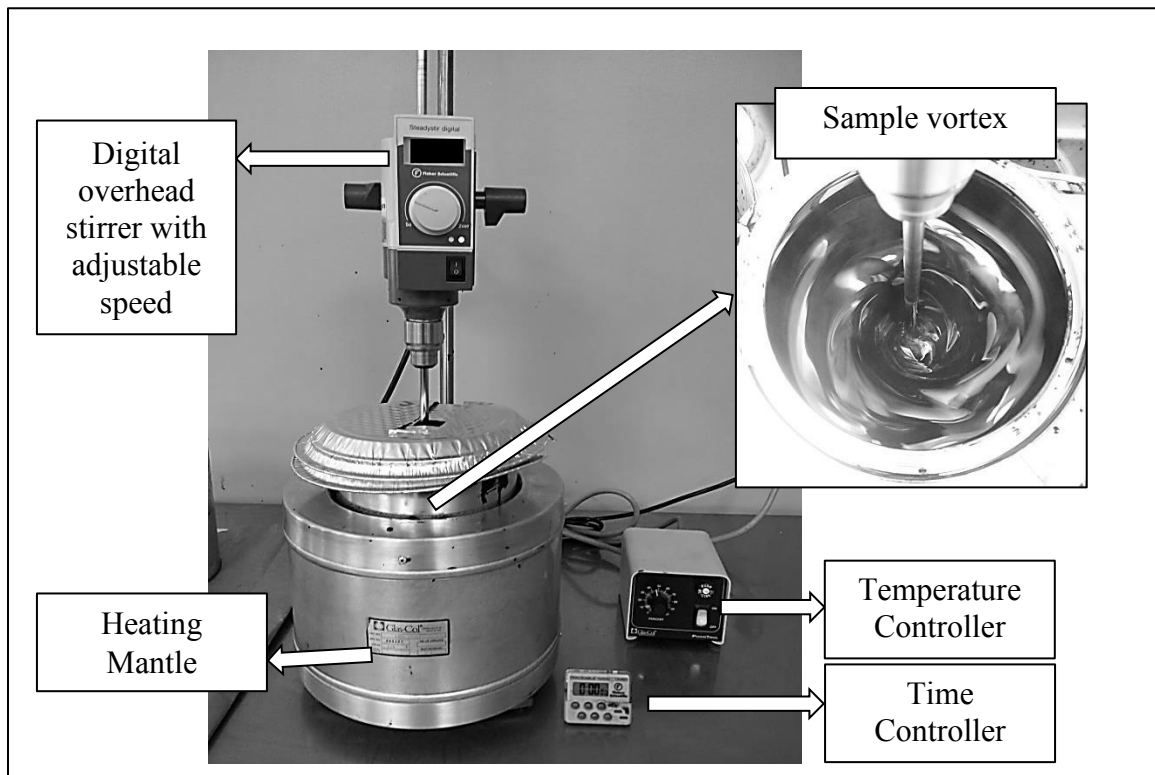


Figure 3-2 Mixing apparatus used to produce MBs

3.1.2. Aggregate Blend

The MBs produced and performance-graded from module 2 were used to prepare asphalt mixtures acceptable for surface course of pavements with high traffic volume. For this matter, a quality aggregate blend consisted of 14mm coarse aggregate, crusher fines (dirty, washed), and blend sand was design to meet physical requirements of C-HF mixture type (also known as “*high-friction surface mix*”) as per the highway design standards utilized by Nova Scotia Transportation Infrastructure Renewal [56]. Physical properties for the aggregate blend are listed in Table 3-2, while Figure 3-3 illustrates the blend gradation and a maximum density line.

In general, the maximum density line is used as a reference which provides the smallest possible volume of space among the aggregate particles [19]. However, a certain amount of asphalt binder is required in the mixture to fill such space, thus enhance the performance of mixture as well as workability of mixture (field placement and compaction). For this matter, the aggregate blend design was manipulated to vary

significantly from the maximum density curve, but still within specification range provided by NSTIR. The maximum density curve was estimated by using Equation 3-1.

$$\%PMD = 100 \times \left(\frac{d}{D}\right)^{0.45} \quad 3-1$$

where

$\%PMD$ = percent passing for maximum density gradation,
 d = Sieve size, mm, and
 D = maximum sieve size for gradation, mm.

A continuous maximum density gradation concept explained in Hot-Mix Asphalt (HMA) design manual prepared by NCHRP [19] was also used to better illustrate the deviation of the aggregate blend gradation from the maximum density gradation. For this matter, Equation 3-2 was used to calculate the continuous maximum density gradation, while Figure 3-4 illustrates the deviation of the blend from maximum density line.

$$P_{CMD}(d_2) = P(d_1) \times \left(\frac{d_2}{d_1}\right)^{0.45} \quad 3-2$$

where

$P_{CMD}(d_2)$ = percent passing, continuous maximum density gradation, for sieve size d_2
 d_1 = one sieve size larger than d_2 , and
 $P(d_1)$ = percent passing sieve d_1 .

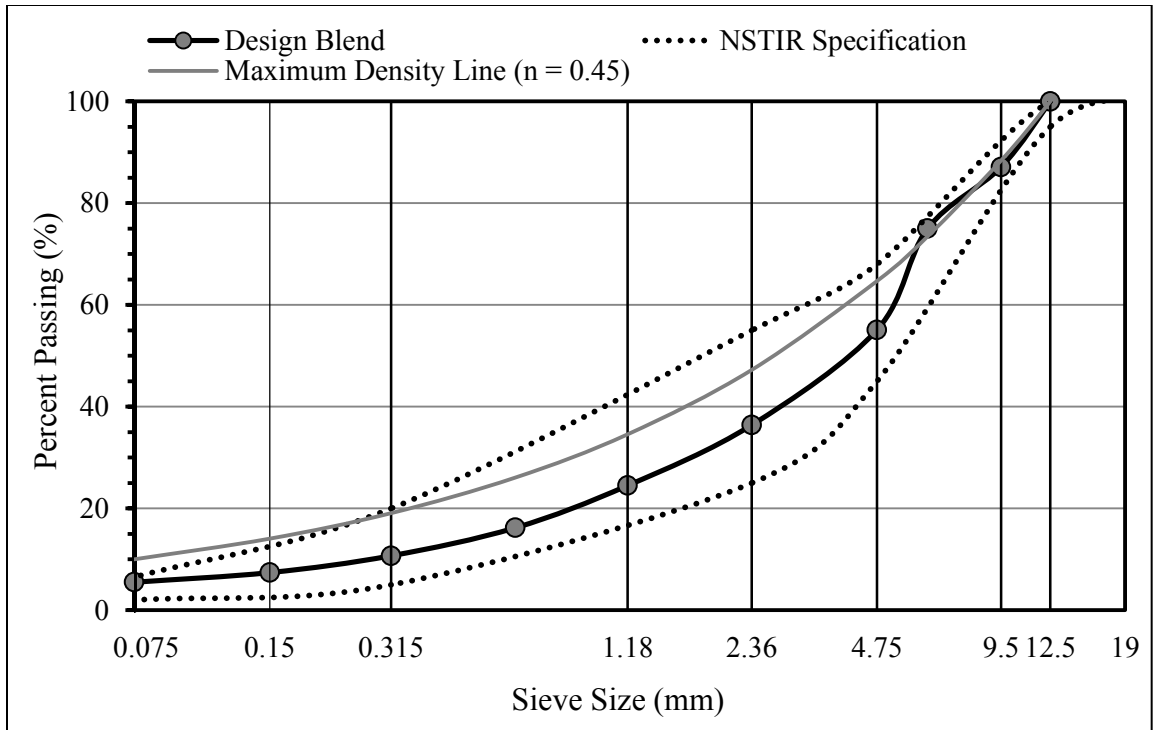


Figure 3-3 Aggregate blend gradation chart

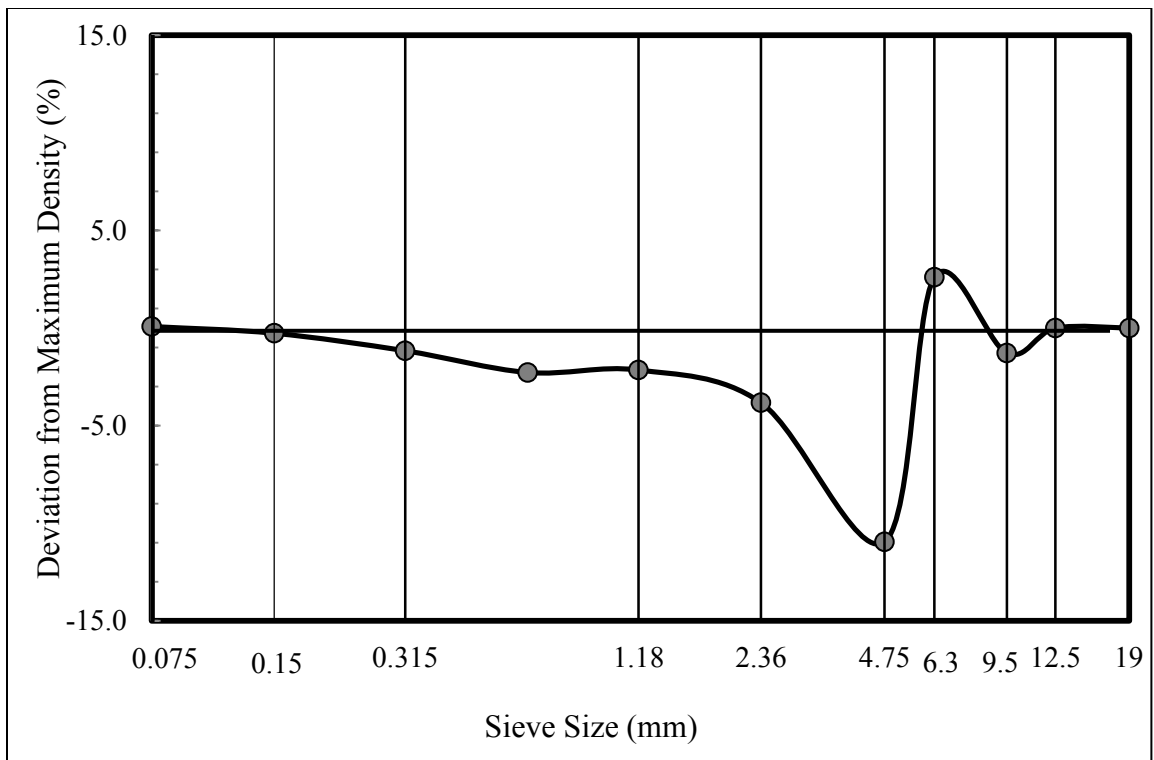


Figure 3-4 Aggregate blend gradation deviation from the continuous maximum density gradation

Table 3-2 Physical properties of aggregate blend

Property	Standard	Aggregate Source				NSTIR Specification
		Coarse	Fine			
		14mm	DCF ^a	WCF ^b	Blend Sand	
Percent Used		41	24	27	8	
Absorption (%)	ASTM C 127	0.47	0.97	0.80	0.93	Maximum 1.75
Soundness (%)	ASTM C88	0.80	3.20	3.50	1.90	Maximum 10
Micro Deval	DOT&PW TM-1 ^c	9.9	-	-	-	Maximum 20
Los Angeles Abrasion (%)	ASTM C 131	13.8	-	-	-	Maximum 30
Flat & Elongated Particles	ASTM D 4791	9.5	-	-	-	Maximum 10
Fractured Particles (%)	DOT&PW TM-1	100	-	-	-	Minimum 95
Sand Equivalent (%)	ASTM D 2419	-	65	96	73	Minimum 50
Fine Aggregate Angularity (%)	AASHTO TP 33	-	46.4	46.3	51.3	Minimum 45

^aDCF: Dirty Crusher Fine, ^bWCF: Washed Crusher Fine, and ^cDOT&PW TM-1: a procedure provided by Nova Scotia Department of Transportation and Public Works

3.2. Asphalt Binders Characterization

The Superpave™ and MSCR PG binder specification of AASHTO M320 and MP19 were used to characterize each binder through an array of rheological tests associated with the control of workability, rutting (permanent deformation), fatigue cracking, and thermal cracking at specific temperatures and aging conditions [25]. Figure 3-5 illustrates the way in which both Superpave™ and MSCR performance grading tests are used in combination with other additional tests.

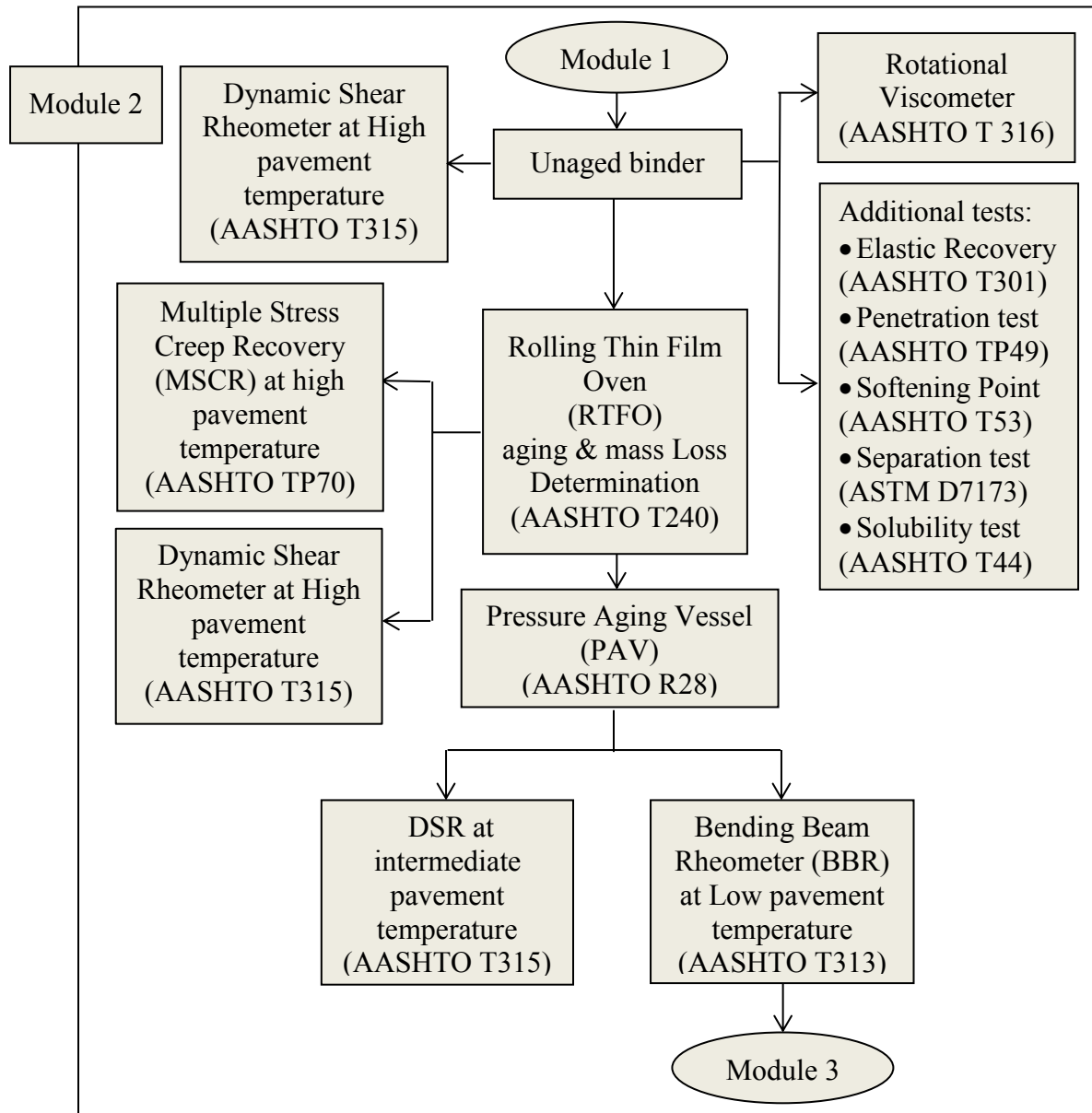


Figure 3-5 Modified binders characterization flow chart

3.2.1. Workability

To prepare ASTM viscosity-temperature plot [44] that can be used to determine mixing and compaction temperatures, a Rotational Viscometer (RV) at GLC laboratory was used to measure viscosity of binders in temperature range of 135 to 165°C in accordance with AASHTO T 316-11, “Viscosity Determination of Asphalt Binder Using Rotational Viscometer” [43]. The viscosity values at 135°C were also used to determine flow characteristics of binders at pumping and handling stage.

In this test method, a specific amount of asphalt binder is weighed into a preheated cylindrical sample chamber. The sample chamber is then placed in a preheated thermocontainer operating at testing temperature. A preheated cylindrical spindle is also immersed into the sample chamber creating thick layer of asphalt binder centered between the wall of the sample chamber and the spindle (Figure 3-6). After 30 minutes waiting for the testing temperature to stabilize in the sample chamber, the RV started to rotate the spindle at a prescribed rate of 20 rpm for 10 minutes. During this period with the spindle rotating, the RV measures and displays the torque required to maintain the rotational rate of 20 rpm. For this study, viscosity values at testing temperatures of 135, 150, and 165°C were evaluated.

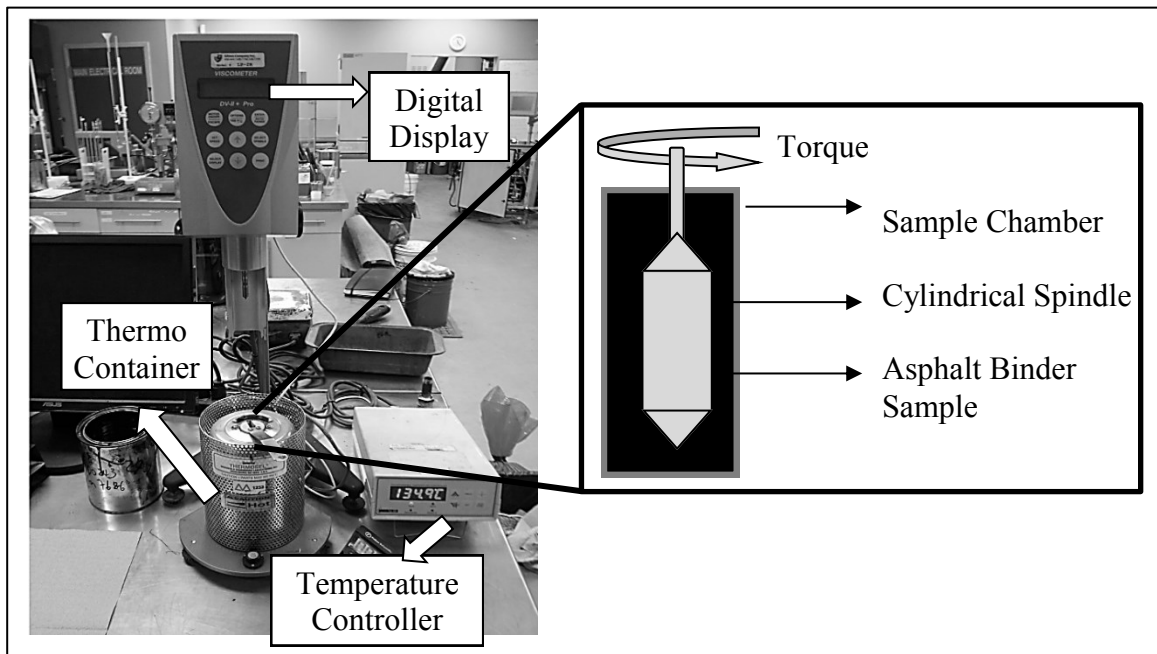


Figure 3-6 Rotational Viscometer, sample chamber and spindle

The procedures outlined in ASTM D 2493 were used to plot the logarithm of measured viscosity values versus the testing temperatures. Then, the mixing and compaction temperature ranges were determined related to viscosity of 0.17 ± 0.02 , and 0.28 ± 0.03 Pa.s respectively. The linearity of the resulting viscosity-temperature curve was verified for all MBs.

3.2.2. Aging

To simulate hardening (oxidative aging) that occurs during mixing at the hot-mix plant and construction as well as mass loss determination, a Rolling Thin-Film Oven (RTFO) at GLC laboratory was used in accordance with AASHTO T240-09, “Effect of Heat and Air on a Moving Film of Asphalt Binder (Rolling Thin-Film Oven Test) [41]. To further simulate long-term aging of asphalt binder in field, a Pressure-Aging Vessel (PAV) was also used in accordance with AASHTO R 28-12, “Accelerated Aging of Asphalt Binder Using a Pressurized Aging Vessel (PAV)” [42].

As per AASHTO T 240-09, a cylindrical glass bottle was filled with 35 ± 0.5 grams of asphalt binder. Immediately after filling, the bottle was turned to horizontal position, rotated for at least one full turn to pre-coat, and placed on the cooling rack. These steps were repeated for five more bottles. After 60 to 180 minutes of cooling, all bottles were placed horizontally in a vertically rotating frame (also called “carriage”). The frame rotates at speed of 15 ± 0.2 revolutions per minute causing the sample to flow along the walls of glass bottle. During each rotation, taking few seconds, air was blown once into each glass bottle. This action continued for 85 minutes in an oven with a constant operating temperature of 163°C . Bottles were then removed, and the aged asphalt sample was poured into thin cans for further rheological testing and long-term aging. RTFO aging of MBs was done at GLC laboratory by using a RTFO oven shown in Figure 3-7.

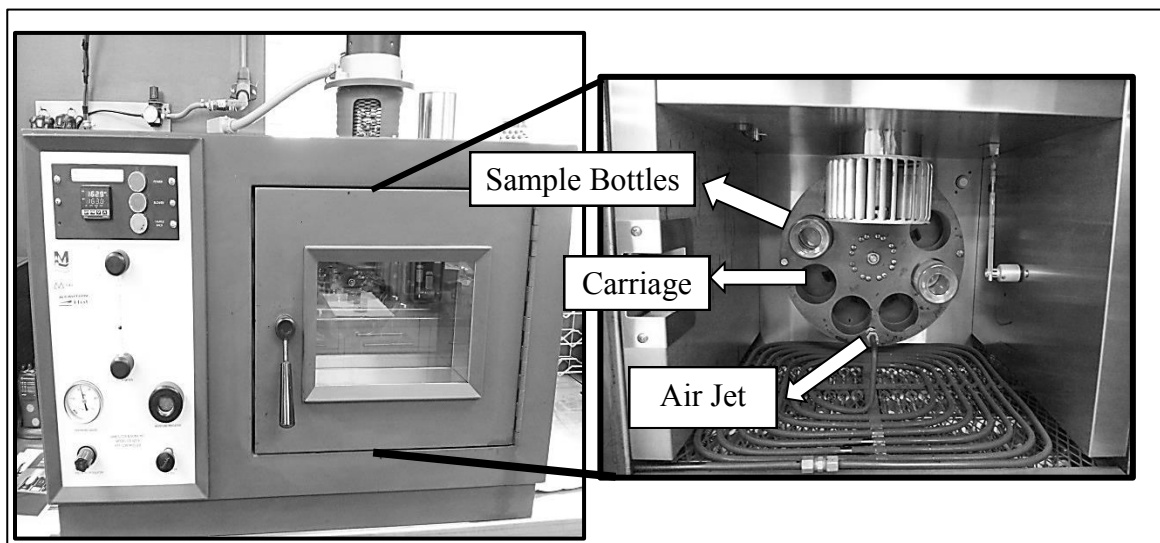


Figure 3-7 Rolling Thin-Film Oven (RTFO)

As part of the RTFO procedure, mass of volatiles loss from the asphalt binder can be determined. For this purpose, a minimum of two glass bottles were weighed to the nearest 0.001 grams before and after filling with the binder sample. After RTFO aging, bottles were cooled on the cooling rack and weighed again. Finally, mass loss was calculated by using Equation 3-3.

$$\text{Mass change} = 100 \times \left[\frac{A - B}{A} \right] \quad 3-3$$

where:

- A = (weight of bottle + binder before aging) – (weight of empty bottle), and
- B = (weight of bottle + binder after aging) – (weight of empty bottle)

To simulate long-term aging, a Pressure-Aging Vessel (PAV) at GLC laboratory was used. In this test method, residue collected from RTFO aging was poured on three stainless pans weighing 50 ± 0.5 grams each. The pans were placed vertically on a pan holder, which the pan was then placed in a sealed pressure vessel (Figure 3-8). The aging conditioning was then performed by 20 hours \pm 10 minutes of constant pressure of 2.10 MPa at conditioning temperature of 100 °C. The PAV test procedure does not produce a test result; it outlines details on how to produce residue, which can be used for additional rheology tests described in following sections.



Figure 3-8 Pressure Aging Vessel (PAV)

3.2.3. Permanent Deformation

To evaluate permanent deformation resistance of MBs, a Dynamic Shear Rheometer (DSR) was used to measure the $|G^*|/\sin(\delta)$ parameter in accordance with AASHTO T 315-12, “Determining the Rheological Properties of Asphalt Binder Using a Dynamic Shear Rheometer (DSR)” [46].

The $|G^*|/\sin(\delta)$ was measured at 10 rad/s and at the maximum pavement temperature of 64°C for both unaged binders and binders subjected to RTFO aging. Testing was done at GLC laboratory by using the DSR apparatus shown in Figure 3-9.

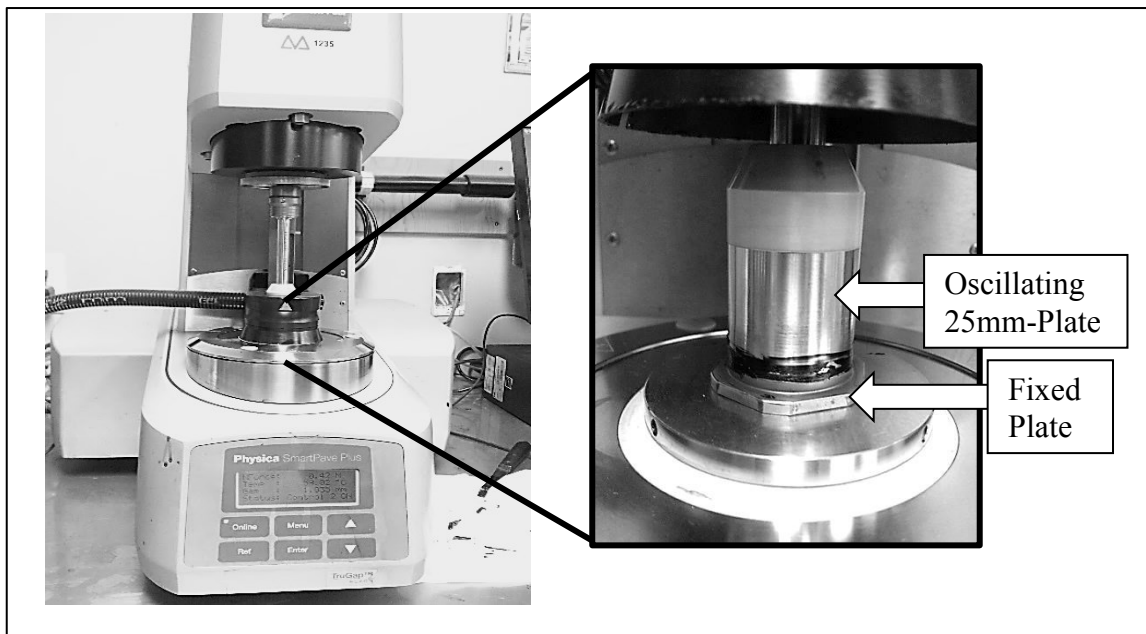


Figure 3-9 Dynamic Shear Rheometer (DSR)

In this test, a certain amount of sample is sandwiched between a fixed plate and an oscillating plate. The geometry of plates and thickness of sample between the two plates depend on the aged state. Unaged and RTFO aged binders are tested with 25 ± 0.05 mm diameter plates and sample thickness of 1 mm. When torque is applied, the oscillating plate traversed from points shown in Figure 3-10 to complete one cycle of oscillation. During the operation of DSR, the resulting strain is recorded and then used to determine the G^* and δ , as described in 2.4.1.2.

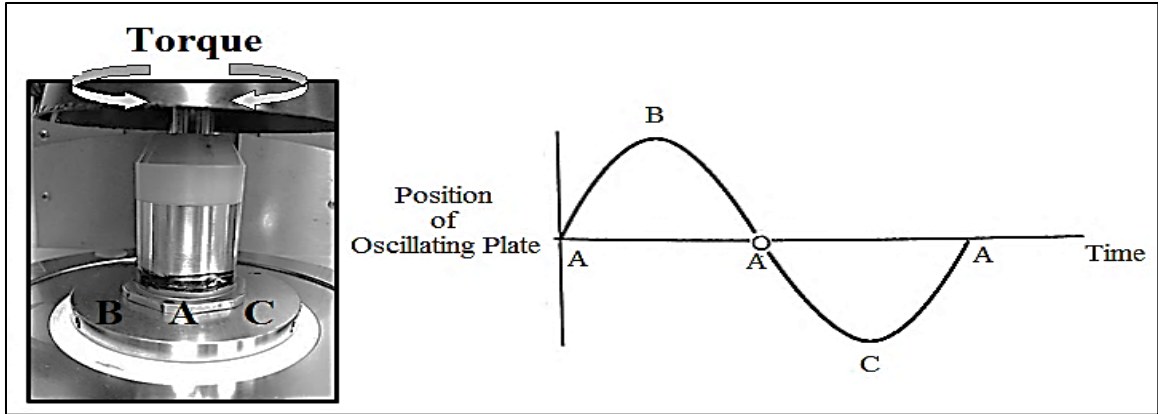


Figure 3-10 DSR cycle of oscillation

In addition to the $|G^*|/\sin(\delta)$ parameter, the DSR was again used to measure non-recoverable creep compliance (J_{nr}) and percentage of recovery (R%) in accordance with AASHTO TP 70-12, “The Multiple Stress Creep Recovery (MSCR) Test of Asphalt Binder Using a Dynamic Shear Rheometer (DSR)” [52].

The MSCR test uses the creep and recovery test concept, explained in chapter 2 of this thesis, to evaluate permanent deformation resistance of binders. For this test, by using the DSR, an RTFO aged binder was subjected to 10 cycles of 1-second creep load and subsequent 9-second recovery at two stress levels of 0.1 and 3.2 kPa. Figure 3-11 illustrates the response of a binder tested for this study under the MSCR test.

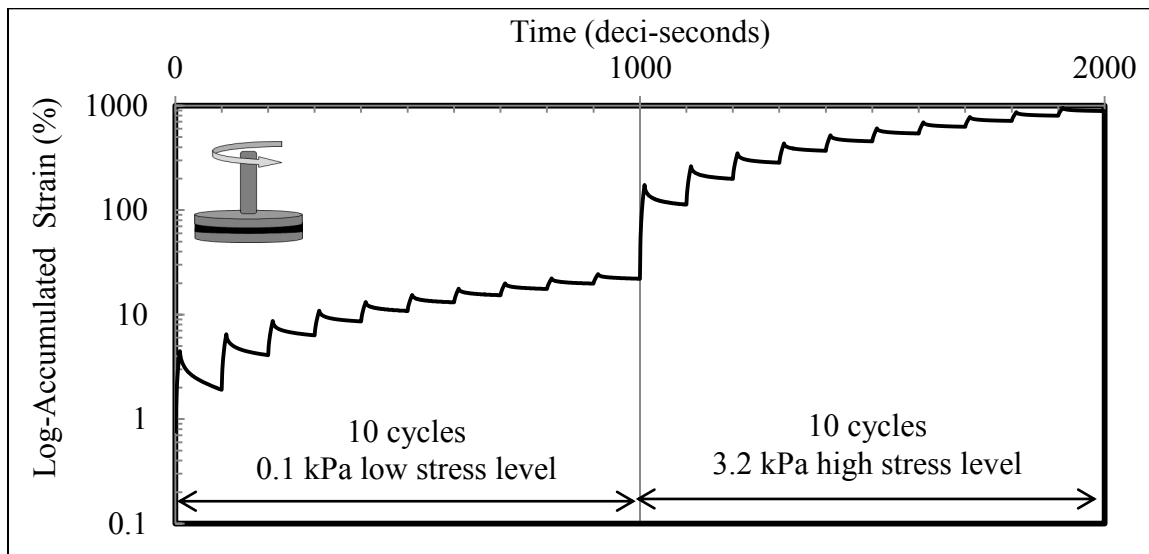


Figure 3-11 MSCR creep-recovery response

For this study, the J_{nr} and $R\%$ were measured at both environmental and bumped maximum pavement temperatures of 58, and 64°C for binders subjected to RTFO. Additionally, the J_{nr} values were used to performance grade binders as part of AASHTO MP 19-10, “Performance-Graded Asphalt Binder Using Multiple Stress Creep Recovery (MSCR) Test” [51].

3.2.4. Fatigue and Thermal Cracking

To evaluate fatigue resistance of MBs, the DSR was used to measure $|G^*|\sin(\delta)$ parameter at an intermediate pavement temperature of 22°C for PAV-aged binders in accordance with AASHTO T 315-12, “Determining the Rheological Properties of Asphalt Binder Using a Dynamic Shear Rheometer (DSR)” [46]. For this test, binders were tested with 8 ± 0.02 mm diameter plates and sample thickness of 2 mm.

The resistance to thermal cracking was evaluated by using a Bending Beam Rheometer (BBR) to measure the creep stiffness (S) and creep rate (m-value) at two low temperatures of -18 and -22°C for PAV-aged binder in accordance with AASHTO T313-12, “Determining the Flexural Creep Stiffness of Asphalt Binder Using the Bending Beam Rheometer (BBR)” [57]. Testing was done at GLC laboratory by using the BBR apparatus shown in Figure 3-13.

The BBR procedure outlines steps to prepare asphalt binder beam specimen measuring 125 mm in length, 6.35 mm in width, and 12.7 mm in height. Beam is formed by pouring heated PAV-aged residue into a rectangular aluminum mold assembly, as shown in Figure 3-12.

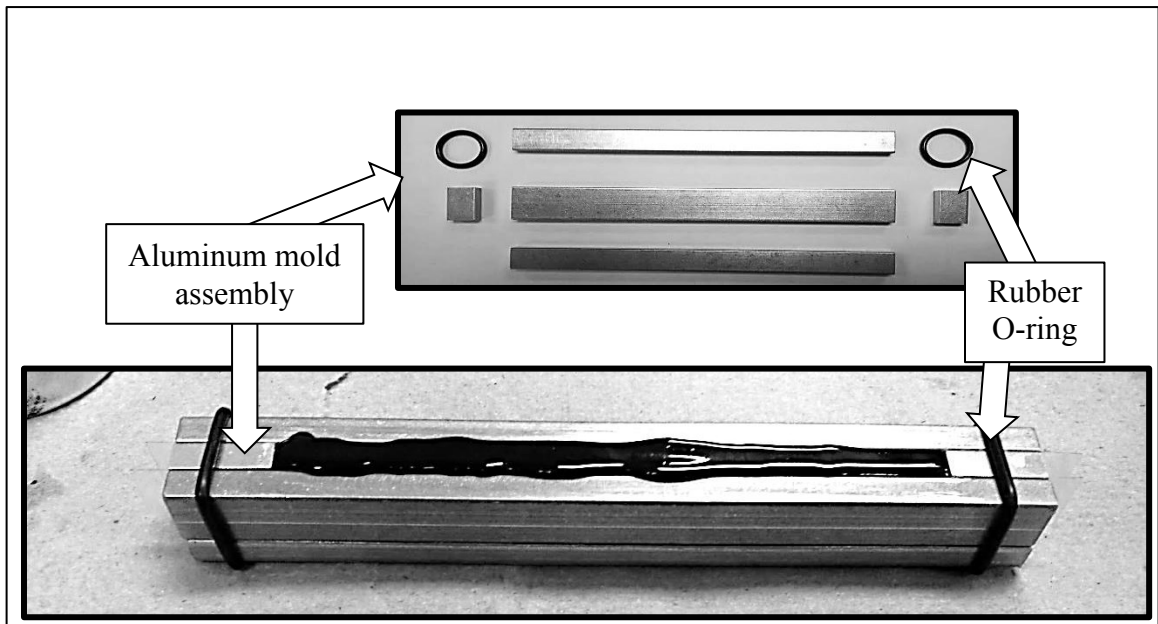


Figure 3-12 Bending Beam Rheometer (BBR) mold assembly

The mold was disassembled after cooling in a freezer for 5 to 10 minutes and the asphalt beam was transferred immediately to the BBR bath for conditioning at the test temperature for 60 ± 5 minutes. After conditioning in the bath, the asphalt beam was subjected to a constant creep load of 980 mN for 240 seconds at the testing temperature. During the test, load and beam deflection were continuously measured by the BBR software at 8, 15, 30, 60, 120, and 240 seconds. At the end of the test, two parameters of creep stiffness (S) and creep rate (m-value) were calculated automatically by the software. For the performance-grading purposes, S and m-value at 60 seconds are only reported.

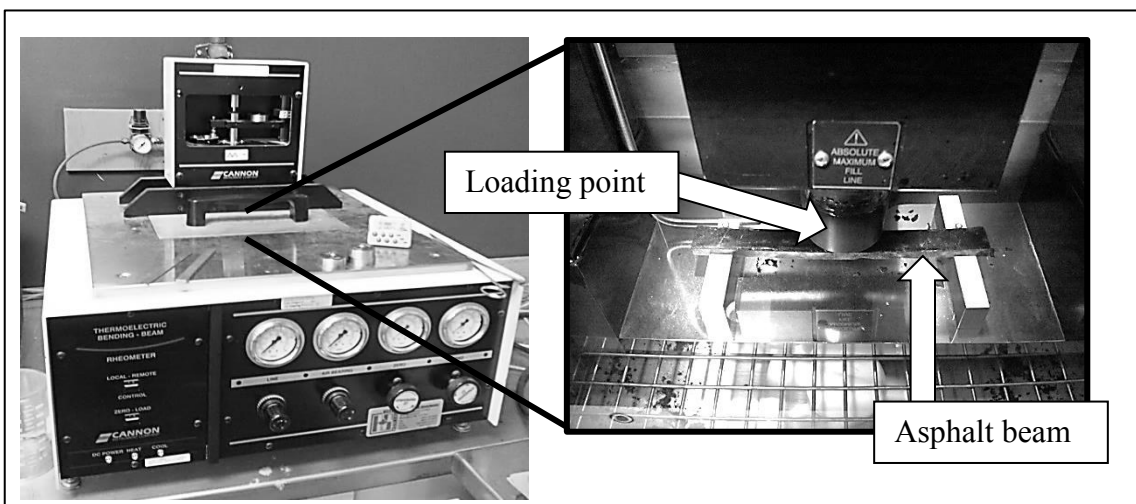


Figure 3-13 BBR apparatus

3.2.5. Additional Empirical Tests

For further characterization of MBs, additional empirical tests such as Elastic Recovery (ER), penetration, Ring-and-Ball (R&B) softening point, the separation, and solubility test were employed.

3.2.5.1. Elastic Recovery (ER):

The ER test is used by many transportation authorities, including NSTIR, to complement the PG grading system in identifying the presence of polymer and quality of blending. For this thesis, the ER test was performed on unaged binder at a temperature of 10°C in accordance with AASHTO T301-11, “Elastic Recovery Test of Asphalt Materials by Means of a Ductilometer” [58]. The ER test was performed at GLC laboratory.

To perform the ER test, a specimen is prepared by pouring heated unaged binder into brass assembly mold, as shown in Figure 3-14. After filling the mold with asphalt binder, the mold assembly goes through a conditioning process including 30 minutes cooling to room temperature, 30 minutes conditioning in the Ductilometer bath at the test temperature of $10 \pm 0.5^\circ\text{C}$, removing from the bath for trimming the asphalt binder flush with the mold surface, and 85 minutes conditioning in the Ductilometer bath. After the conditioning process, the ER test starts by removing side and base plates from mold assembly, mounting the specimen in the testing apparatus, and pulling the clips apart at the speed rate of 5 cm/min until 20 cm of elongation. After reaching 20 cm, the specimen is held in its elongated position for 5 minutes, severed at its center (10 cm) with a pair of scissors, and remained in the bath for another 60 minutes. Finally, after the end of 60 minutes, the half of the specimen is retracted until the ends of the severed sample just touch; marking a length reading which is used for Equation 3-4 to calculate percent Elastic Recovery (% ER).

$$\% ER = 100 \times \left[\frac{20 \text{ cm} - X}{20 \text{ cm}} \right] \quad 3-4$$

where:

X = final reading of length after retracting severed ends together, cm

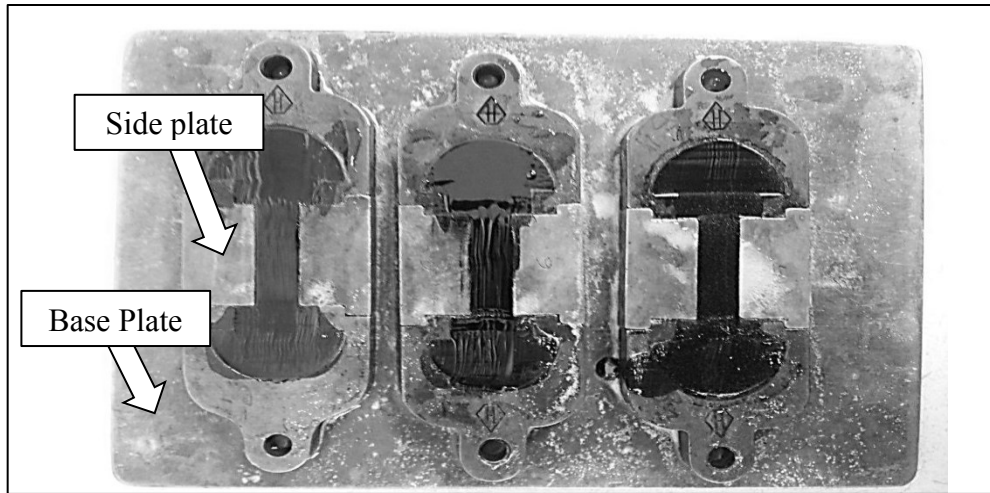


Figure 3-14 Filled and trimmed ER molds

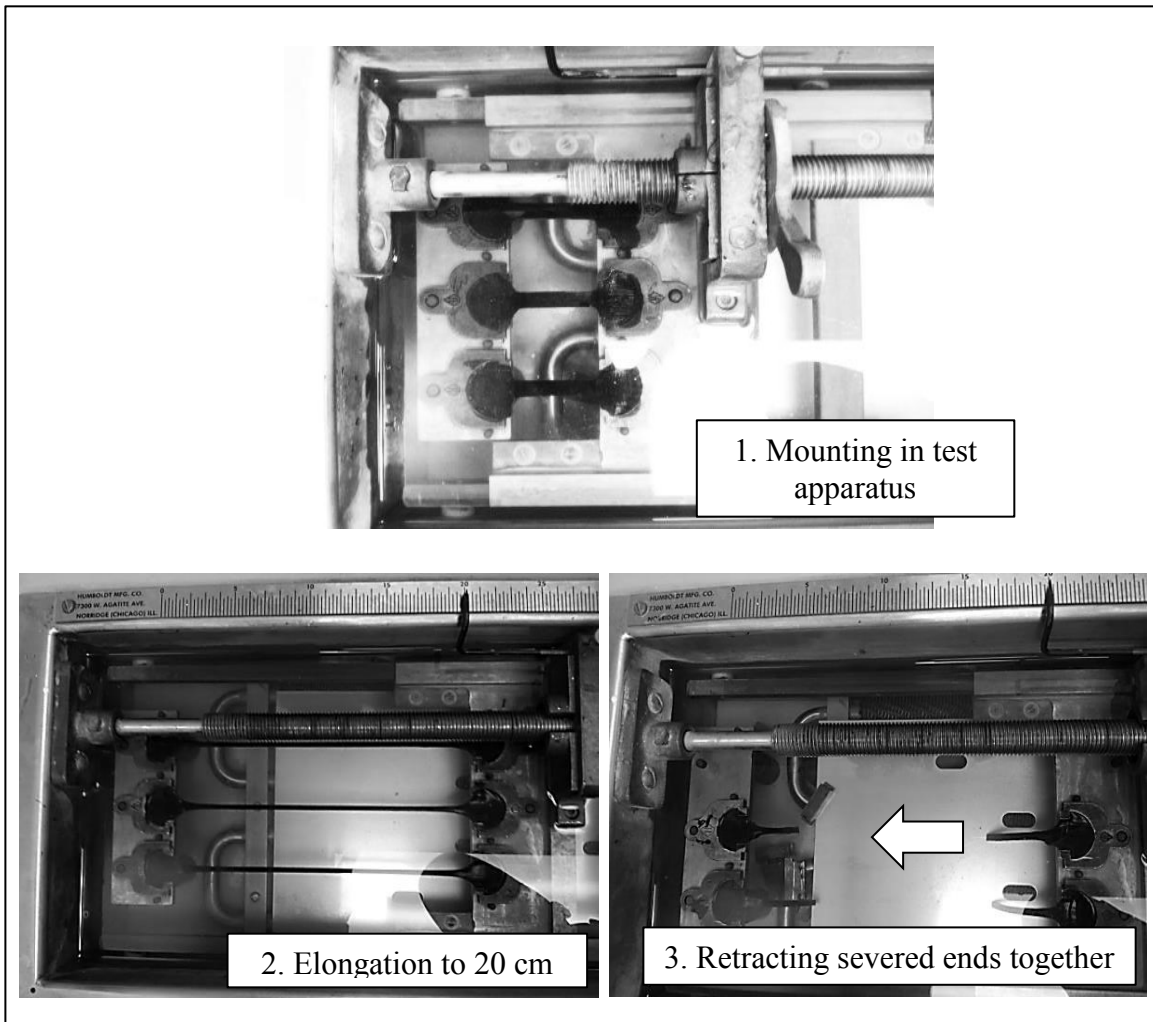


Figure 3-15 ER molds mounting, elongation and recovery

3.2.5.2. Penetration:

To evaluate the consistency of the MBs, the penetration test was performed on the unaged asphalt binder at a temperature of 25°C in accordance with AASHTO, “Standard Method of Test for Penetration of Bituminous Materials” [59]. To conduct the test, the heated asphalt binder is poured into a 3-ounce tin can, which then goes through a conditioning process of 60 minutes cooling to room temperature, and 60 minutes in a temperature-controlled water bath at the test temperature of $25 \pm 0.5^\circ\text{C}$.

After conditioning process, the sample container is placed under a needle of prescribed dimensions. The needle is loaded with 100 grams weight and is allowed to penetrate the asphalt sample for five seconds. After five seconds, the penetrated depth is measured in units of 0.1 mm (dmm) and is reported as penetration units. Figure 3-16 shows the penetration test apparatus used at GLC laboratory.

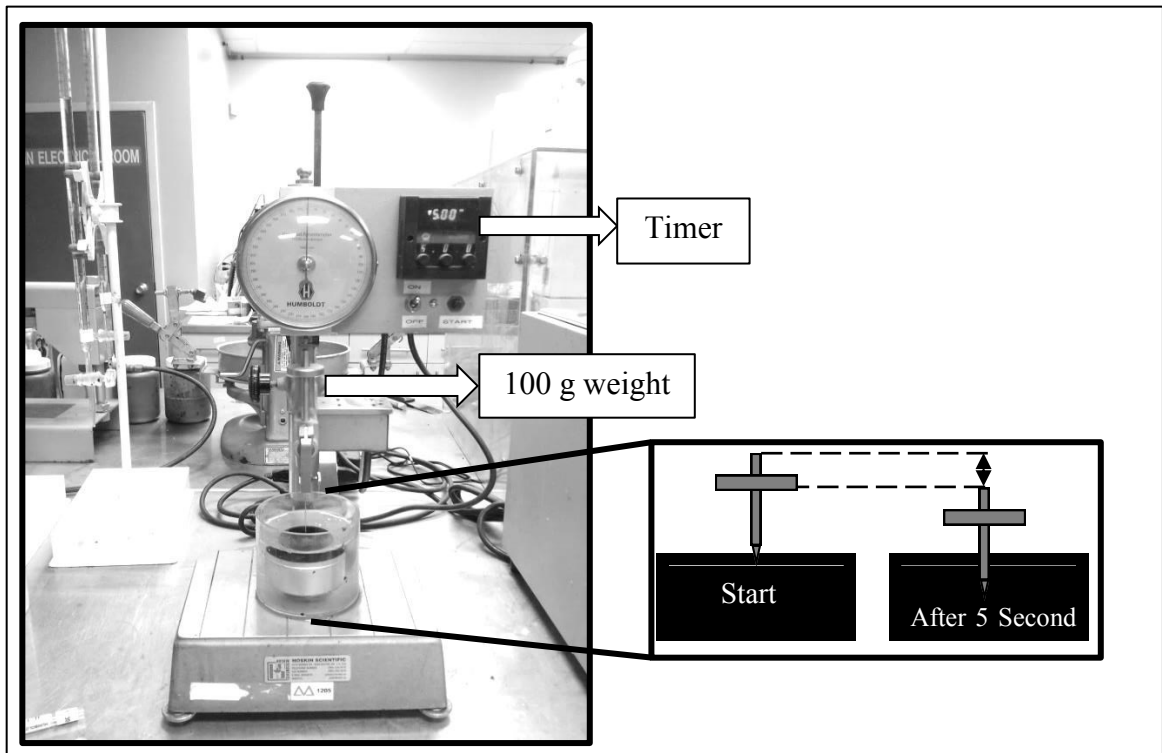


Figure 3-16 Penetration test apparatus

3.2.5.3. Separation test & Ring-and-Ball (R&B) softening point:

Separation of polymers from liquid asphalt in a storage tank under heated static conditions is a concern of asphalt producers and users. For this purpose, all MBs were assessed in accordance to the ASTM D 7173, “Standard Practice for Determining the Separation Tendency of Polymer from Polymer Modified Asphalt” [60]. As part of the separation test, the R&B softening point test was also used to evaluate the degree of separation. The R&B softening test was performed in accordance with the AASHTO T 53-09 “Softening Point of Bitumen (Ring-and-Ball Apparatus)” [61]

To perform separation test, an aluminum ointment tube (also known as “cigar tube”, Figure 3-17) measuring 25 mm in diameter and 140 mm in height is filled with 50 grams of unaged asphalt binder and stored at temperature of 163 ± 5 °C for two days in a vertical position. After storage, the tube is frozen at -10 ± 1 °C for minimum of four hours. Finally, the tube is removed and cut into three equal portions from which the top and bottom portions are used for measuring the softening points.



Figure 3-17 Separation tubes

Measuring the softening point of each binder was performed by pouring heated sample into brass rings. The rings were trimmed and placed on the assembly, while supporting a steel ball in the center. The assembly was then suspended in a beaker filled with water

which was heated at rate of 5 °C per minute. The heating continued until the binder in the rings soften enough to allow the steel balls sink for 25 mm. The temperature of water in the beaker was determined as the softening point of the binder. Figure 3-18 shows an apparatus used for this test at GLC laboratory.

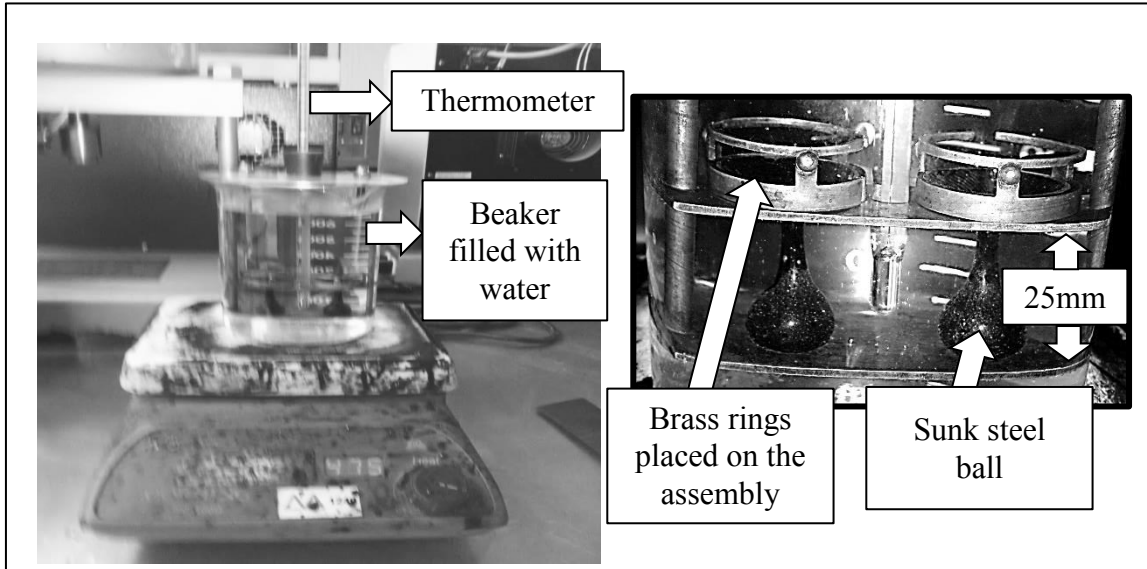


Figure 3-18 Ring and Ball (R&B) softening point test

Solubility test:

The solubility test was performed to measure the purity of modified binders by measuring the soluble portion of the binder in Trichloroethylene solvent in accordance with the AASHTO T 44, “Standard Method of Test for Solubility of Bituminous Materials” [62]

The solubility test was performed by dissolving 2 g of asphalt binder in 100 mL of Trichloroethylene solvent. The solution was then filtered through a filter paper placed in a porcelain crucible (also called “Gooch”) with holes in the bottom allowing solution to pass (Figure 3-19). After all solution was filter through, the solubility was calculated by using Equation 3-5:

$$\% \text{ soluble} = 100 \times \left(\frac{B - (C - A)}{B} \right) \tag{3-5}$$

where

- A = mass of crucible and filter (g),
- B = mass of sample, and
- C = mass of crucible, filter and insoluble material

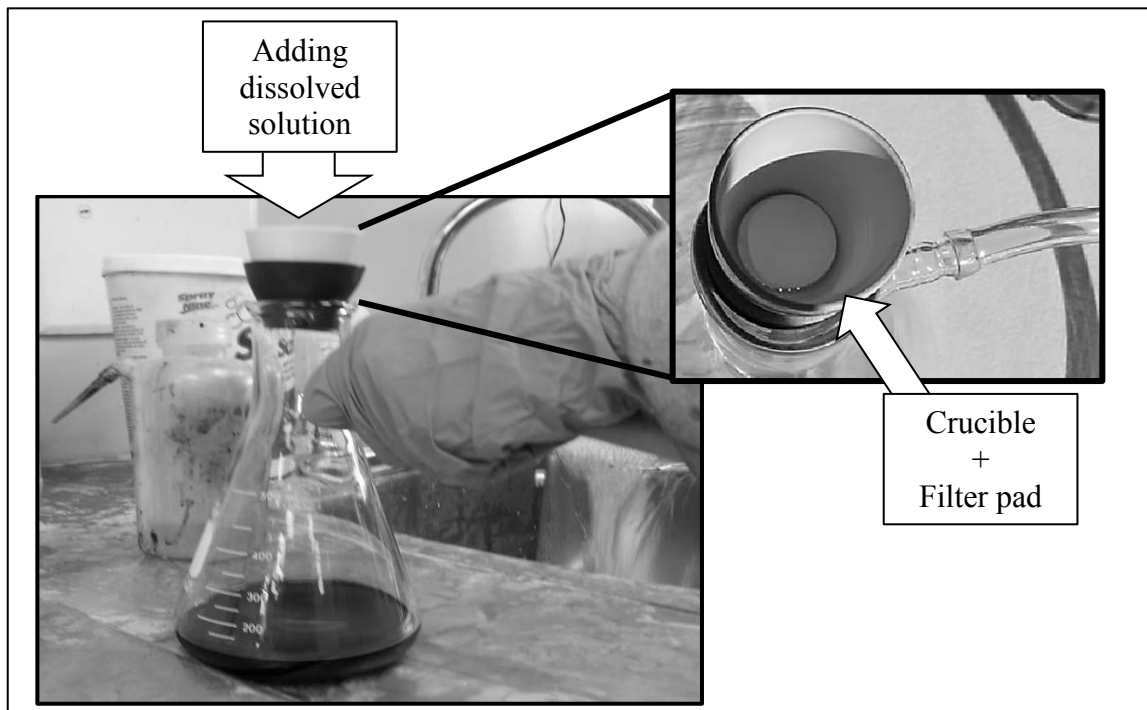


Figure 3-19 Solubility test

3.3.Mixture Design

Marshall method of mixture design was used to determine job-mix formula, which can be used for preparing Marshall size specimens for tests such as Indirect Tensile Strength (IDT) and moisture susceptibility Test. Additionally, a Superpave™ Gyratory Compactor (SGC) was used to produce relatively larger specimen compare to Marshall sized specimens, which can used for permanent deformation (rutting) evaluation. Figure 3-20 illustrates a flow chart used for design, production, and characterization of mixtures containing MBs.

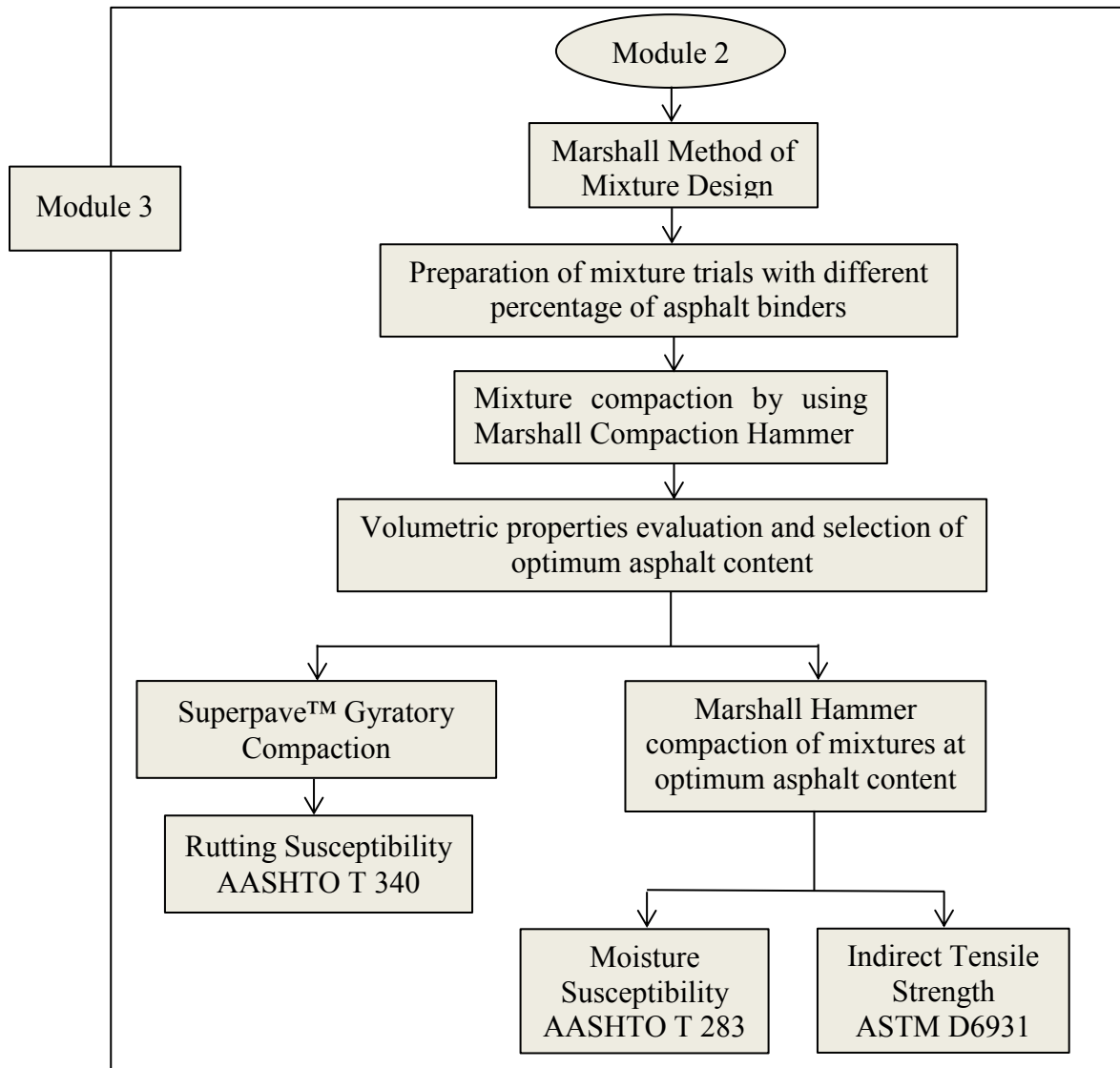


Figure 3-20 Mixture design and characterization flow chart

3.3.1. Mixture Volumetric Analysis

The volumetric proportions of asphalt binder and aggregate components affect asphalt mixtures performance and constructability [21]. To determine volumetric properties of a mixture, a three-phase system consisting of aggregate blend, asphalt binder, and air is most commonly used (Figure 3-21). Combinations of these properties with other properties, such as unit weight of mixture, are then used to select the optimum asphalt content based on mixture design procedure. For this study, Marshall method of mixture design was used, which is explained in more in details in section 3.3.2.

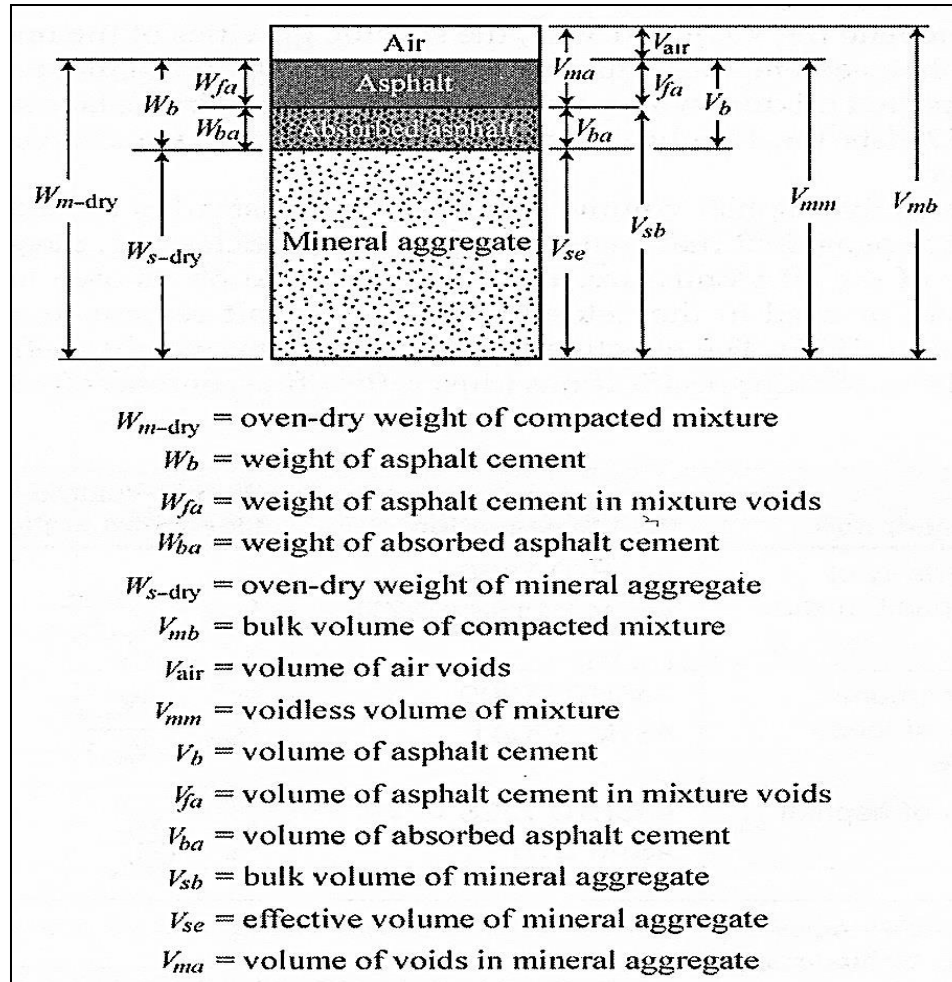


Figure 3-21 Volumetric properties of an asphalt mixture [20]

3.3.2. Marshall Method of Mixture Design

Marshall method of mixture design includes major steps such as: specimen preparation by using Marshall compactor, density and voids analysis, conducting Marshall stability and flow tests, analysis of data, and determination of optimum asphalt content. These steps are explained in following sections.

Step A: Preparation of Marshall Specimen

Marshall sized cylindrical specimens measuring 102 mm (4 in.) in diameter and approximately 64 mm (2.5 in.) in height were fabricated in accordance with ASTM D 6926-10, “Standard Practice for Preparation of Bituminous Specimens Using Marshall Apparatus” [63]. Figure 3-22 shows the Marshall apparatus used for this study.

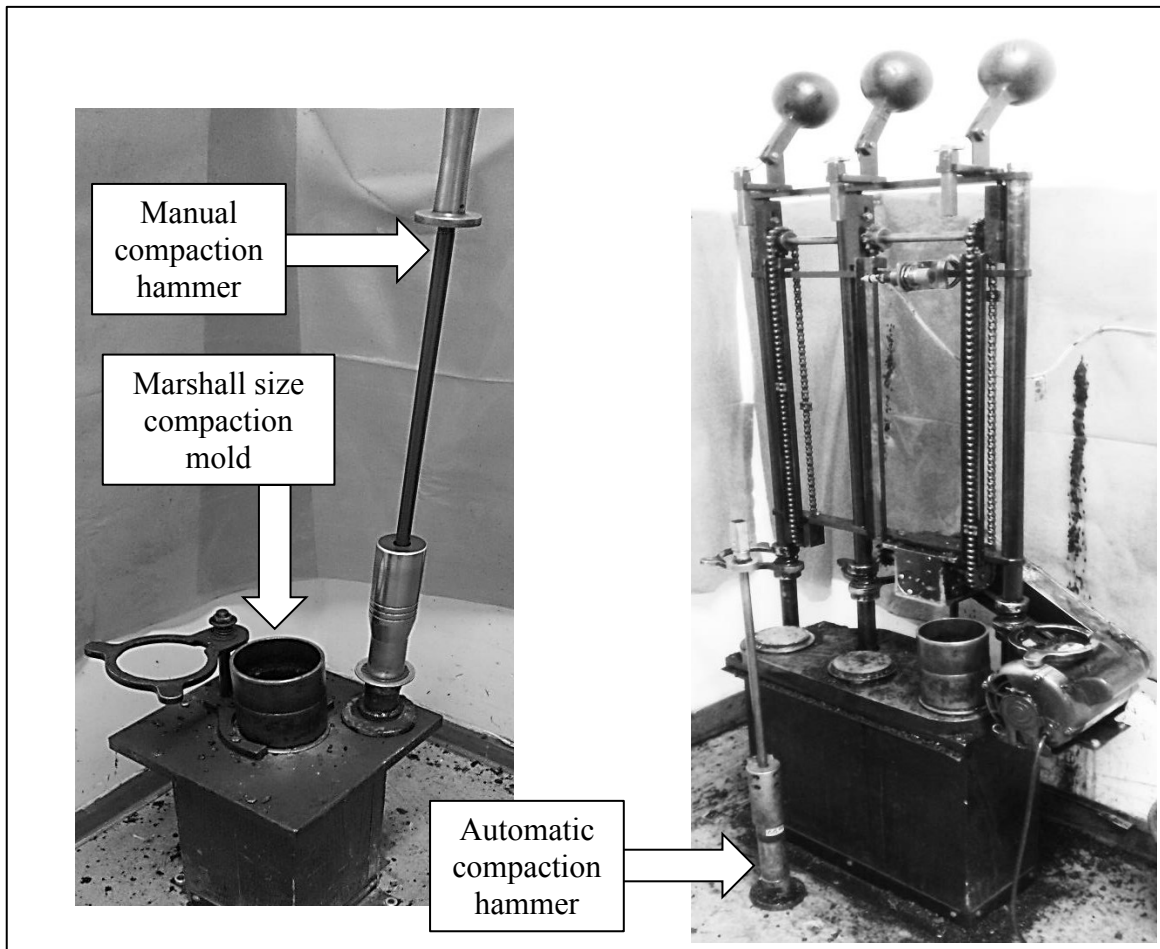


Figure 3-22 Marshall compaction apparatus

Five asphalt contents were used for this study range between 4.50 to 6.50 percent at 0.5 percent increments. The specimens were compacted at the compaction temperatures by 75 blows per side with a manual compaction hammer. After compaction, specimens were extracted from the compaction mold and allowed to cure at room temperature overnight before further testing.

Step B: Calculation of Density and Voids

Theoretical maximum specific gravity (G_{mm}) is an essential parameter in determining volumetric properties of a mixture such as air void and VMA. G_{mm} was determined by measuring the specific gravity of loose mixture after removal of the air entrapped in the mixture by using a vacuum saturation, as shown in Figure 3-23. Equation 3-6 was used

to determine G_{mm} values in accordance with AASHTO T 209-12, “Standard Method of Test for Theoretical Maximum Specific Gravity (G_{mm}) and Density of Hot Mix Asphalt (HMA)” [64].

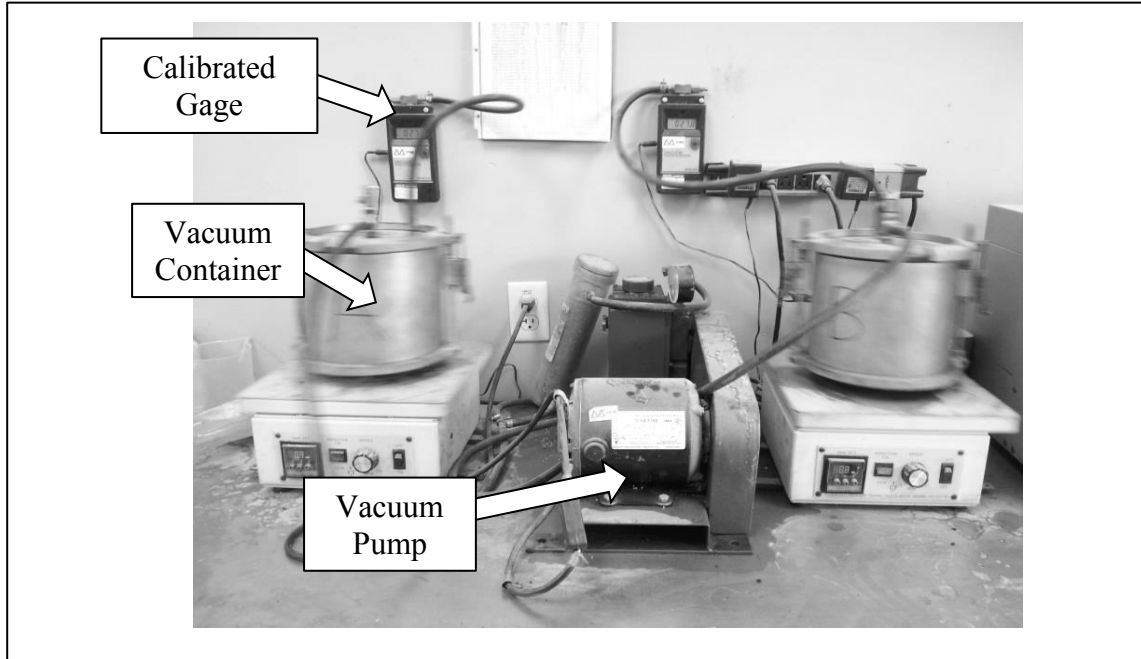


Figure 3-23 Vacuum apparatus for determination of G_{mm}

$$G_{mm} = \frac{A}{A + B - C} \quad 3-6$$

where:

- G_{mm} = theoretical maximum specific gravity of loose mixture
- A = mass of oven-dry specimen in air, g
- B = mass of container filled with water at 25°C, g, and
- C = mass of container with specimen filled with water at 25°C, g

Compacted bulk specific gravity (G_{mb}) refers the specific gravity of compacted specimen, which includes the volume of air voids within the specimen. Determination of G_{mb} was performed in accordance with AASHTO T 166-13. “Standard Method of Test for Bulk Specific Gravity (G_{mb}) of Compacted Hot Mix Asphalt (HMA) Using Saturated Surface-Dry Specimens” [65]. G_{mb} is calculated by using Equation 3-7. Figure 3-24 shows an apparatus employed to weight compacted specimen in water.

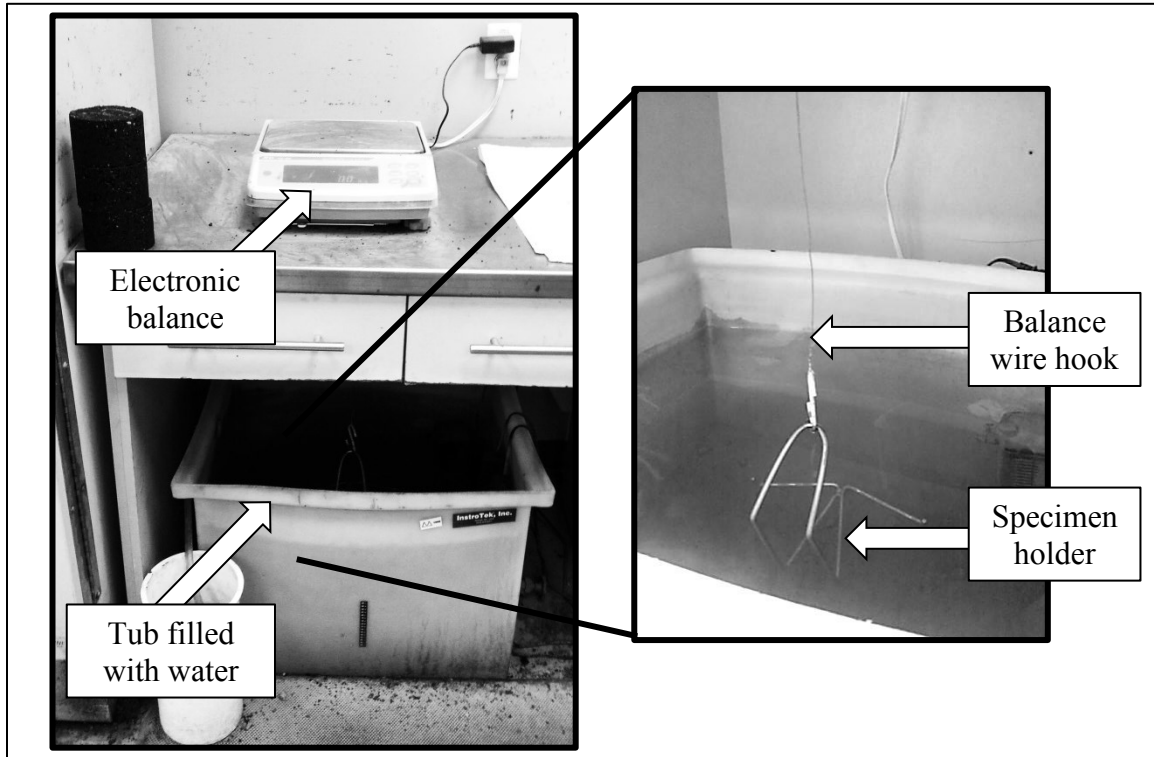


Figure 3-24 Apparatus used to determine weight of compacted specimen in water

$$G_{mb} = \frac{A}{D - E} \quad 3-7$$

where:

- G_{mb} = bulk specific gravity of compacted specimen
- A = mass of dry specimen in air, g
- D = mass of the saturated surface-dry specimen in air, g, and
- E = mass of the specimen in water at 25°C, g

To calculate other required volumetric properties of compacted specimens, following equations were used:

$$VTM = 100 \left(1 - \frac{G_{mb}}{G_{mm}} \right) \quad 3-8$$

where:

- VTM = air voids in compacted mixture, %
- G_{mb} = bulk specific gravity of compacted specimen and
- G_{mm} = theoretical maximum specific gravity of loose mixture

$$VMA = 100 \left[1 - \frac{G_{mb}(1 - P_b)}{G_{sb}} \right] \quad 3-9$$

where:

VMA = volume of voids in mineral aggregate, % and
 G_{sb} = bulk specific gravity of the compacted mix, and
 P_b = the asphalt content by weight of total mix, %

$$VFA = 100 \left(\frac{VMA - VTM}{VMA} \right) \quad 3-10$$

where:

VFA = voids filled with asphalt, (%)

Step C: Marshall Stability and Flow Test

As part of the Marshall method, resistance of compacted specimen to plastic flow was measured using of Marshall Stability-Flow apparatus in accordance with ASTM D 6927-06, “Standard Test Method for Marshall Stability and Flow of Bituminous Mixtures” [66]. Figure 3-25 shows a Marshall Stability-Flow tester located at GLC laboratory, which was used for this study. As shown, each specimen was loaded in compression by means of a testing head (also called “breaking head”) at the loading rate of 50 ± 5 mm/min. Prior to loading, specimens were conditioned at $60 \pm 1^\circ\text{C}$ in a water bath for 30 to 40 minutes.

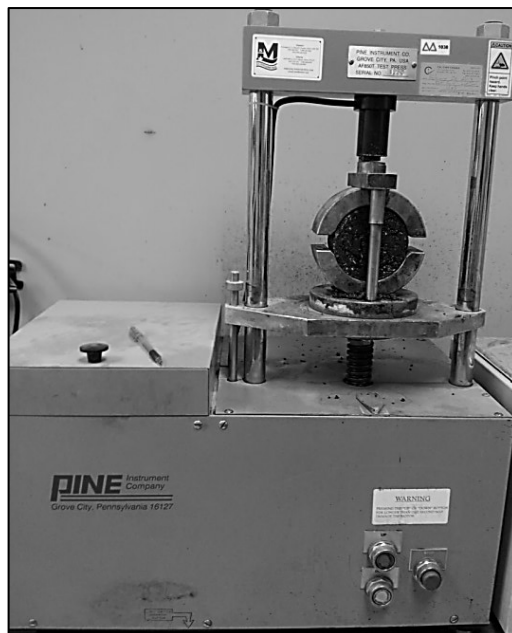


Figure 3-25 Marshall Stability-Flow tester

From this test, two values were measured. First, Marshall stability which was recorded as the peak resistance load obtained during constant loading. Secondly, Marshall flow which was recorded as vertical deformation of specimen during the peak resistance load. These two values were then used for further analysis.

Step D: Tabulating and Plotting Test Results

For this step, results of pervious steps were used to prepare plots of:

- asphalt content versus air voids (or VTM),
- asphalt content versus VMA,
- asphalt content versus VFA,
- asphalt content versus G_{mb} ,
- asphalt content versus Marshall stability, and
- asphalt content versus Marshall flow

Step E: Optimum Asphalt Content Determination

Two methods are commonly used to determine the optimum asphalt content: NAPA procedure [67], and Asphalt Institute (A.I) method in MS-2 [21]. For this study, A.I method was used as per NSTIR requirements by performing following steps:

- 1) asphalt content at maximum Marshall stability,
- 2) asphalt content at maximum density,
- 3) asphalt content at mid-point of specified air void range,
- 4) average the three asphalt contents obtained through steps 1 to 3,
- 5) for the average asphalt content obtained from step 4, determination of following properties based on step D plots and curves: stability, flow, air voids, and VMA
- 6) comparison of step 5 results with respect to NSTIR specification.

3.3.3. Superpave™ Gyratory Compactor

The Superpave™ Gyratory Compactor (SGC) was used to fabricate compacted specimens, which can be tested for the rutting susceptibility. The Gyratory sized specimens measuring 152 mm in diameter and approximately 115mm in height were compacted with SGC at pressure of 600 kPa in accordance with AASHTO PP 060-13, “Standard Practice for Preparation of Cylindrical Performance Test Specimens Using the

Superpave Gyratory Compactor (SGC)” [68]. Figure 3-26 shows the SGC apparatus used at GLC laboratory.

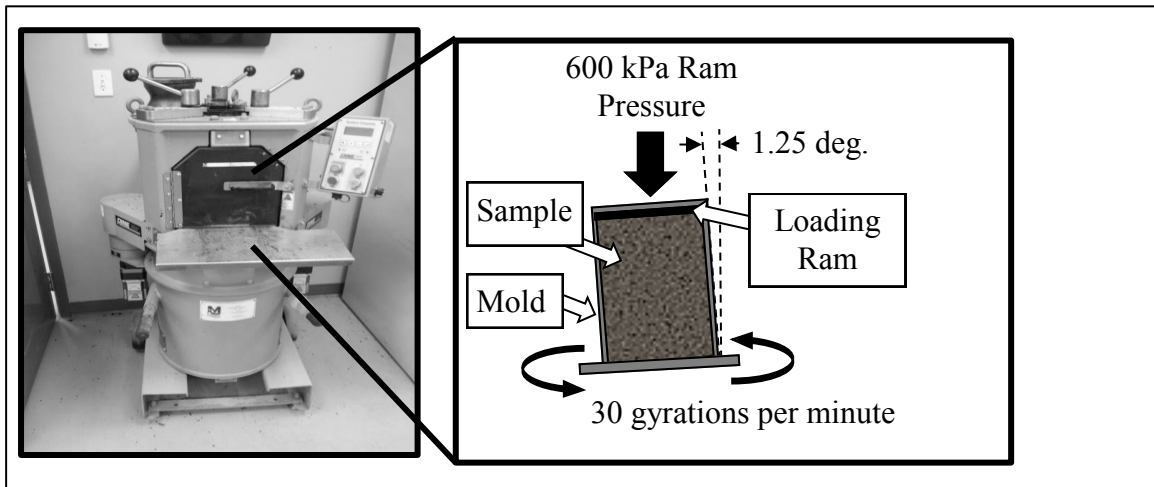


Figure 3-26 Superpave™ Gyratory Compactor

The SGC is capable of recording the position of the loading ram as well as specimen height throughout the compaction. This measurement was used to achieve a target air void of 7 percent for each specimen. In order to do so, a trial specimen for each mixture was compacted to 100 gyrations (N_{100}). Volumetric properties such as G_{mb} , and G_{mm} were then calculated for this specimen. Finally, a plot of percent air void versus number of gyrations was developed for each mixture by using Equation 3-11 and 3-12. Figure 3-27 shows an example of a plot constructed for a mixture tested for this study.

$$G_{mb@Nx} = \frac{h_{@N100} \times G_{mb@N100}}{h_{@Nx}} \quad 3-11$$

where

- $G_{mb@Nx}$ = estimated bulk specific gravity of compacted specimen at x gyrations
- $G_{mb@N100}$ = bulk specific gravity of compacted trial specimen at 100 gyrations
- $h_{@N100}$ = final height of trial specimen compacted at 100 gyrations, mm
- $h_{@Nx}$ = height of specimen throughout the compaction at x gyrations, mm

$$VTM_x = 100 \left(1 - \frac{G_{mb@Nx}}{G_{mm}} \right) \quad 3-12$$

where

- VTM_x = estimated air voids in compacted mixture at x gyrations, %
- G_{mm} = theoretical maximum specific gravity of loose trial mixture

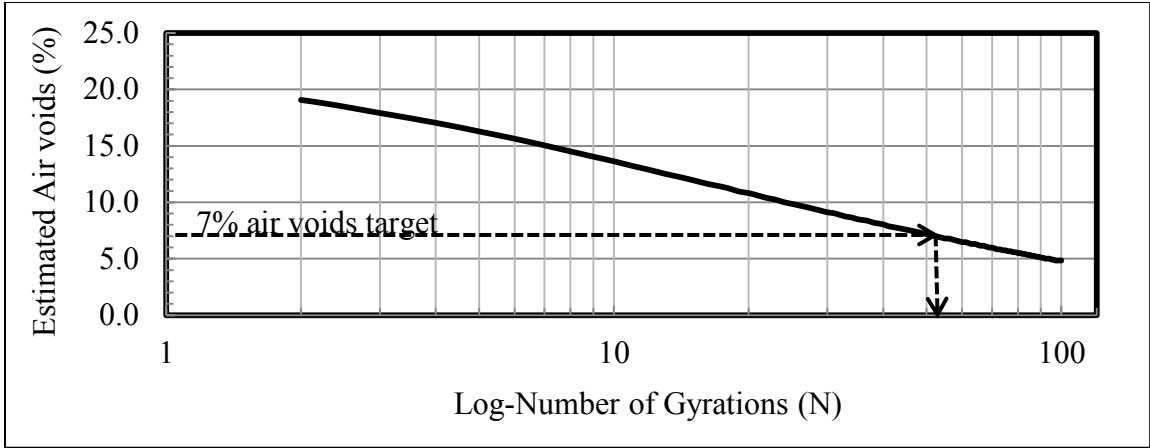


Figure 3-27 A sample plot of SGC trial specimen compaction characteristic

3.4. Asphalt mixture characterization

3.4.1. Rutting Susceptibility

For evaluating the rutting susceptibility of HMA mixtures, the Asphalt Pavement Analyzer (APA) was used to test Superpave™ gyratory compacted specimens at the high temperature of 64°C in accordance with AASHTO T 340-10, “Standard Method of Test for Determining the Rutting Susceptibility of Hot Mix Asphalt Using the Asphalt Pavement Analyzer (APA)” [69]. For this test, Superpave™ gyratory specimens were trimmed to height of approximately 75 mm. The trimmed specimens were then placed in the APA to condition for 6 hours at the test temperature of 64 ± 1 °C, as shown in Figure 3-28. After conditioning, testing started by applying a wheel load of 445 ± 22 N on the hose pressurized at 690 ± 35 kPa.

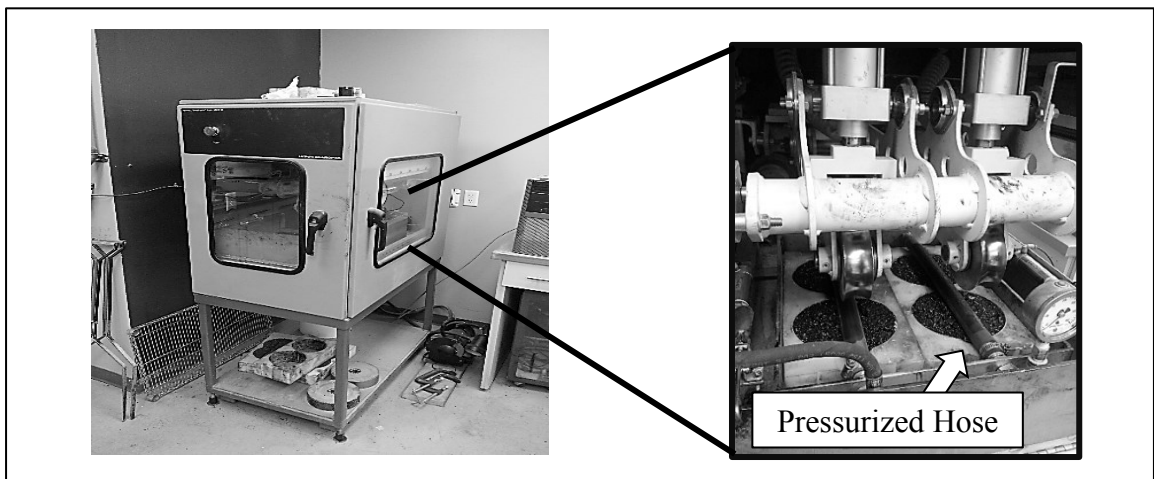


Figure 3-28 The APA test apparatus

The loading continued for 8,000 cycles. For each mixture, two replicates were tested simultaneously, with one in front of the other. Figure 3-29 shows a sample rut curve over course of loading cycles for a mixture tested for this study. The APA testing was performed at GLC laboratory.

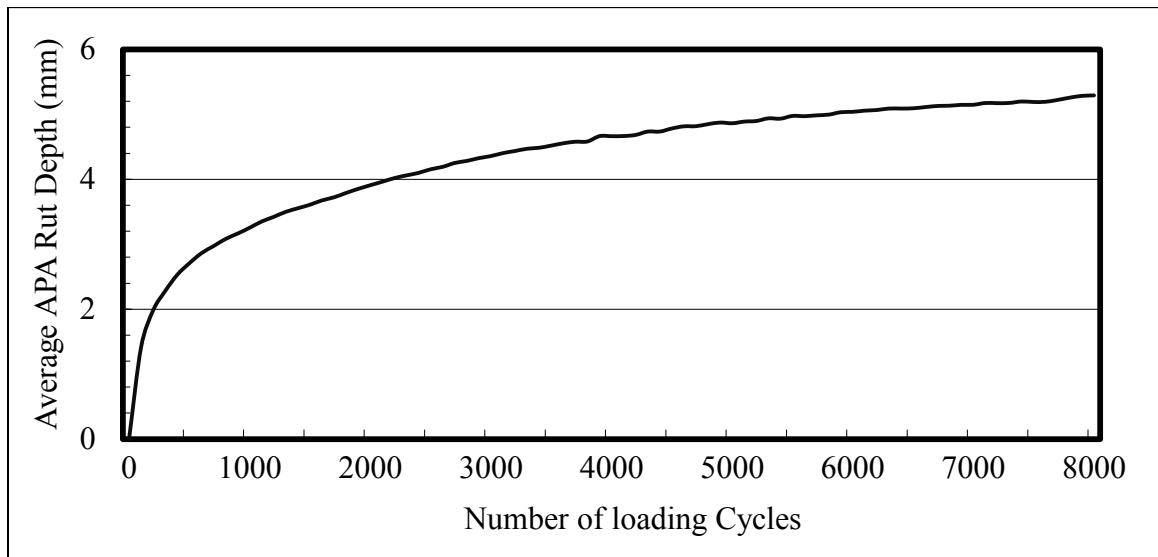


Figure 3-29 A sample the APA test result

3.4.2. Tensile Strength

The Indirect Tensile Strength (IDT) test was used to evaluate tensile strength of modified mixtures in accordance with ASTM D6931-12, “Standard Test Method for Indirect Tensile Strength of Bituminous Mixtures” [70]. For this test, three Marshall sized specimens were prepared as per job-mix formula for each mixture measuring 102 mm in diameter and approximately 51 mm in thickness. Samples were tested at an ambient temperature of 25°C for evaluation of resistance to cracking at intermediate pavement temperature.

Specimens were first conditioned in a water bath for 30 minutes at temperature of 25°C. Once conditioned, specimens were loaded in compression at the rate of 50 mm/min until the maximum load was reached. The IDT was then calculated by using Equation 3-13. Testing was performed at GLC laboratory on the testing apparatus shown in Figure 3-30.

$$S_t = \frac{2000P}{\pi tD}$$

3-13

where:

- S_t = IDT strength, kPa
- P = maximum load, N
- t = sample thickness immediately before test, mm
- D = sample diameter, mm
- π = 3.14

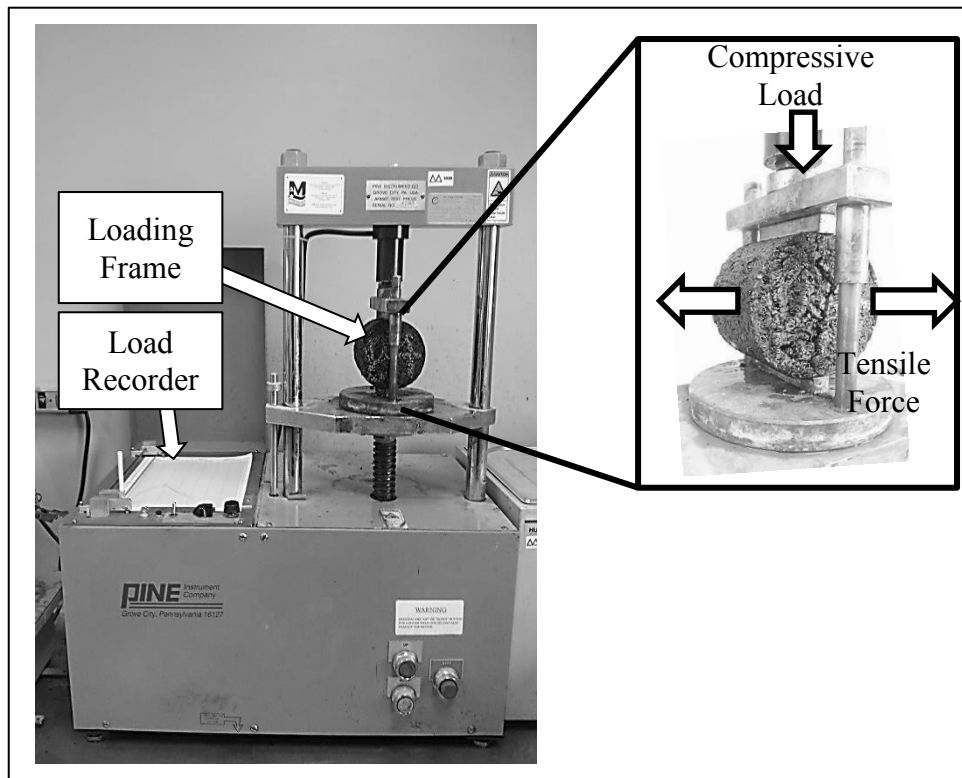


Figure 3-30 IDT test apparatus and load configuration

3.4.3. Moisture Susceptibility

To evaluate resistance of compacted samples to moisture-induced damage, the IDT test apparatus were used in accordance with AASHTO T 283-11, “Standard Method of Test for Resistance of Compacted Hot Mix Asphalt (HMA) to Moisture-Induced Damage” [71]. This test method is usually referred to as “Modified Lottman Test”.

For each mixture, at least ten Marshall size specimens were compacted to an air void target of 7.0 ± 0.5 percent in accordance with ASTM D 6926-10 [63]. Specimens were then cured to room temperature for 24 ± 3 hours. After curing, following tests and measurements were performed for each specimen:

- Theoretical maximum specific gravity (G_{mm}) – AASHTO T 209;
- Thickness (t) and diameter (D) – ASTM D 3549;
- Bulk specific gravity of compacted specimen (G_{mb}) – AASHTO T 166; and
- The percent air voids– AASHTO T 269

Specimens were then separated into two subsets, of at least three specimens each, so that average air voids of two subsets were approximately equal. One subset was tested dry, while other subset was conditioned before testing. Conditioning included vacuuming to saturation range of 70 to 80 percent, a freezing cycle, and a thaw cycle in warm-water. Figure 3-31 illustrates more details of conditioning cycles used for this study.

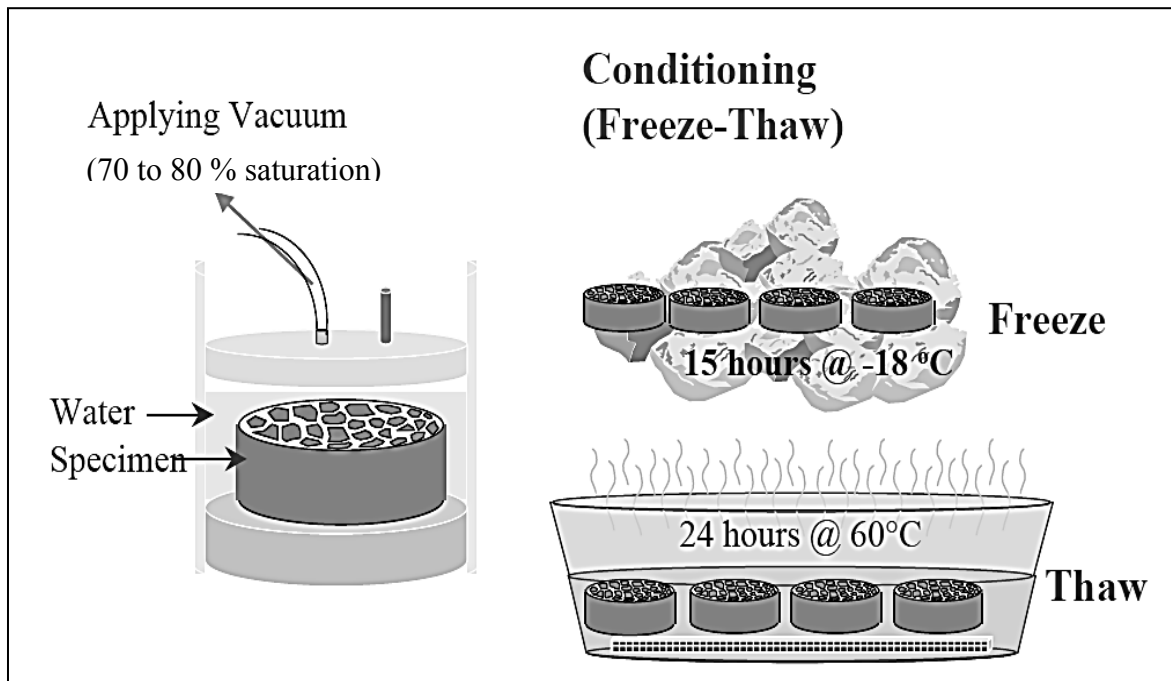


Figure 3-31 AASHTO T 283-11 conditioning cycles [72]

The moisture susceptibility was evaluated as the ratio of the tensile strength (Equation 3-14) of two dry and conditioned subsets.

$$TSR = \frac{S_{t2}}{S_{t1}} \quad 3-14$$

where:

TSR = tensile strength ratio

S_{t1} = average tensile strength of the dry subset, kPa

S_{t2} = average tensile strength of the conditioned subset, kPa

CHAPTER 4: RESULTS AND DISCUSSION

To achieve the targeted PG 64-28 binder from the PG 58-28 base asphalt, several trial blends of the Low Density Poly-Ethylene (LDPE) and Poly-styrene (PS) modifiers (Figure 4-1) were optimized in the laboratory to produce proprietary binder prototypes exhibiting similar high and low temperature performance grades, as illustrated in Figure 4-2. It should be noted that a temperature of 67°C was targeted in Figure 4-1 to achieve PG 64-28, while accounting for possible temperature changes after addition of additives [A] and [B].

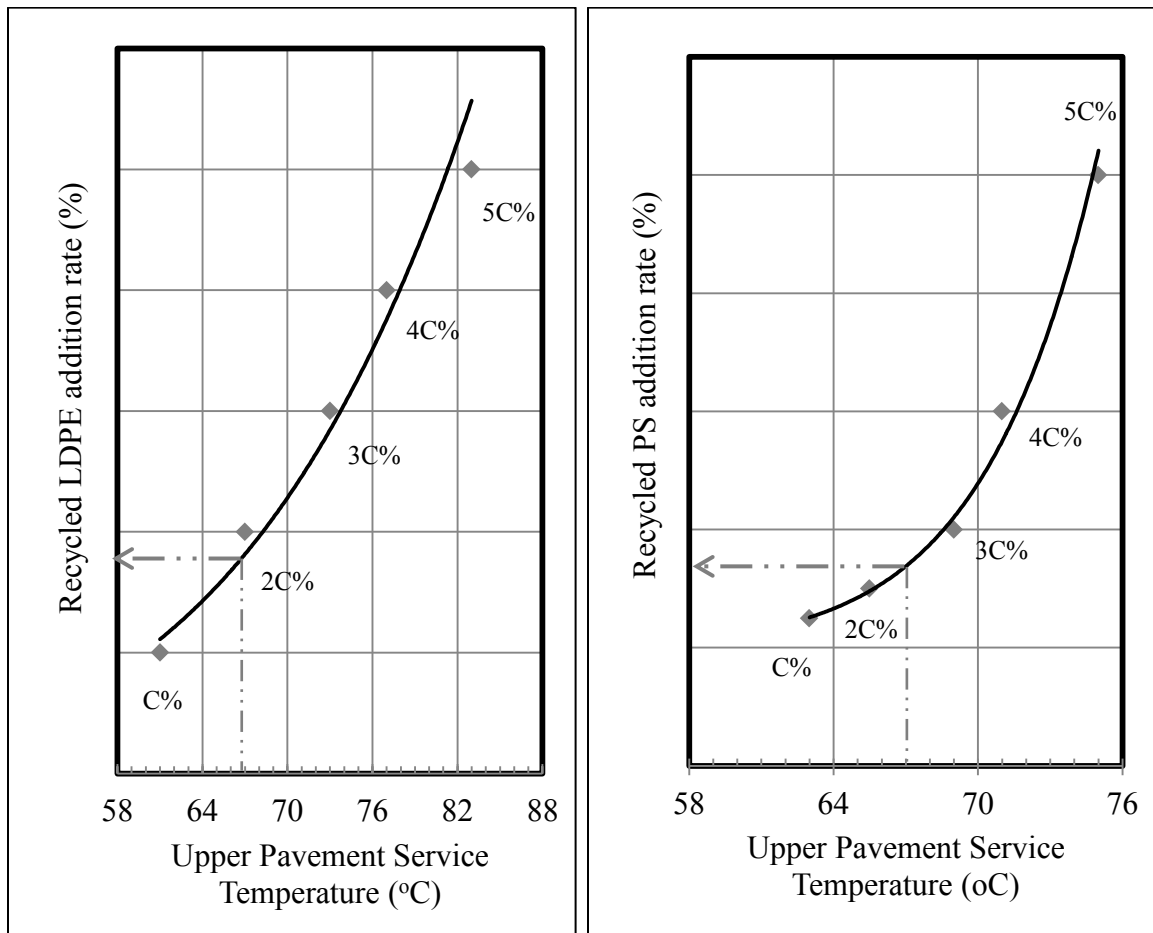


Figure 4-1 Optimization of trial blends of LDPE and PS to produce final binders

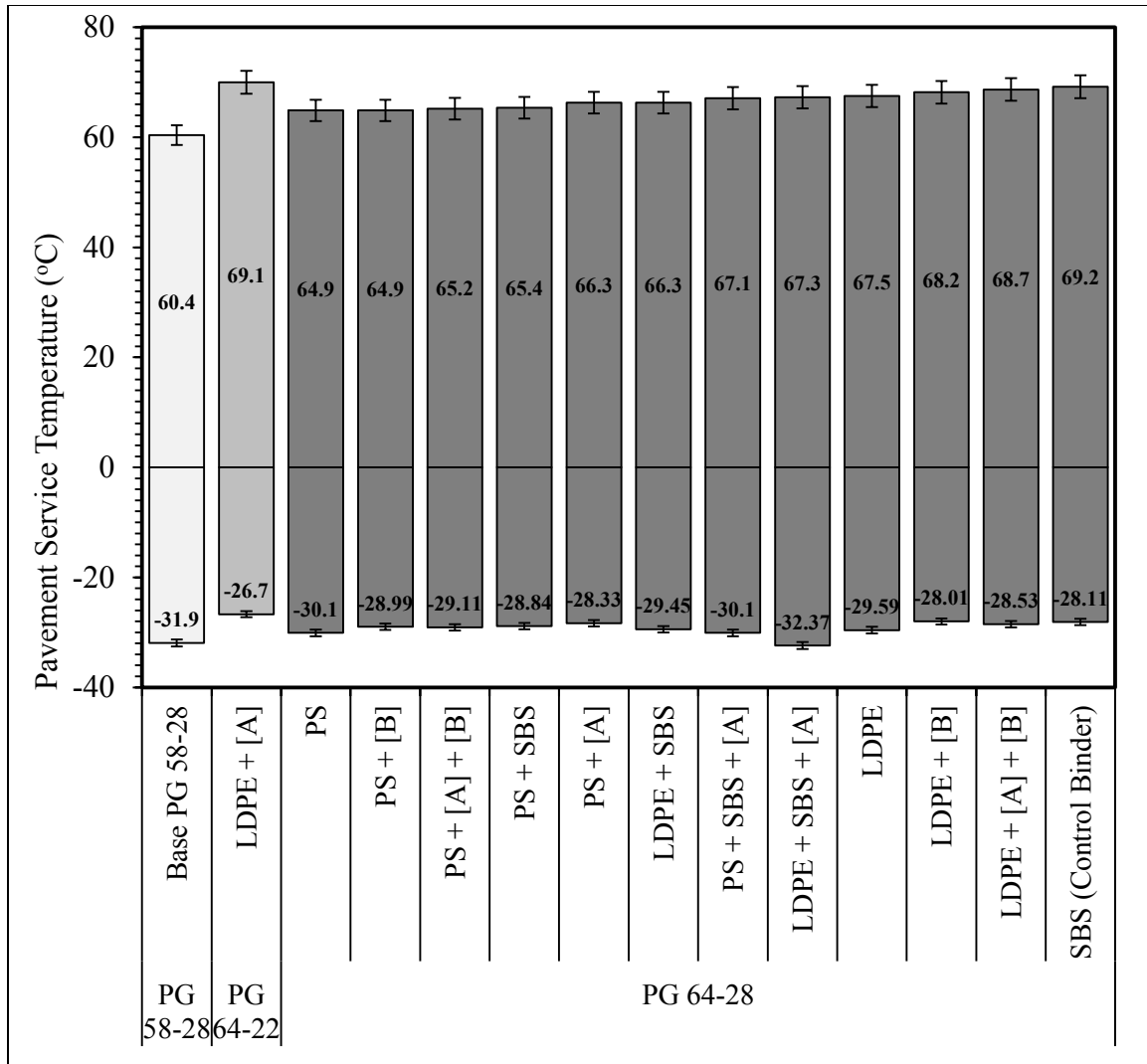


Figure 4-2 Superpave™ Performance Grade (PG) of Modified Binders (MBs)

The Marshal method of volumetric mix design was used to produce a hot mix asphalt concrete for high traffic volume freeways as per the highway design standards utilized by NSTIR [56]. The mixture was designed with an optimum PG 64-28 (SBS-control Binder) asphalt binder content of 5.5 percent. Figure 4-3 illustrates the results of the marshal mixture design, while the physical and volumetric properties are listed in Table 4-1.

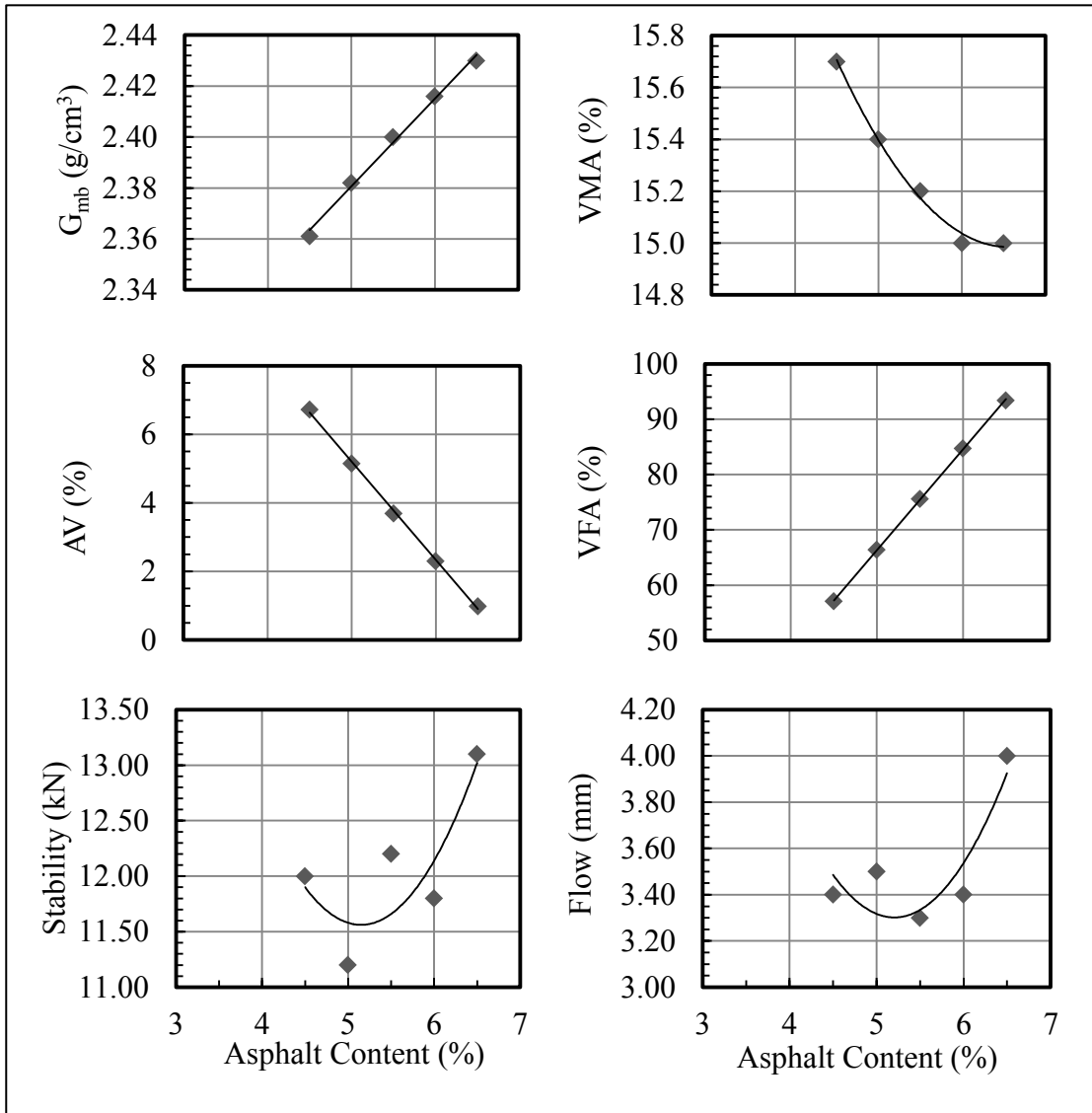


Figure 4-3 Plots required for Marshall mixture design

Table 4-1 Hot-Mix Asphalt (HMA) mixture physical properties

Property	Selected	NSTIR Specification
Asphalt Content, P_b (%)	5.5	-
Marshall Stability (kN)	12.2	Minimum 7.5
Air Voids, AV (%)	3.69	3.5 – 4.5
Voids in Mineral aggregate, VMA (%)	15.2	Minimum 14
Voids Filled with Asphalt, VFA (%)	75.6	65 – 78
Marshall Flow (mm)	3.30	2 – 4
Mixture Maximum Specific Gravity, G_{mm} (g/cm ³)	2.492	-
Compacted Bulk Specific Gravity, G_{mb} (g/cm ³)	2.400	-

3.5.Effect of Modification on Workability

The rotational viscometer was used to determine temperatures related to mixing and compaction viscosity values of 0.17 and 0.28 Pa.S respectively in accordance with AASHTO T 316-11, “Viscosity Determination of Asphalt Binder Using Rotational Viscometer” [43]. The mixing and compaction temperatures of all binders are listed in Table 4-2.

Table 4-2 Mixing and compaction temperature range for all MBs

Blend Type	Mixing Temperature (°C)		Viscosity at 135°C (Pa.S)	Compaction Temperature (°C)	
	Range	Mid point		Range	Mid point
SBS (Control Binder)	165 - 170	167.5	0.686	153 - 158	155.5
LDPE+[A]	162 - 167	164.5	0.646	151 - 156	153.5
LDPE+SBS+[A]	160 - 166	163	0.519	148 - 153	150.5
PS+SBS+[A]	160 - 166	163	0.516	148 - 153	150.5
LDPE	158 - 165	161.5	0.416	144 - 150	147
LDPE+[B]	158 - 164	161	0.511	147 - 152	149.5
LDPE+SBS	157 - 163	160	0.466	145 - 150	147.5
LDPE+[A]+[B]	154 - 164	159	0.542	133 - 142	137.5
PS+SBS	155 - 161	158	0.429	143 - 148	145.5
PS+[A]	155 - 161	158	0.439	143 - 149	146
PS+[A]+[B]	154 - 160	157	0.416	142 - 148	145
PS	153 - 159	156	0.396	141 - 146	143.5
PS+[B]	153 - 159	156	0.356	141 - 147	144
Base PG 58-28	146 - 152	149	0.295	134 - 139	136.5

The results of above table indicate that binders containing RPM had lower mixing and compaction temperature compare to the control binder. It is also noticeable that recycled-PS exhibited lower mixing and compaction temperatures than LDPE, which may indicate a potential for reduced short term aging effects and emissions during HMA production.

The viscosity values at 135°C were evaluated with respect to the upper limit of 3.0 Pa.S as per the AASHTO M320 criterion for the proper pumping and handling. For this study, all modified binders exhibited viscosities that were well below the limit, as listed in Table 4-2. It should be also noted that all modified binders exhibited a linear viscosity-temperature curve.

3.6. Effect of Modification on Permanent Deformation

The Superpave™ rutting parameter of $|G^*|/\sin(\delta)$ for modified binders was measured in accordance with AASHTO T 315-12, “Determining the Rheological Properties of Asphalt Binder Using a Dynamic Shear Rheometer (DSR) [46]. The $|G^*|/\sin(\delta)$ values for each unaged binder at maximum temperature range of 58 to 70°C are illustrated in Figure 4-4.

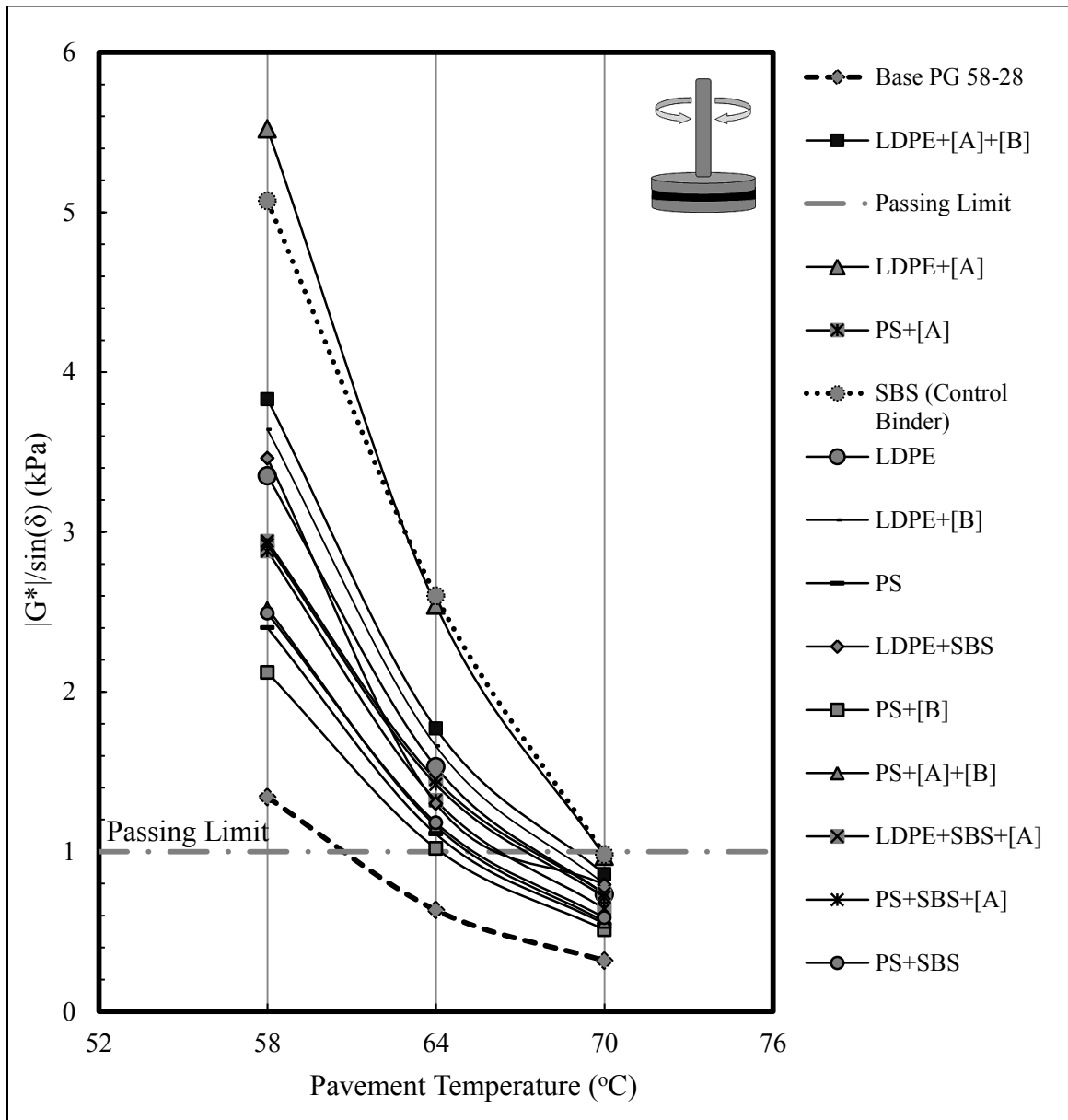


Figure 4-4 Comparison of rutting parameter of $G^*/\sin(\delta)$ for all binders at different maximum pavement temperatures

As illustrated in Figure 4-4, the $|G^*|/\sin(\delta)$ values of the base PG 58-28 binder were significantly increased at maximum pavement temperature of 64°C. It is also noticeable that SBS modified binder (control binder) exhibited highest $|G^*|/\sin(\delta)$ value at temperature of 64°C, which may indicate a potential for increased permanent deformation resistance of HMA. Figure 4-4 also illustrates that all binders (except base PG 58-28) met the lower limit of 1.0 kPa at 64°C, as per the AASHTO M320 criterion for the $|G^*|/\sin(\delta)$ value for unaged binder.

The $|G^*|/\sin(\delta)$ values for each unaged binder at a maximum pavement temperature of 64°C are illustrated in Figure 4-5, but are normalized with respect to the value obtained for the SBS modified control binder.

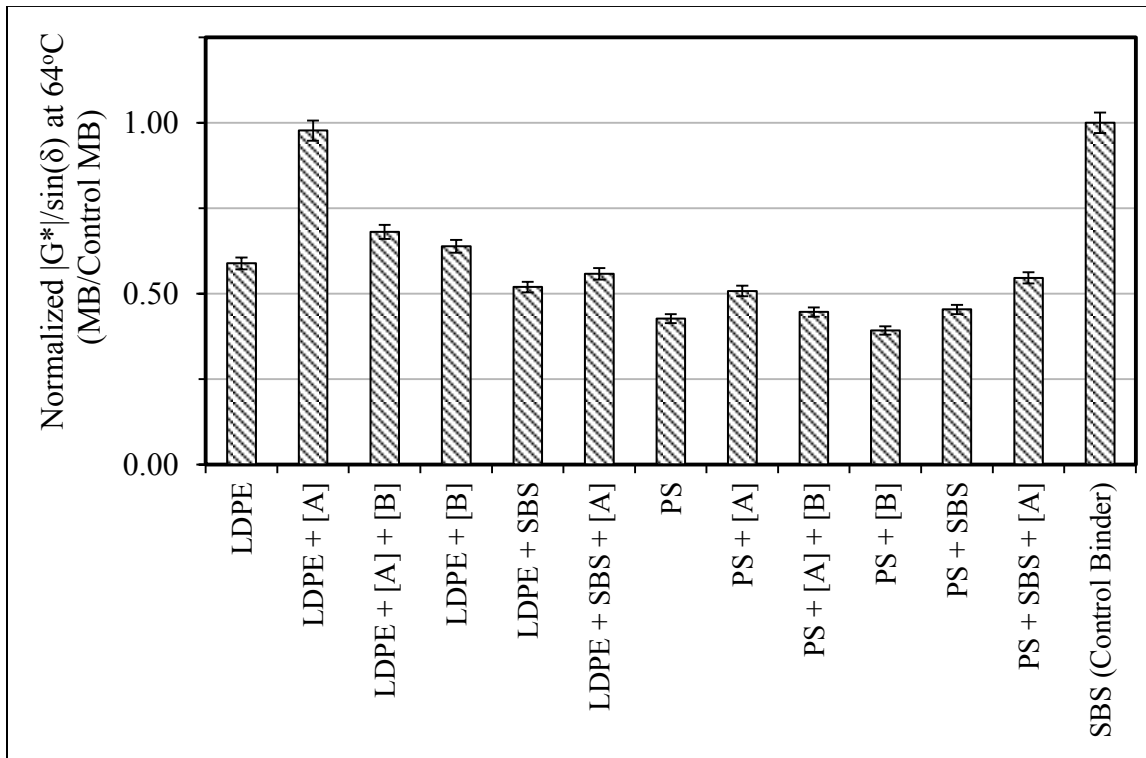


Figure 4-5 Comparison of rutting performance for unaged binders based on Superpave™ $G^*/\sin(\delta)$ parameter

The following trends can be observed from Figure 4-5:

- Generally, modified binders containing RPM resulted in lower values of $|G^*|/\sin(\delta)$ compared to the virgin SBS modified control binder, except LDPE+[A]. However, RPM's still provided favourable enhancement of $|G^*|/\sin(\delta)$ for the base asphalt;

- Although the $|G^*|/\sin(\delta)$ parameter was expected to be improved by using combination of RPM-LDPE and Virgin-SBS, a reduction was instead observed. However, this reduction was slightly improved by using the cross linking agent;
- Slight improvement was observed for the $|G^*|/\sin(\delta)$ parameter by using the combination of RPM-PS and Virgin-SBS. This improvement was further improved by using a cross linking agent in the binder; and
- As expected, an improvement was observed for the $|G^*|/\sin(\delta)$ parameter by using the cross-linking agent [A]. The aromatic oil [B] did soften MBs causing expected decrease in the $|G^*|/\sin(\delta)$.

In order to measure the RTFO $|G^*|/\sin(\delta)$ parameter, all MBs were RTFO aged in accordance with AASHTO T240-09, “Effect of Heat and Air on a Moving Film of Asphalt Binder (Rolling Thin-Film Oven Test) [41]. As part of this test, mass loss percentage was measured for all binders, as illustrated in Figure 4-6.

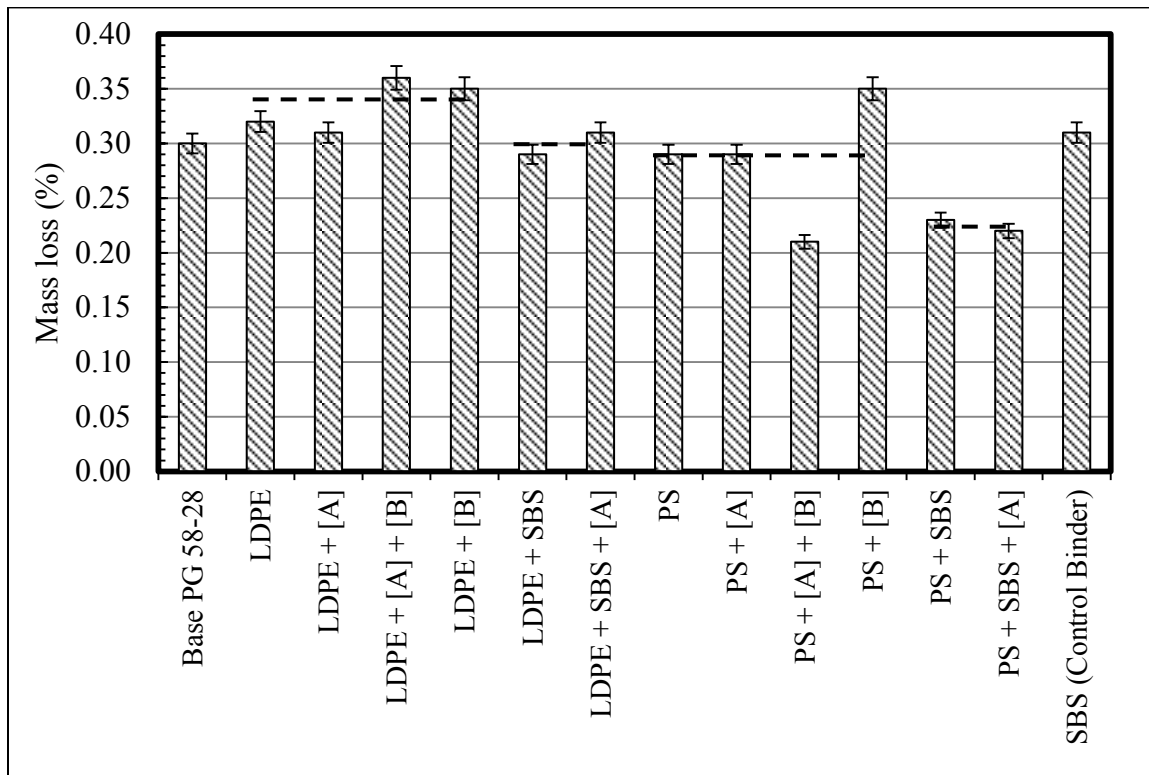


Figure 4-6 RTFO Mass loss percentage for all MB

As shown in Figure 4-6, on average, the effect of recycled LDPE modification appears to result in greater mass loss (0.34%) compare to both base asphalt binder (0.30%) and the SBS modified control binder (0.31%). However, an improvement of 4% was observed by using the combination of RPM-LDPE and Virgin-SBS. On the other hand, the recycled PS modification appears to resulted in lower mass loss (0.29%), which was further improved by 6% by addition of Virgin-SBS. Finally, all the MBs exhibited mass losses that were well below the limit upper limit of 1.0 percent mass loss as per the AASHTO M320 criterion.

The $|G^*|/\sin(\delta)$ values for each RTFO binder at a maximum pavement temperature of 64°C are illustrated in Figure 4-7, but compared to the values obtained for the values obtained from unaged binders.

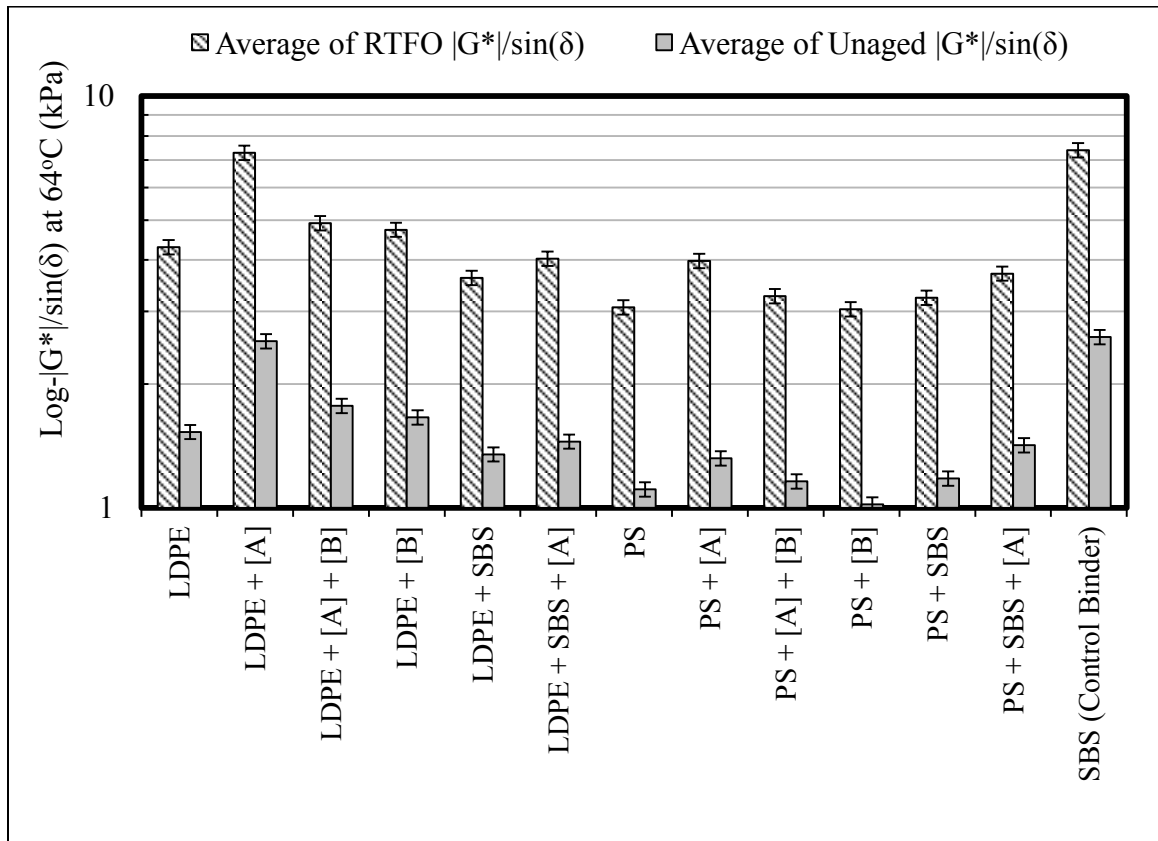


Figure 4-7 Values of $|G^*|/\sin(\delta)$ at 64°C for all unaged and RTFO aged MBs

As shown above, for all binders, an improvement was observed in the value of $|G^*|/\sin(\delta)$ after RTFO aging. Such improvement was observed to follow the same trends in the unaged $|G^*|/\sin(\delta)$ parameter. Moreover, as Figure 4-7 shows, all binders met the lower stiffness limit of 2.2 kPa at 64°C, as per the AASHTO M320 criterion for the $|G^*|/\sin(\delta)$ value for RTFO binder.

In order to verify these observed trends in the $|G^*|/\sin(\delta)$ parameter, the Asphalt Pavement Analyzer (APA) was used to measure rutting susceptibility of asphalt mixtures produced from the modified binder prototypes as listed in Table 1. The mixtures were conditioned and tested at a high service temperature of 64°C for 8,000 cycles of loading. Each cycle of loading includes two passes of a wheel load applied over the specimen. For each mixture, two replicates were compacted by using the Superpave™ gyratory compactor in accordance with procedure described in section 3.3.3 of this thesis. The APA test results are listed in Table 4-3, while illustrated in Figure 4-8 and Figure 4-9.

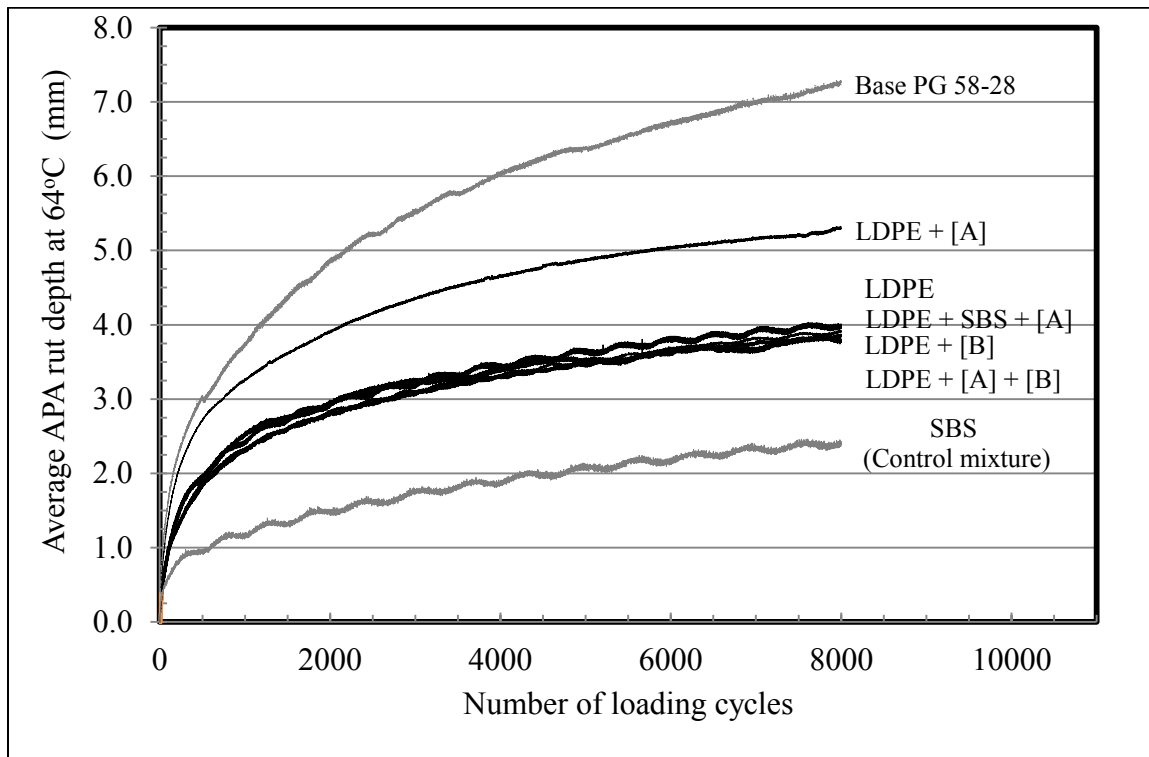


Figure 4-8 APA results for mixtures containing LDPE RPM

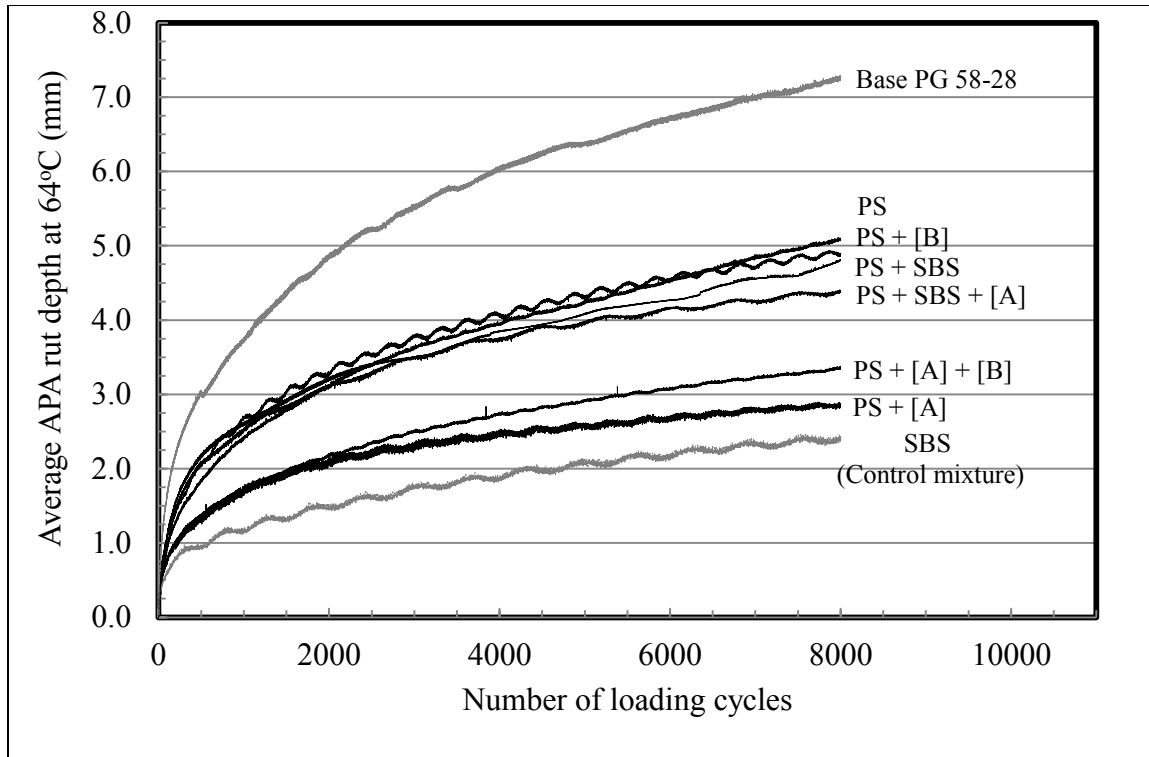


Figure 4-9 APA results for mixtures containing PS RPM

Table 4-3 Summary of Asphalt Pavement Analyzer (APA) test results

Binder Composition	PG Grade	Continuous PG Grade (° C)	Average APA Rut Depth At 64°C (mm)
SBS (Control mixture)	64-28	69.2-28.1	2.419
PS + [A]	64-28	66.3-28.3	2.841
PS + [A] + [B]	64-28	65.2-29.1	3.352
LDPE + [A] + [B]	64-28	68.7-28.5	3.765
LDPE + [B]	64-28	68.2-28.0	3.839
LDPE + SBS + [A]	64-28	67.3-32.4	3.905
LDPE	64-28	67.5-29.6	3.956
LDPE + SBS	64-28	66.3-29.5	4.226
PS + SBS + [A]	64-28	67.1-30.0	4.393
PS + SBS	64-28	65.4-28.8	4.800
PS + [B]	64-28	64.9-29.0	4.878
PS	64-28	64.9-30.1	5.077
LDPE + [A]	64-22	69.1-26.7	5.292
Base PG 58-28	58-28	60.4-31.9	7.264

The APA results indicated that mixtures containing recycled plastics exhibit similar, yet slightly less, rut resistance compared to the SBS-modified control mixture. However, the degree of rutting resistance in mixtures is not uniform across modifier and additive combinations. As illustrated in Figure 4-10, it was observed, on average, that mixtures containing RPM-PS exhibited more resistance to rutting compared to mixtures modified with RPM-LDPE. The results also indicated that a combination of RPM and virgin-SBS did not improve the rutting resistance of the mixtures.

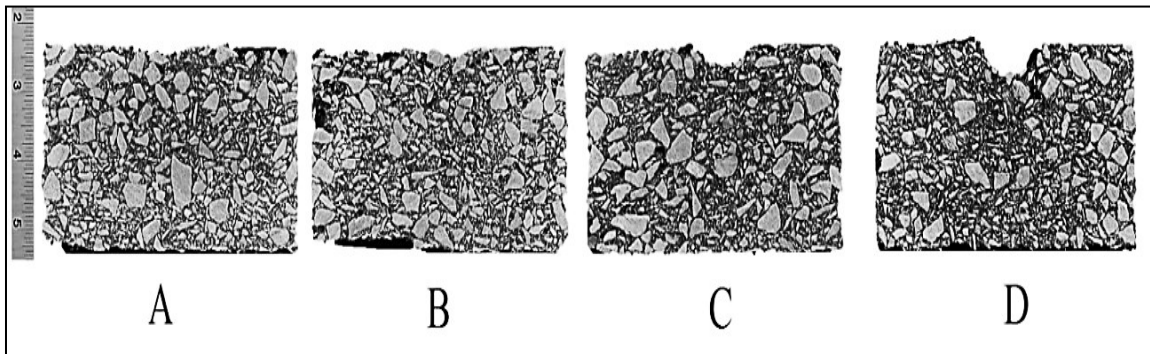


Figure 4-10 Cross sections of APA specimens after 8,000 load repetitions at 64°C containing: A (SBS-control binder), B (PS+[A]), C (LDPE+[A]+[B]), and D (Base PG 58-28)

The Superpave™ rutting parameter of $|G^*|/\sin(\delta)$ and non-recoverable compliance (J_{nr}) were both compared to the APA results. Figure 4-11 and Figure 4-12 illustrate the relationship of $|G^*|/\sin(\delta)$ to the mixtures rutting results for unaged and RTFO-aged conditions, respectively.

As shown in Figure 4-11, a linear relationship between the unaged $|G^*|/\sin(\delta)$ and the average rut depth exhibits a poor coefficient of determination (R^2) equal to 0.20. Modeling this relationship using a power function did slightly improve R^2 to a value of 0.30, but there was still a great deal of scatter in the data.

The RTFO-aged $|G^*|/\sin(\delta)$ parameter demonstrated a slightly stronger relationship with the APA rutting results. Figure 4-12 shows both linear and power function models of the relationship between the RTFO-aged $|G^*|/\sin(\delta)$ to the mixtures rutting results with R^2 values of 0.23, and 0.36 respectively.

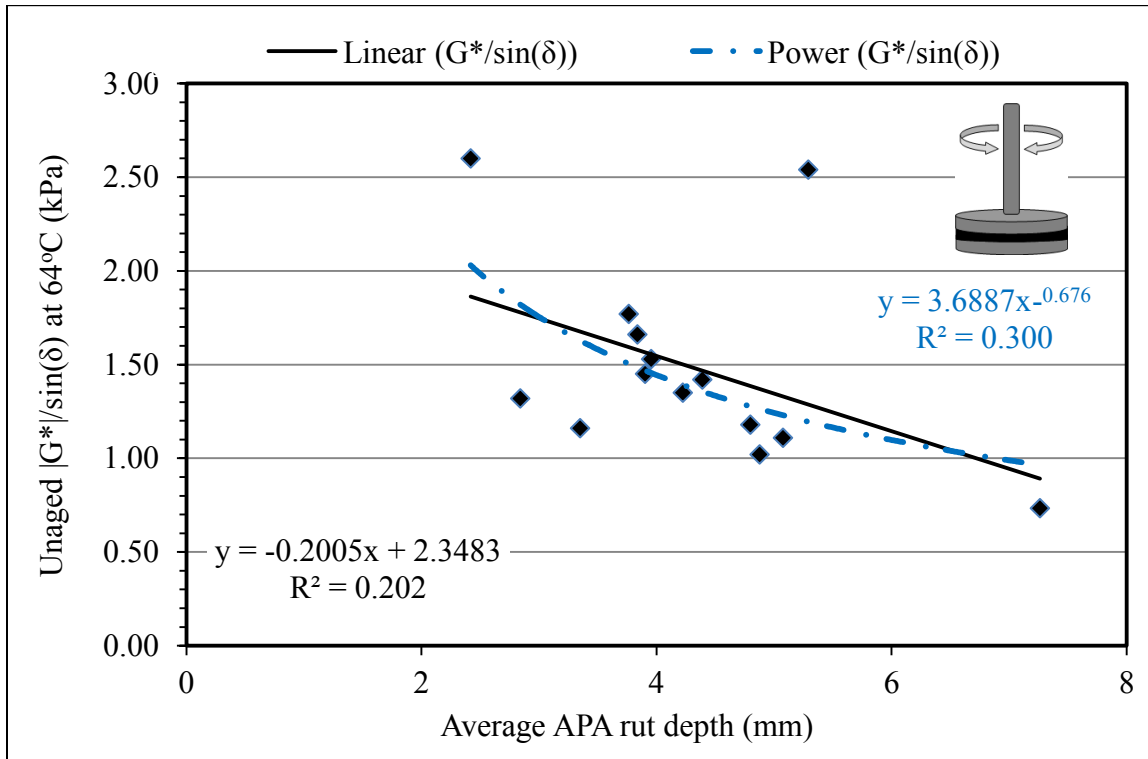


Figure 4-11 Relationship Between unaged $G^*/\sin(\delta)$ at 64°C and Mixture Rut Depth

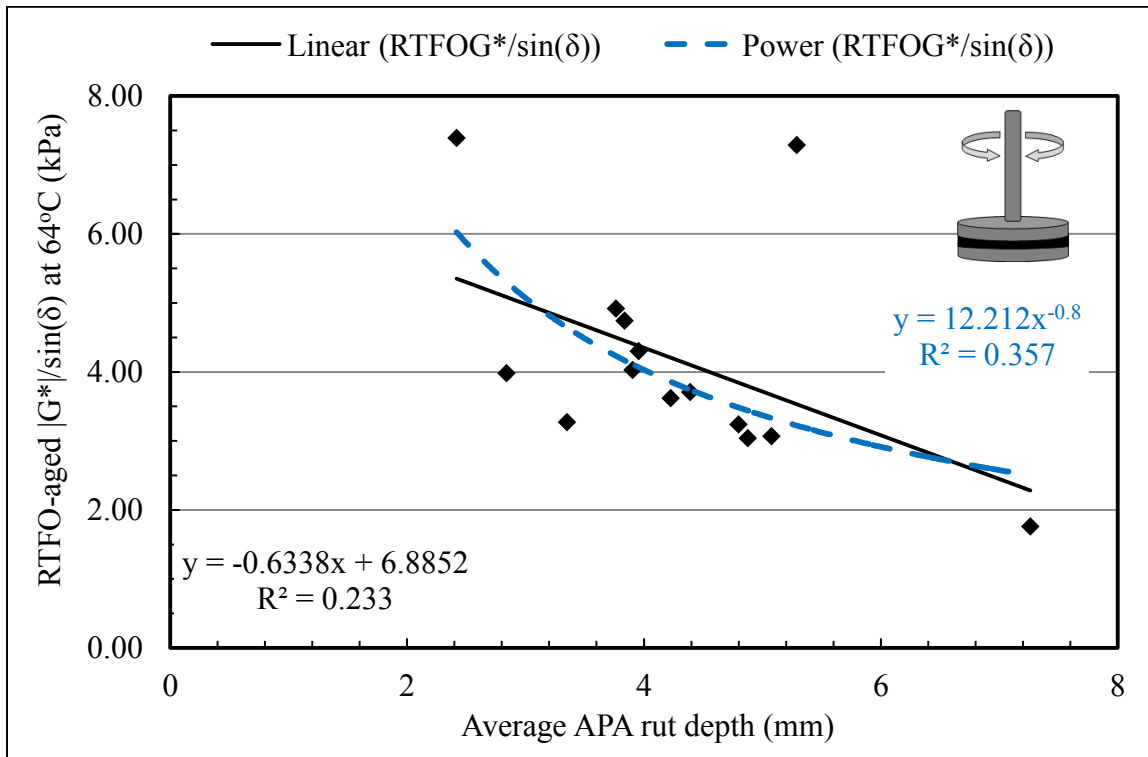


Figure 4-12 Relationship Between RTFO $G^*/\sin(\delta)$ at 64°C and Mixture Rut Depth

In recent years, the non-recoverable creep compliance (J_{nr}) has been proposed as a more appropriate alternative to the Superpave™ rutting parameter of $|G^*|/\sin(\delta)$ for both neat and polymer modified. Figure 4-13 illustrates a linear relationship of J_{nr} values, measured at stress level of 3.2 kPa, to the APA rutting results with R^2 values of 0.64. These results appear to indicate that the J_{nr} provides a better indication of rutting susceptibility for modified binders than the $|G^*|/\sin(\delta)$ parameter.

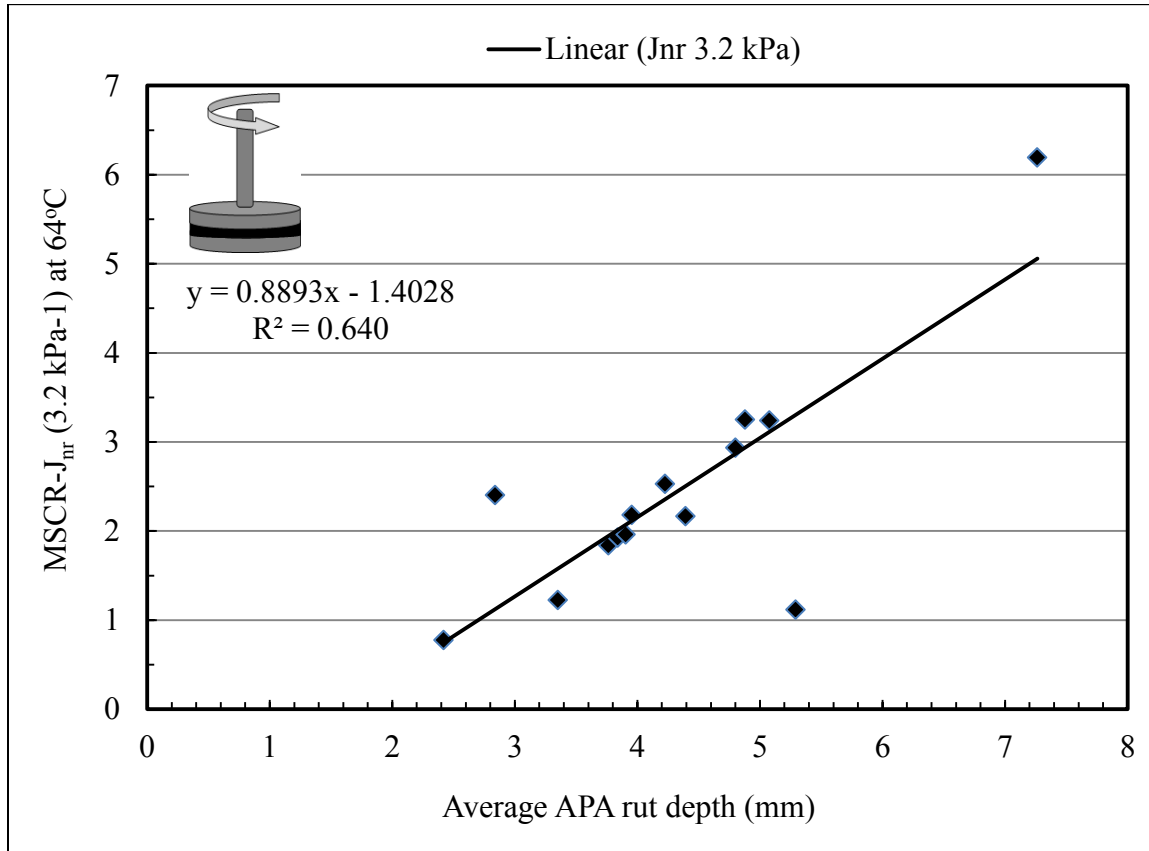


Figure 4-13 Relationship Between Non-Recoverable Creep Compliance, J_{nr} (3.2 kPa), and Mixture Rut Depth

Table 4-4 lists different rankings for the modified binders based on both RTFO-aged and unaged $|G^*|/\sin(\delta)$ and J_{nr} (3.2 kPa) parameters. It is observed that the non-recoverable creep compliance (J_{nr}) correlated well to APA rut ranks compared to the Superpave™ parameter $|G^*|/\sin(\delta)$. However, all three parameters identically ranked the neat PG58-28 binder indicating that both parameters are adequate in describing rutting behaviour of unmodified binders, and possibly binders contain elastomeric modifiers (i.e. SBS).

Table 4-4 Hot Mix Asphalt Rutting Susceptibility Rankings

Binder Composition	APA Rut Rank	MSCR J_{nr} (3.2kPa) at 64°C Rank	Unaged $ G^* /\sin(\delta)$ at 64°C Rank	RTFO $ G^* /\sin(\delta)$ at 64°C Rank
SBS (control binder)	1	1	1	1
PS + [A]	2	9	9	7
PS + [A] + [B]	3	3	11	10
LDPE + [A] + [B]	4	4	3	3
LDPE + [B]	5	5	4	4
LDPE + SBS + [A]	6	6	6	6
LDPE	7	8	5	5
LDPE + SBS	8	10	8	9
PS + SBS + [A]	9	7	7	8
PS + SBS	10	11	10	11
PS + [B]	11	13	13	13
PS	12	12	12	12
LDPE + [A]	13	2	2	2
Base PG 58-28	14	14	14	14

As part of the MSCR test, accumulated strain can be also measured at stress levels of 0.1 and 3.2 kPa. Figure 4-14 illustrates the accumulated strain for all binders. In general, It can be observed that modification of base PG 58-28 significantly decrease accumulated deformation. The SBS modified binder exhibits the lowest amount of accumulated deformation in compare to all binders. An improvement was also observed for the accumulated deformation by using the combination of RPM-PS, Virgin-SBS, and a cross linking agent in the binder. In general, all modified binders (except LDPE + [A], and SBS-Control Binder) exhibited accumulated strains ranging similar to each other.

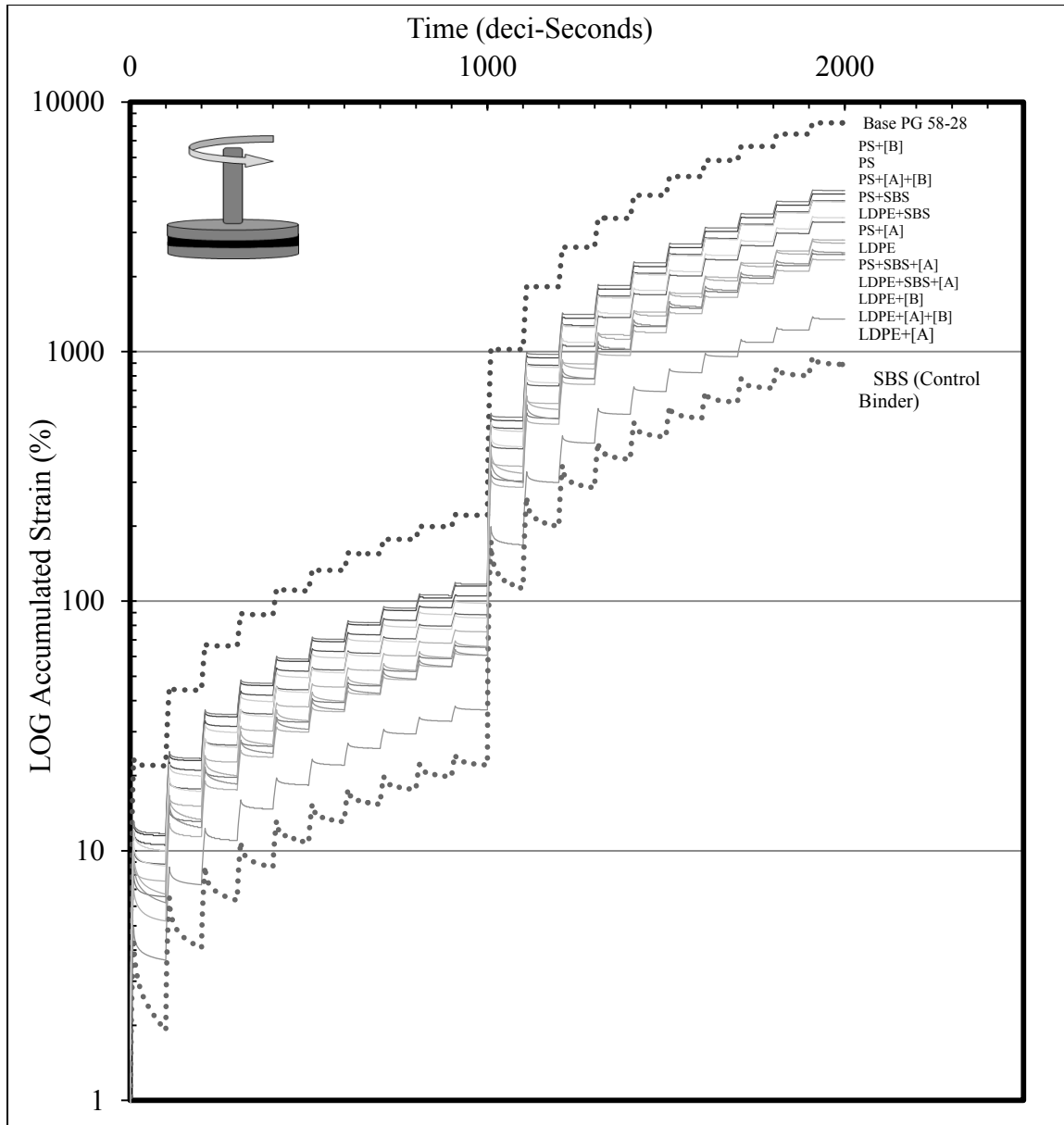


Figure 4-14 Results of the accumulated strain under MSCR testing at maximum pavement temperature of 58 °C.

The J_{nr} values can also be used to performance grade binders as part of AASHTO MP 19-10, “Performance-Graded Asphalt Binder Using Multiple Stress Creep Recovery (MSCR) Test” [51]. It should be noted that high temperature grading in AASHTO MP 19-10 specification is related to the average seven-day maximum pavement temperature (i.e. environmental temperature) as oppose to the bumped-grade temperature. For this purpose, the J_{nr} values were also measured for all modified binders at a temperature of 58°C and are listed in Table 4-5.

As illustrated, the base-asphalt (PG 58-28) was graded as suitable for standard traffic levels (“S” grade) corresponds to traffic levels fewer than 10 million equivalent single axle loads (ESALs) and traffic speed of more than 70 km/hr as per AASHTO MP 19-10. The SBS-modified control binder and cross-linked LDPE modified binder met the requirements of the extreme high traffic level, grade “E”, which corresponds to traffic levels greater than 30 million ESALs and standing traffic with speed of less than 20 km/hr. The majority of the modified binders were graded as “V” and “H”. The grade “H” corresponds to the ESAL of 10 to 30 million or slow moving traffic with speed between 20 to 70 km/hr. On the other hand, grade “V” corresponds to ESALs of greater than 30 million with or standing traffic with speed of less than 20 km/hr.

Table 4-5 AASHTO MP 19-10 Performance-Grading (PG) of MBs

Blend Type	AASHTO M 320-10 PG	AASHTO MP 19-10				
		$J_{nr,0.1}$ (kPa ⁻¹)	$J_{nr,3.2}$ (kPa ⁻¹)	$J_{nr,diff.}$ (%)	Traffic Level Grade	Traffic ESALs (millions)
SBS (Control Binder)	PG 64-28	0.22	0.27	22.81	E	> 30
LDPE+[A]	PG 64-22	0.37	0.41	11.69	E	> 30
LDPE+[A]+[B]	PG 64-28	0.61	0.71	16.72	V	>30
LDPE+[B]	PG 64-28	0.65	0.74	13.83	V	>30
LDPE+SBS+[A]	PG 64-28	0.61	0.76	25.19	V	>30
PS+SBS+[A]	PG 64-28	0.66	0.83	25.91	V	>30
LDPE	PG 64-28	0.75	0.85	12.92	V	>30
PS+[A]	PG 64-28	0.89	1.00	13.47	V	>30
LDPE+SBS	PG 64-28	0.86	1.05	22.17	H	10 to 30
PS+SBS	PG 64-28	0.98	1.21	23.89	H	10 to 30
PS	PG 64-28	1.15	1.30	13.50	H	10 to 30
PS+[B]	PG 64-28	1.17	1.35	14.82	H	10 to 30
Base PG 58-28	PG 58-28	2.21	2.51	13.41	S	< 10
PS+[A]+[B]	PG 64-28	2.55	3.00	17.54	S	< 10

Utilization of recycled plastic modifiers resulted in significant increase in in high temperature stiffness of the base-asphalt. Recycled plastics may behave similarly to engineered virgin-SBS modifier as an effective means of increasing the contribution of binders to rutting resistance with relatively lower cost of construction (Figure 4-15).

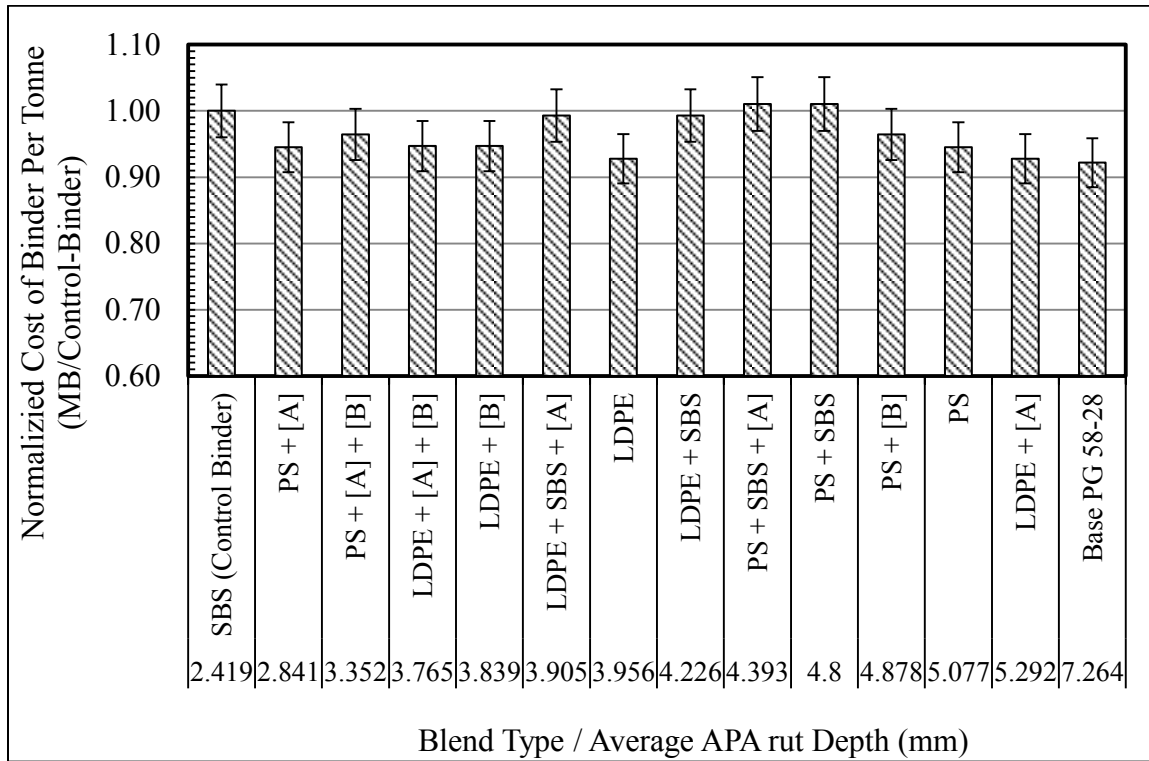


Figure 4-15 Relationship between mixture rut depth and cost of MB per Tonne

3.7.Effect of Modification on Fatigue and Thermal Cracking

Figure 4-16 illustrates the relative difference in the fatigue parameter $G^*\sin(\delta)$ for the modified binders, as normalized by the $G^*\sin(\delta)$ value for the SBS-modified control binder, at intermediate pavement temperature of 22°C. Binders with a lower $G^*\sin(\delta)$ parameter deform without developing large stresses which relate to higher resistance to fatigue cracking at intermediate pavement temperatures [25].

As illustrated in Figure 4-16, some of modified binders exhibited relatively similar $G^*\sin(\delta)$ values as the control binder. However, some other modified binders exhibited higher stiffness than the control binder which may result in less resistance to fatigue cracking.

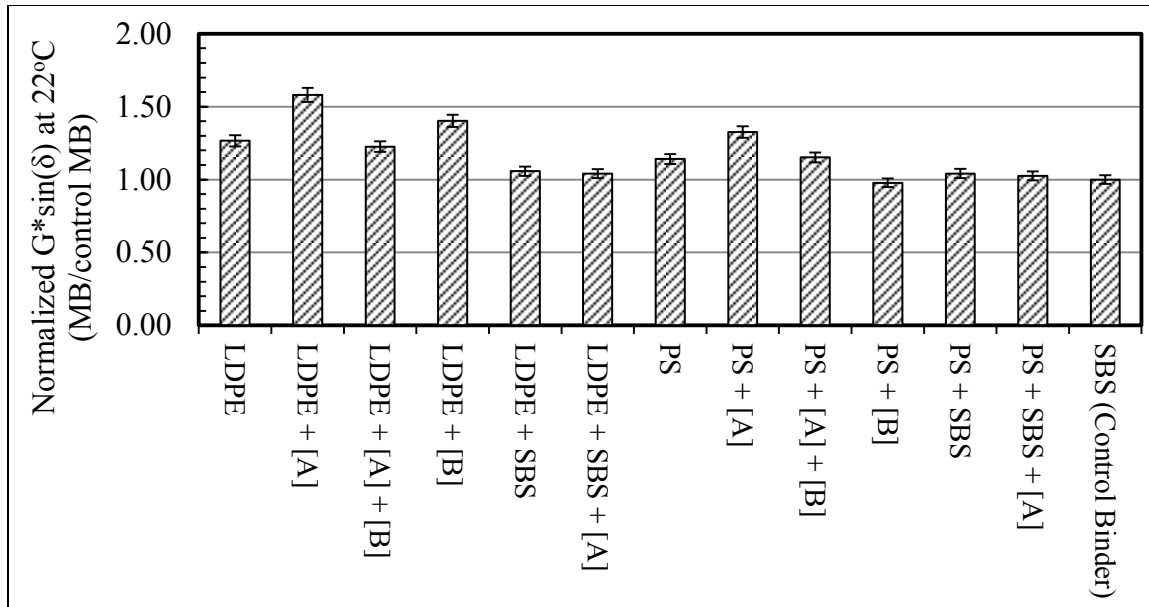


Figure 4-16 Fatigue parameter of $G^* \sin(\delta)$ at intermediate pavement temperature of 22°C

The tensile strength of bituminous mixtures can be related to fatigue performance of mixtures. Mixtures with higher tensile strengths tend to exhibit higher resistance to fatigue loading, resulting in the development of less cracks [73]. For this study, the tensile strength of mixtures was evaluated by performing the indirect tensile (IDT) strength on Marshall compacted specimens in accordance with ASTM D 6931-12 [70]. For each combination of modifiers, three replicates of Marshall specimens were prepared with minimum of 102 mm in diameter and 51 mm in thickness. Specimens were tested at an ambient temperature of 25°C.

Figure 4-17 illustrates the IDT strength ratio of modified mixtures (MM) normalized to the SBS-modified control binder at a temperature of 25°C. On average, it was observed that mixtures containing RPM exhibited similar tensile strengths as the control binder. Utilization of recycled plastic modifiers resulted in significant increase in high temperature stiffness of the base-asphalt. Recycled plastics may behave similarly to engineered virgin-SBS modifier as an effective means of increasing the contribution of binders to fatigue resistance with relatively lower cost of construction (Figure 4-18).

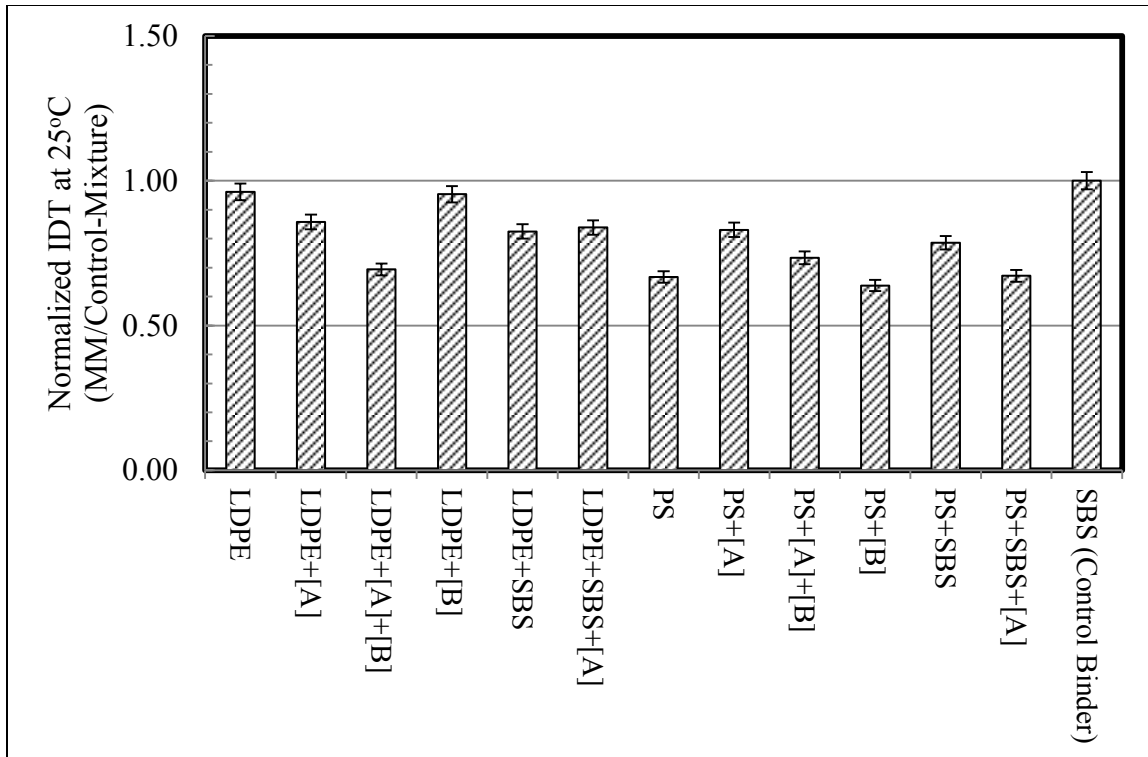


Figure 4-17 Indirect Tensile Strength (IDT) of Modified Mixtures (MM) at testing temperature of 25°C

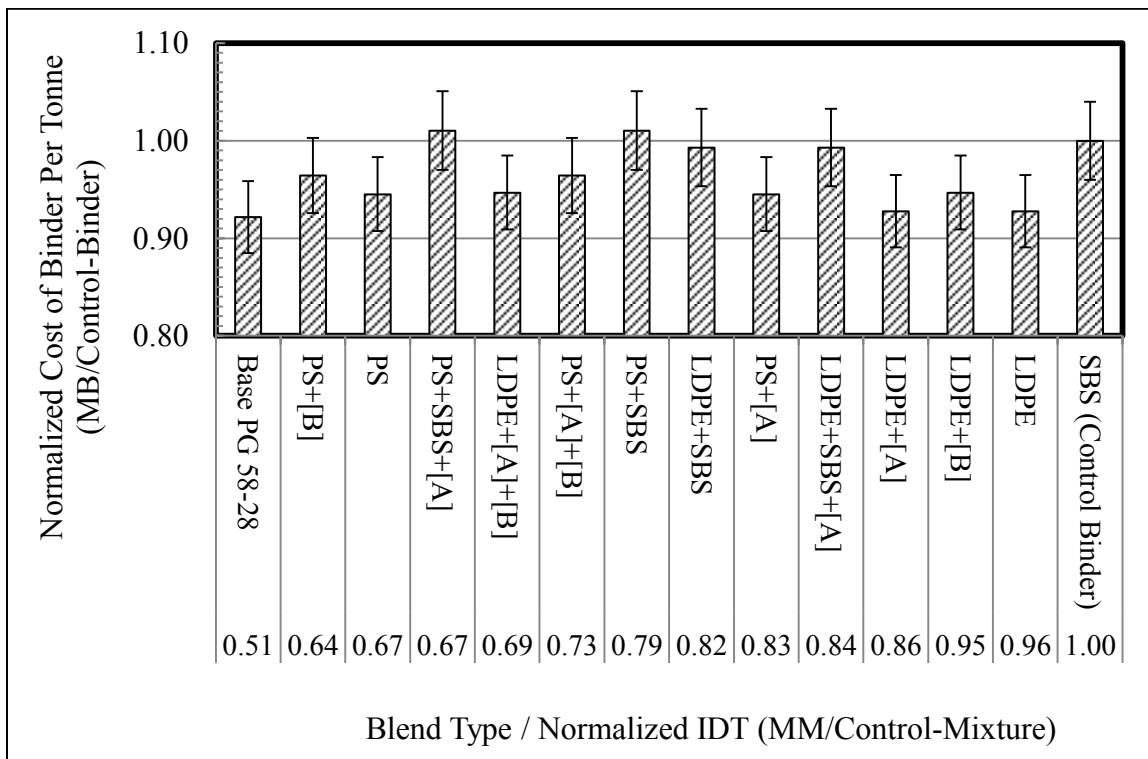


Figure 4-18 Relationship between mixture IDT and cost of MB per Tonne

Figure 4-19 and Figure 4-20 illustrate the values of creep stiffness (S) and creep rate (m -value), measured with Bending Beam Rheometer (BBR) in accordance with AASHTO T 313, “Determining the flexural creep stiffness of asphalt binder using the bending beam rheometer (BBR)” [57]. For this study, the test temperature of -18°C was used to simulate the minimum pavement temperature of -28°C . Furthermore, the BBR test was performed on PAV-aged binders to simulate mixing, and in-service aging.

As illustrated in Figure 4-19 all modified binders show an increase in the creep stiffness ($S(60)$) value when compared to the base-asphalt. However, the changes (ranging between 2 and 57 MPa) are not significant and considered minimal. Moreover, all modified binders (except LDPE + [A]) show minor reductions (ranging between 0 to 0.004) in the creep rate ($m(60)$).

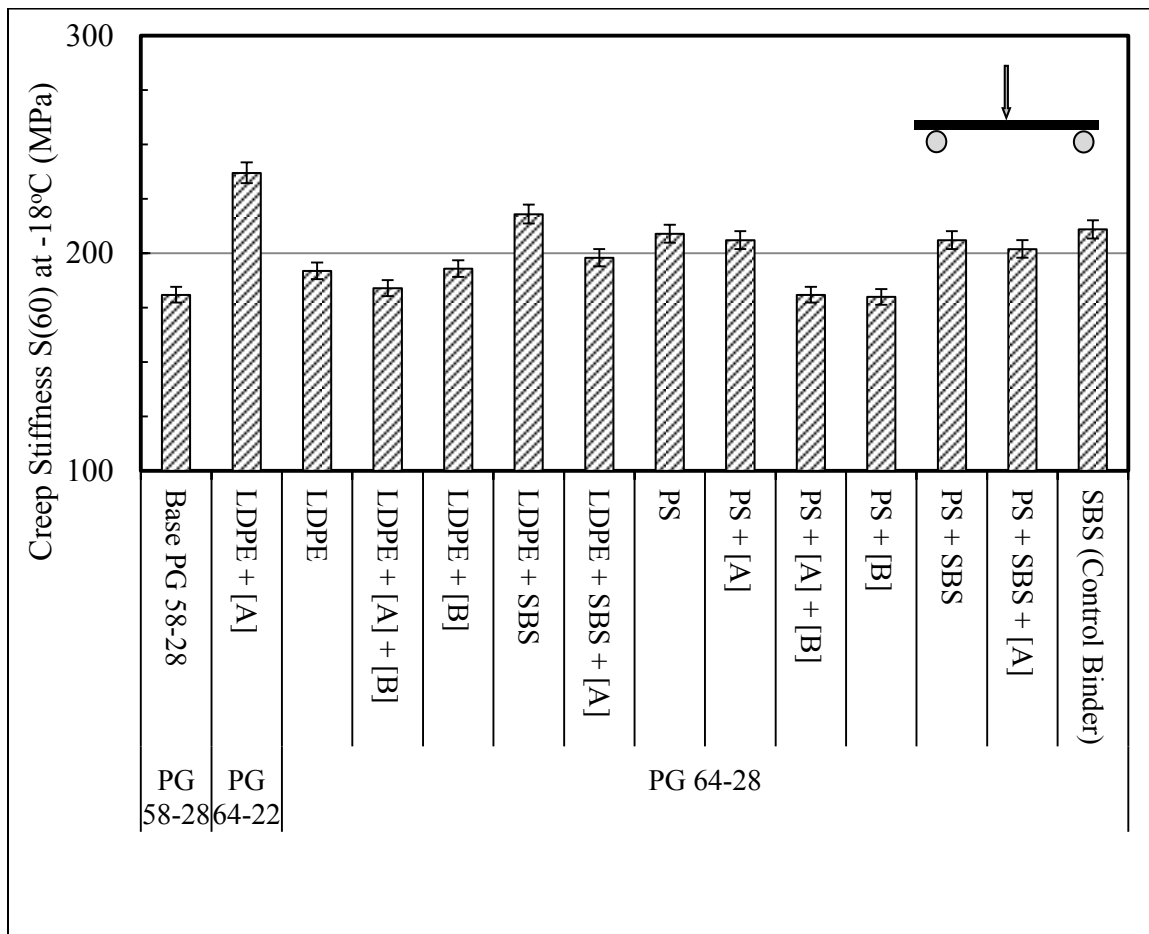


Figure 4-19 Creep stiffness $S(60)$ at minimum pavement temperature of -18°C

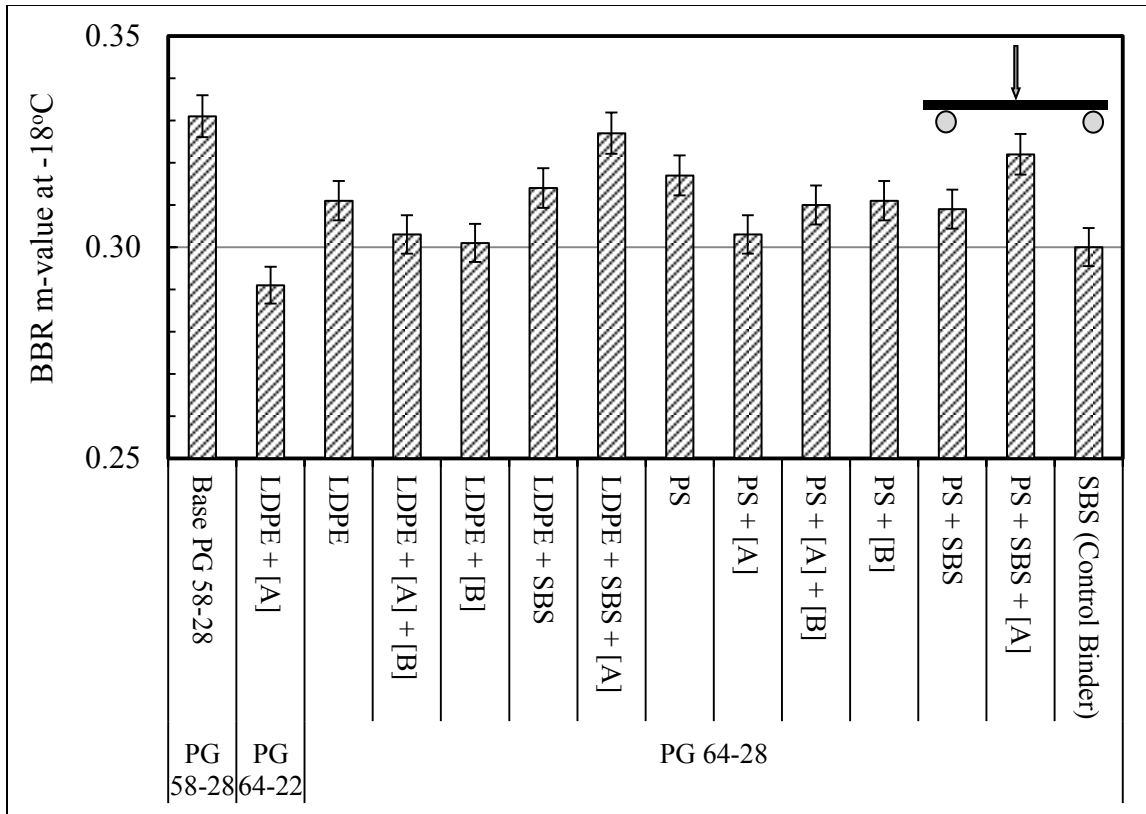


Figure 4-20 Creep rate $m(60)$ at minimum pavement temperature of -18°C

3.8. Effect of Modification on Moisture Susceptibility

For limited number of mixtures, the moisture susceptibility was evaluated in accordance with AASHTO T 283-11, “Resistance of Compacted Hot Mix Asphalt (HMA) to Moisture-Induced Damage” [71]. The indirect tensile strength (S_t) of two subsets of dry and conditioned were determined, and subsequently used to evaluate Tensile Strength Ratio (TSR). More details of volumetric design and measurements are provided in Appendix A, while Table 4-6 summarizes the results of the test.

Table 4-6 Moisture susceptibility test results

Binder	Subset (Specimen ID)		P (kN)	Air Voids (%)	Degree of Saturation (%)	S_t (kPa)	Average S_t (kPa)	TSR (%)
	Dry	Wet						
PG 58-28 (Baser Binder)	A3		6250	7.04		574.5	507.0	78.52
	A5		5450	7.29		506.8		
	A11		4750	7.50		439.5		
		A4	4450	7.50	79.0	405.2	398.1	
		A7	3300	7.82	76.7	330.6		
		A12	4900	6.98	79.7	458.5		
SBS (Control Binder)	B4		8625	7.5		776.5	766.9	77.94
	B5		8500	7.3		780.2		
	B8		7950	6.8		744.1		
		B6	6000	7.0	76.1	565.2	597.7	
		B9	6750	7.2	74.1	622.2		
		B10	6450	7.2	75.6	605.7		
LDPE	C8		6575	6.7		617.6	630.9	73.09
	C9		6750	7.5		622.6		
	C10		7000	7.4		652.3		
		C11	5325	6.7	73.3	488	461.1	
		C5	3950	7.3	76.9	363.4		
		C12	5750	7.3	79.7	531.9		
PS+[A]	D7		7750	7.2		704.9	717.8	68.80
	D8		7275	7.2		678.7		
	D11		8250	6.9		769.7		
		D3	5750	6.9	71.5	486.7	493.9	
		D4	5000	7.1	79.0	459.8		
		D5	5250	7.1	78.0	535.2		

As indicated in Table 4-6, the mixtures containing MBs exhibited higher tensile strengths than the base PG 58-28 binder for both dry and conditioned subsets. However, an increase in TSR values was noted for the mixtures containing MBs. It should be also noted that the NSTIR recommends the minimum TSR value of 73 percent, which all mixtures passed the limit except the PS+[A] mixture. To investigate the source of difference between the TSR values, the broken specimens shown in Figure 4-21 were used to visually comparison. However, no major difference was observed.

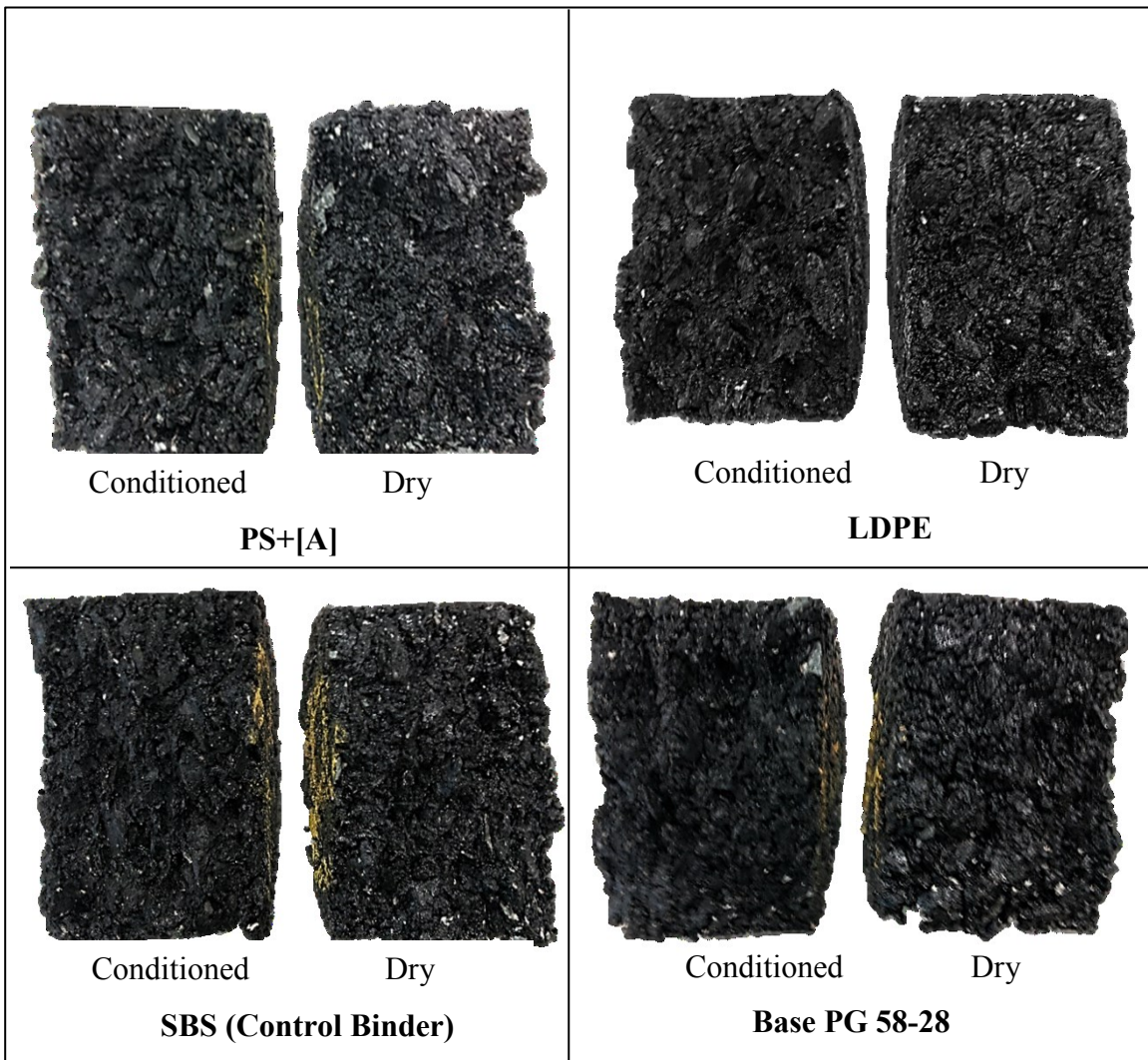


Figure 4-21 Moisture susceptibility test visual inspection

3.9.Effect of Modification on Additional Empirical Tests

The solubility test was performed to measure the purity of modified binders by measuring the soluble portion of the binder in Trichloroethylene solvent in accordance with the AASHTO T 44 [62]. For this study, all modified binders were found to be well above the minimum limit of 99.0 percent solubility.

Separation of polymers from liquid asphalt in a storage tank under heated static conditions is a concern of asphalt producers and users. For this purpose, all modified binders were assessed in accordance to the ASTM D 7173, “Standard Practice for Determining the Separation Tendency of Polymer from Polymer Modified Asphalt” [60]. The results of the separation tests are listed in Table 4-7. All modified binders exhibited no significant separation compared to the SBS-modified control binder. It should be noted that there is no pass/fail specification for this test.

Table 4-7 Softening point and separation test results

Blend Type	Softening Point (°C)	Top & Bottom Difference (°C)
LDPE + [A]	53	1.2
LDPE + [A] + [B]	50	1.7
LDPE	51	2.3
LDPE + [B]	50	2.1
PS + [A]	46	1.4
PS + [A] + [B]	47	1.6
PS	46	2.5
PS + [B]	46	1.8
SBS (Control Binder)	56	0.6
Base PG 58-28	44	0.2
LDPE + SBS + [A]	49	0.7
LDPE + SBS	46	1.5
PS + SBS + [A]	49	0.9
PS + SBS	47	1.7

In addition to AASHTO M 320-10, many transportation authorities, including NSTIR, have used the empirical ER test for modified binders to complement the PG grading system. As per the highway design standards utilized by NSTIR, a minimum of 50 percent elastic recovery is required for modified binders in order to help avoid excessive permanent deformation as well as identifying the presence of polymer and quality of blending. However, there is significant debate about the real value and benefits of the ER test.

The ER test was performed on unaged binder at a temperature of 10°C in accordance with AASHTO T301-11 [58]. Figure 4-22 illustrates a weak correlation between the ER results and the APA rut results using both linear and power function models. As a result, the ER test does not appear to provide a reliable prediction rutting performance for modified binders.

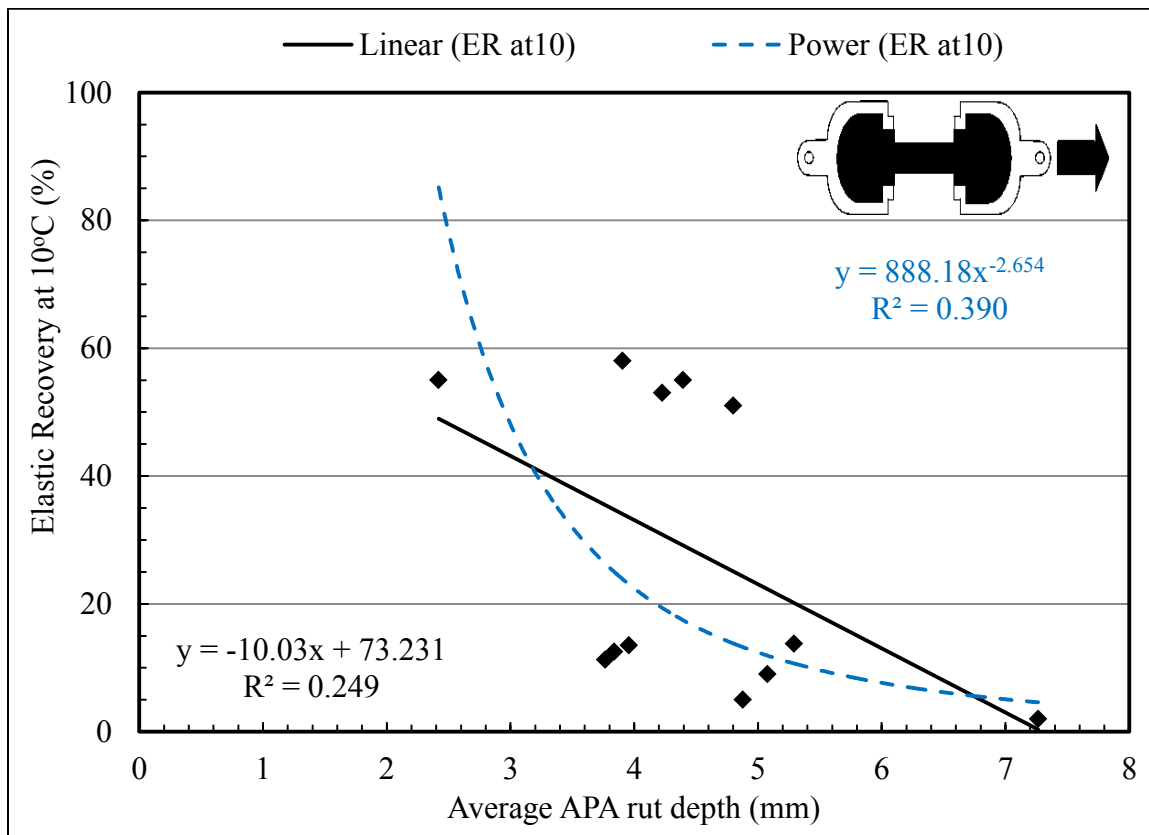


Figure 4-22 Relationship between ER % at 10°C and rutting susceptibility

As part of AASHTO MP 19-10 [51], the MSCR test can be also used to measure the amount of percent recovery at stress level of 3.2 kPa ($R_{3.2}$). Figure 4-23 illustrates the correlation between the $R_{3.2}$ measured at environmental temperature of 58°C. As it illustrated, the $R_{3.2}$ provides a better indication of rutting susceptibility for modified binders than the ER test.

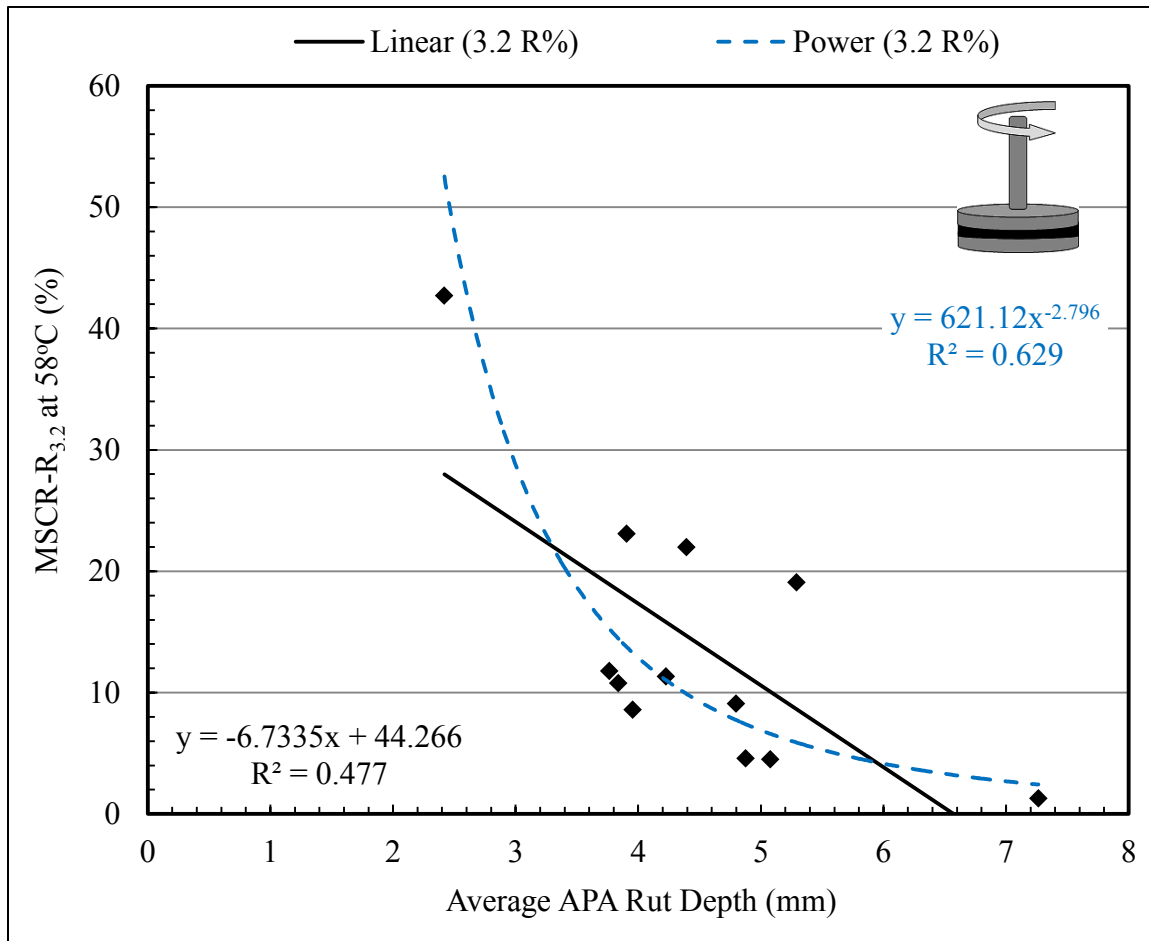


Figure 4-23 Relationship between MSCR percent recovery at 3.2 kPa at 58°C and rutting susceptibility

The penetration test was performed on unaged binder at a temperature of 25°C in accordance with AASHTO T 49-11 [59]. As shown in Figure 4-24, MBs exhibited much lower penetration values than base PG 58-28, more stiffness at intermediate pavement temperature.

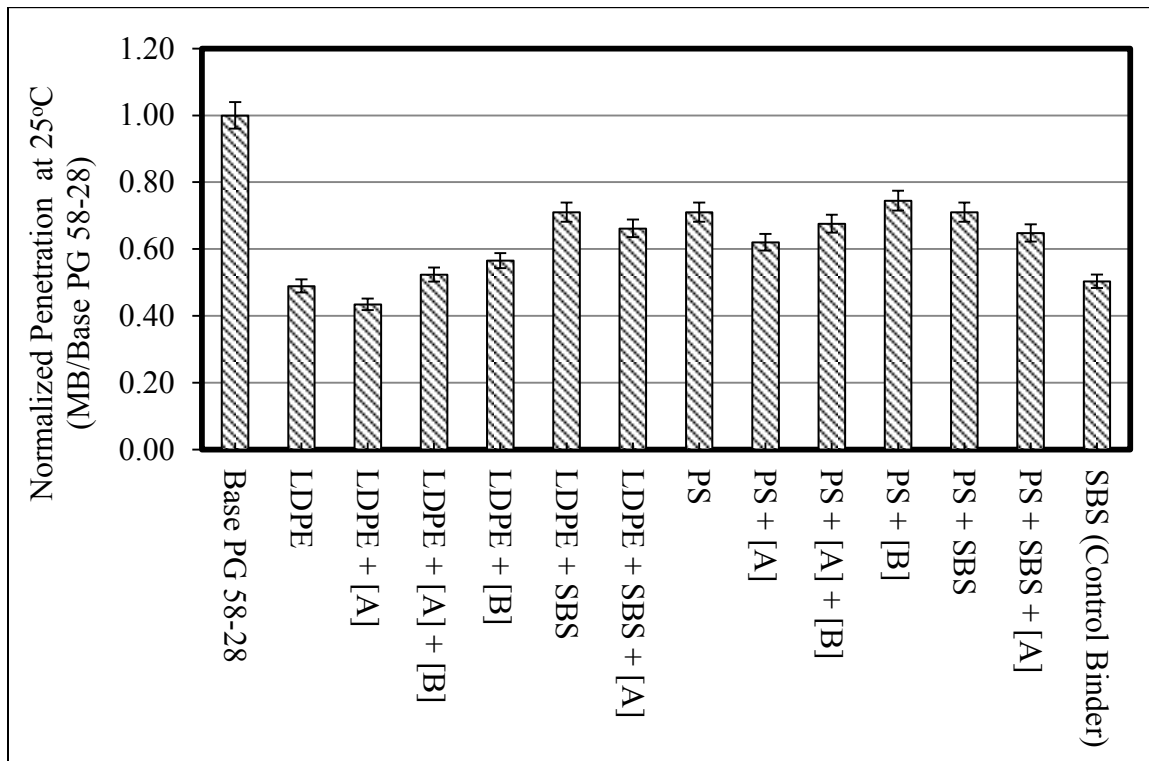


Figure 4-24 Penetration values of modified binder at testing temperature of 25°C

CHAPTER 5: CONCLUSIONS AND RECOMMENDATIONS

5.1. Conclusions

The objective of this study was to investigate the feasibility of utilizing recycled plastics generated in Atlantic Canada as more cost effective alternatives to the typical virgin modifier (SBS) for application of HMA. The experimental work entailed analyzing physical characteristics of a range of modified binders and HMA mixtures containing recycled Low Density Poly-Ethylene (LDPE), recycled Poly-styrene (PS), and virgin Styrene-Butadiene-Styrene (SBS). The following conclusions can be drawn from the results:

- All Modified Binders (MBs) except the cross-linked recycled-LDPE met the criteria for performance grade specification of PG 64-28. The cross-linked recycled-LDPE was graded as PG 64-22;
- The Superpave™ rutting parameter of $G^*/\sin(\delta)$ was not able to predict the high temperature rutting susceptibility of modified binders as observed by the APA rutting results. The MSCR non-recoverable creep compliance (J_{nr}) provided a stronger correlation to mixture rutting results;
- Utilization of Recycled Plastic Modifiers (RPMs) resulted in significant increase in high temperature stiffness of the base-asphalt. Recycled plastics may behave similarly to engineered virgin-SBS modifier as an effective means of increasing the contribution of binders to rutting resistance while limiting the increase in cost of the modified binder;
- All modified binders met the percent difference criterion between the J_{nr} at stress levels of 0.1 and 3.2 kPa, indicating that the modifiers used in this study were not stress sensitive;
- Mixtures containing RPM exhibited similar tensile strengths as the virgin-SBS modifier;
- The effect of recycled plastic modifiers on low temperature characteristics of base-asphalt was observed to be marginal;
- Modified binders containing RPMs resulted in lower laboratory mixing and compaction temperatures compared to the SBS-modified control binder. This may

- indicate that mixtures modified with RPMs might result in fewer emissions during mixing at the hot-mix plant and construction in the field, and lower fuel consumption;
- All modified binders exhibited no significant separation compared to the SBS-modified control binder. However, the addition of cross-linking agent, and oil softener, as well as co-blending with virgin polymer did reduce the separation tendency of MBs containing only recycled-plastic modifiers (RPM);
 - All MBs were found to be well above the minimum limit of 99.0 percent solubility in Trichloroethylene solvent;
 - The MSCR average percent recover (R%) provided a stronger correlation to mixture rutting results than ER test; and
 - Results presented in this thesis validated claims that the MSCR test provides a better understanding of polymer behaviour at high temperature as well as quality of modification compare to Superpave™ PG specification. Moreover, the one test of MSCR could potentially eliminate the need of performing additional Superpave™-Plus tests such as Elastic Recovery (ER).

In conclusion, this study suggests that recycled plastics can be successfully utilized as cost effective, environment-friendly, and energy efficient asphalt binder modifiers for the construction and preservation of roads and highways. The utilization of recycled plastics in pavement applications (i.e. HMA) not only may result in economic benefits, it also creates environmental benefits by creating a market for such underutilized resources, as opposed to a disposal mechanism or energetic recycling (i.e. incineration, pyrolysis, gasification).

5.2.Recommendations for Future Work

For future, a strong emphasize must be put on the development of RPM modified binders that allow production and construction of asphalt mixtures at much lower temperatures than HMA. By reducing production temperatures, additional benefit of reduced emissions from burning fuels and odors generated at the hot-plant as well as the construction site can be achieved.

REFERENCES

- [1] B. N. Mills, S. L. Tighe, J. Andrey, J. T. Smith, S. Parm and K. Huen, "The Road Well-Traveled: Implications of Climate Change for Pavement Infrastructure in Southern Canada," Waterloo, Ontario, Canada, 2007.
- [2] Environment Canada, *Weathering of building infrastructure and the changing climate: adaptation options*, J. K. a. N. C. Heather Auld, Ed., 2007.
- [3] S. L. Tighe, J. Smith, B. Mills and J. Andrey, "Using the MEPDG to Assess Climate Change Impacts on Southern Canadian Roads," in *the 7th International Conference on Managing Pavements and Other Roadway Assets (ICP7)*, Calgary, Alberta, Canada, 2008.
- [4] R. Hass and G. Kennepohl, "The Legacy of Four Decades of Asphalt Research at Canadian Universities," in *Canadian Technical Asphalt Association*, Edmonton, Alberta, Canada, 2010.
- [5] C. Macosko, R. Larson, T. Lodge, J. Mewis and M. Tirrel, "Rheology principles, measurements and applications," University of Minnesota, 1994.
- [6] PHA Consulting Associates, "Plastics Study," Resource Recovery Fund Board, Halifax, 2006.
- [7] Resource Recovery Fund Board Inc. (RRFB Nova Scotia), "<http://www.rrfb.com>," 2013. [Online]. Available: <http://www.rrfb.com/problematic-waste.asp>.
- [8] P. Haberl, "Method of mixing materials of construction with minor amounts of addition agents". Patent US4228052 A, 1980.
- [9] S. Zoorab and L. Suparma, "Laboratory design and performance of improved bituminous composites utilizing recycled plastics packaging waste," in *Technology watch and innovation in the construction industry*, Brussels, Belgium, 2000.
- [10] S. Zhang, Z. Zhang, K. Pal, Z. Xin, J. Suh and J. Kim, "Prediction of mechanical properties of waste polypropylene/waste ground rubber tire powder blends using artificial neural networks," *Materials and Design*, pp. 3624-3629, 2010.
- [11] R. S. S. S. Vasudevan R, "Utilization of plastics waste in construction of flexible pavement," in *The nations seminar on "Integrated development of rural & arterial road network for socio-economic growth"*, 2003.

- [12] M. Naskar, T. Chaki and K. Reddy, "Effect of waste plastic as modifier on thermal stability and degradation kinetics of bitumen/waste plastics blend," *Thermochimica Acta* 509, pp. 128-134, 2010.
- [13] Natural Sciences and Engineering Research Council of Canada (NSERC), "Industrial Postgraduate Scholarships Program," 2013. [Online]. Available: http://www.nserc-crsng.gc.ca/students-etudiants/pg-cs/ips-besii_eng.asp.
- [14] General Liquids Canada Ltd. (GLC), "General Liquids Canada Ltd. (GLC)," 2013. [Online]. Available: <http://general-liquids.ca/>.
- [15] Dalhousie University, "Centres and Institutes," 2013. [Online]. Available: http://www.dal.ca/academics/academic_calendars/Undergraduate_Calendar_2013_2014/Centres_and_Institutes.html.
- [16] Asphalt Institute, The Asphalt Binder Handbook, MS-26, USA: Asphalt Institute, 2011.
- [17] Asphalt Institute, Asphalt Binder Testing MS-25, second ed., Asphalt Institute, 2008.
- [18] Bahia, H. U., W. P. Hislop, H. Zhai and A. Rangel, "NCHRP Report 459, Characterization of Modified Asphalt Binders in Superpave Mix Design. Prepared for the National Cooperative Highway Research Program," Transportation Research Board (TRB), Washington, D.C., 2001.
- [19] National Cooperative Highway Research Program (NCHRP), A Manual for Design of Hot-Mix Asphalt with Commentary, Washington: Transportation Research Board, 2011.
- [20] G. Dore and H. K. Zubeck, Cold Regions Pavement Engineering, ASCE Press, 2009.
- [21] Asphalt Institute, "Superpave Mix Design," 2001.
- [22] R. McGennis, R. Anderson, T. Kennedy and M. Solaimanian, "Background of Superpave Asphalt Mixture Design and Analysis," Federal Highway Administration (FHWA), 1995.
- [23] F. Roberts, P. Kandhal, E. Brown, D.-Y. Lee and T. Kennedy, Hot Mix Asphalt Materials, Design and Construction, 2nd ed., Lanham Md., 1996.
- [24] G. Dore and Y. Savard, "Analysis of Seasonal Pavement Deterioration," *Transportation Research Board*, 1998.

- [25] H. Bahia and D. Anderson, "The New Proposed Rheological Properties of Asphalt Cement," vol. ASTM STP 1241, pp. 1-27, 1995.
- [26] C. L. Barnes and J.-F. Trottiera, "Evaluating Laboratory-Induced Asphalt Concrete Moisture Damage Using Surface Waves," *International Journal of Pavement Engineering*, vol. 11, no. 6, 2010.
- [27] D. A. Anderson and T. W. Kennedy, "Development of SHRP Binder Specification," *The Association of Asphalt Paving Technologists*, vol. 62, pp. 481-507, 1993.
- [28] B. Vallerga, C. Monismith and K. Granthem, "A Study of Some Factors Influencing the Weathering of Paving Asphalts," in *AAPT*, 1957.
- [29] Finn and N. Fred, "Factors involved in the Design of Asphaltic Pavement Structures," NCHRP, 1967.
- [30] R. Traxler, "Durability of Asphalt Cements," in *AAPT*, 1963.
- [31] M. Mirza and M. Witczak, "Development of a Global Aging System for Short and Long Term Aging of Asphalt Cements," *Journal of the Association of Asphalt Pavement Technologists*, vol. 64, p. 393, 1995.
- [32] L. Johansson, *Aging of Road Bitumens-State of the Art*, Stockholm: Royal Institute of Technology, 1998.
- [33] P. Kandhal, L. Sandvig, W. Koehler and M. Wenger, *Asphalt Viscosity-Related Properties of In-service Pavements in Pennsylvania*, ASTM, 1973.
- [34] J. Way and T. Wilkey, "Heating, Mixing and Storing Modified Asphalt," Heatec, Inc, Chattanooga, Tennessee, 1996.
- [35] D. R. a. D. R., "Practical Use of the MSCR Test: Characterization of SBS Dispersion and Other Additives in PMA Binders," in *Transportation Research Board Annual Meeting*, Washington, D.C., 2009.
- [36] J. Read and D. Whiteoak, *The shell bitumen handbook*, 5th ed., Thomas Telford Publishing, 2003.
- [37] M. S.-G. Dave Newcomb, "Polymer Literature Review," Minnesota Local Road Research Board (MLRRB), 1995.

- [38] C. Daranga, C. S. Clopotel, A. Mofolasayo and H. U. and Bahia, "Storage Stability and Effect of Mineral Surface on Polyphosphoric Acid (PPA) Modified Asphalt Binders," in *Transportation Research Board Annual Meeting*, Washington, D.C., 2009.
- [39] A. A. o. S. H. a. T. Officials, Standard Specification for Superpave Volumetric Mix Design, M 323-13, Washington, DC: AASHTO, 2013.
- [40] American Association of State and Highway Transportation Officials (AASHTO) M320. "Standard Specification for Performance-Graded Asphalt Binder", Standard Specifications for Transportation Materials and Methods of Sampling and Testing, Part 1B, Wahington, D.C., 2010.
- [41] American Association of State Highway and Transportation Officials (AASHTO) T 240, "Effect of Heat and Air on a Moving Film of Asphalt Binder (Rolling Thin-Film Oven Test)," 2009.
- [42] American Association of State Highway and Transportation Officials (AASHTO) R 28, "Accelerated Aging of Asphalt Binder Using a Pressurized Aging Vessel (PAV)," in *Standard Specifications for Transportation Materials and Methods of Sampling and Testing, Part 1B*, Washington, D.C., 2012.
- [43] American Association of State Highway and Transportation Officials (AASHTO) T 316, "Viscosity Determination of Asphalt Binder Using Rotational Viscometer," in *Standard Specifications for Transportation Materials and Methods of Sampling and Testing, Part 2B*, Washington, D.C., 2011.
- [44] ASTM International, "Standard Viscosity-Temperature Chart for Asphalts ASTM D2493/D2493M," West Conshohocken, PA, 2009.
- [45] R. C. West, D. E. Watson and P. A. Turner, "Mixing and Compaction Temperatures of Asphalt Binders in Hot-Mix Asphalt," Transportation Research Board, Washington DC, 2012.
- [46] American Association of State Highway and Transportation Officials (AASHTO) T 315, "Determining the Rheological Properties of Asphalt Binder Using a Dynamic Shear Rheometer (DSR)," in *Standard Specifications for Transportation Materials and Methods of Sampling and Testing, Part 2B*, Washington, D.C., AASHTO, 2012.
- [47] H. U. Bahia, "Modeling of asphalt Binder Rheology and Its Application to Modified Binders," in *Modeling of Asphalt Concrete*, McGraw-Hill Construction, 2009, pp. 11-56.

- [48] R. D'Angelo, R. Dongre and G. Reinke, "Evaluation of Repeated Creep and Recovery Test Method as an Alternative to SHRP+ Requirements for Polymer Modified Asphalt Binders," 2006.
- [49] H. Bahia and D. Anderson, "The Pressure Aging Vessel (PAV): A Test to Simulate Rheological Changes Due to Field Aging," *ASTM Special Technical Publication*, vol. 1241, 1994.
- [50] ASM Internation, Standard Test Methods for Flexural Properties of Unreinforced and Reinforced Plastics and Electrical Insulating Materials, ASTM D790, 2010.
- [51] American Association of State Highway and Transportation Officials (AASHTO) MP 19, "Standard Specification for Performance-Graded Asphalt Binder Using Multiple Stress Creep Recovery (MSCR) Test," in *AASHTO PROVISIONAL STANDARDS*, Washington, D.C., 2010.
- [52] American Association of State Highway and Transportation Officials (AASHTO) TP 70, "Standard Method of Test for Multiple Stress Creep Recovery (MSCR) Test of Asphalt Binder Using a Dynamic Shear Rheometer (DSR)," in *AASHTO Provisional Standards*, Washington, D.C, 2012.
- [53] R. D'Angelo, R. Kluttz, R. Dongre, K. Stephens and L. Zanzotto, "Revision of the Superpave High Temperature Binder Specification: The Multiple Stress Creep Recovery Test," *ASPHALT PAVING TECHNOLOGY*, vol. 76, no. 123, 2007.
- [54] H. Bahia, N. TABATABAEE, C. CLOPOTEL and A. GOLALIPOUR, "Evaluation of the MSCR Test for Modified Binder Specification," in *Proceedings of the Fifty-Sixth Annual Conference of the Canadian Technical Asphalt Association (CTAA)* , Quebec City, Quebec, 2011.
- [55] U. Isacson and X. Lu, "Testing and appraisal of polymer modified road bitumens-state of the art," *Materials and Structures* 28, pp. 139-159, 1995.
- [56] Nova Scotia Transportation and Infrastructure Renewal (NSTIR), "Division 4 (Pavements), Section 4 (Asphalt Concrete Hot Mixed-Hot Placed)," in *Standard Specification, Highway Construction and Maintenance*, Halifax NS Canada, Nova Scotia Transportation and Infrastructure Renewal (NSTIR), 2011.
- [57] American Association of State Highway and Transportation Officials (AASHTO) T 313, "Determining the Flexural Creep Stiffness of Asphalt Binder Using the Bending Beam Rheometer (BBR)," in *Standard Specifications for Transportation Materials and Methods of Sampling and Testing, Part 2B*, Washington, D.C., 2012.

- [58] American Association of State Highway and Transportation Officials (AASHTO) T 301, "Elastic Recovery Test of Asphalt Materials by Means of a Ductilometer," in *Standard Specifications for Transportation Materials and Methods of Sampling and Testing, Part 2B*, Washington, D.C., 2011.
- [59] American Association of State Highway and Transportation Officials (AASHTO) T 49, Standard Method of Test for Penetration of Bituminous Materials, 2011.
- [60] ASTM International D 7173, "Standard Practice for Determining the Separation Tendency of Polymer from Polymer Modified Asphalt," West Conshohocken, PA, 2011.
- [61] American Association of State Highway and Transportation Officials (AASHTO) T 53, "Softening Point of Bitumen (Ring-and-Ball Apparatus)," in *Standard Specifications for Transportation Materials and Methods of Sampling and Testing, Part 2A*, Washington, D.C., 2009.
- [62] American Association of State Highway and Transportation Officials (AASHTO) T 44, "Solubility of Bituminous Materials," in *Standard Specifications for Transportation Materials and Methods of Sampling and Testing, Part 2A*, Washington, D.C., 2011.
- [63] ASTM International D 6926, Standard Practice for Preparation of Bituminous Specimens Using Marshall Apparatus, 2010.
- [64] American Association of State Highway and Transportation Officials (AASHTO) T 209, Standard Method of Test for Theoretical Maximum Specific Gravity (Gmm) and Density of Hot Mix Asphalt (HMA), 2012.
- [65] American Association of State Highway and Transportation Officials (AASHTO) T 166, Standard Method of Test for Bulk Specific Gravity (Gmb) of Compacted Hot Mix Asphalt (HMA) Using Saturated Surface-Dry Specimens, 2013.
- [66] ASTM International D 6297, Standard Test Method for Marshall Stability and Flow of Bituminous Mixtures, 2006.
- [67] National Asphalt Pavement Association (NAPA), "Mix Design Techniques-Part I," NAPA, 1982.
- [68] American Association of State Highway and Transportation Officials (AASHTO) PP 060, Standard Practice for Preparation of Cylindrical Performance Test Specimens Using the Superpave Gyrotory Compactor (SGC), AASHTO, 2013.

- [69] American Association of State Highway and Transportation Officials (AASHTO) T 340, "Standard Method of Test for Determining the Rutting Susceptibility of Hot Mix Asphalt (APA) Using the Asphalt Pavement Analyzer (APA)," in *Standard Specifications for Transportation Materials and Methods of Sampling and Testing, Part 2B*, Washington, D.C, 2010.
- [70] ASTM International, "Standard Test Method for Indirect Tensile (IDT) Strength of Bituminous Mixtures ASTM D6931," in *Annual book of ASTM standards*, West Conshohocken, PA, 2012.
- [71] American Association of State Highway and Transportation Officials (AASHTO) T 283, Standard Method of Test for Resistance of Compacted Hot Mix Asphalt (HMA) to Moisture-Induced Damage, AASHTO, 2011.
- [72] M. Solaimanian, J. Harvey, M. Tahmoressi and V. Tandon, *Test Methods for Determination of Moisture Damage for Hot-Mix Asphalt Pavements*, Transportation Research Board (TRB), 2003.
- [73] K. C. Mahboub, "An Introduction to Superpave," in *Pavement Analysis and Design*, Upper Saddle River, NJ, Pearson Education, Inc, 2004.
- [74] M. B. Rajib and E.-k. Tahar, *Pavement Engineering : principles and practice*, Boca Raton: Taylor & Francis Group, 2009.
- [75] Transportation Research Board (TRB), *National Cooperative Highway Research Program Overview*, 2013.
- [76] Canadian Strategic Highway Research Program, "Canadian Strategic Highway Research Program," 2013. [Online]. Available: <http://www.cshrp.org/english/programoverview.html>.

APPENDIX A

(TEST RESULTS)

Hot-Mix Asphalt (HMA) Concrete Mix Design

Aggregate Physical Properties

Property	Coarse Aggregate			Fine Aggregate			Combined	Materials Sources		
	CA1	CA2	CA3	FA1	FA2	FA3				
Gsb	2.706			2.663	2.660	2.588	2.673	CA1	14-mm	Rocky Lake Quarry
Gmm	-			-	-	-	Specification	CA2	-	-
Absorption	0.47			0.97	0.80	0.9	Max. 1.75	CA3	-	-
SS Soundness	0.8			3.2	3.5	1.9	Max 10	FA1	DCF	Rocky Lake Quarry
Micro Deval	9.9			-	-	-	Max 20	FA2	WCF	Rocky Lake Quarry
LA Abrasion	13.8			-	-	-	-	FA3	Blend Sand	Cary Pit
PN	123			-	-	-	-	AC	PG 64-28P	Polymer Research GLC/DAL
Flat & Elong	9.5			65	96	73	Min. 50			
% Fractured	100			46.4	46.3	51.3	Min. 45			

Aggregate Blend Information

Sieve Size	CA1	CA2	CA3	FA1	FA2	FA3	Cumulative	Aggregate Breakdown	Design Blend	NSTIR Specification
% Used	44.2	0	0	19.9	25.9	10	100			
28mm	100.0			100.0	100.0	100.0	100.0	0	100.0	-
20mm	100.0			100.0	100.0	100.0	100.0	0.0	100.0	100
14mm	100.0			100.0	100.0	100.0	100.0	0.0	100.0	95-100
10mm	67.4			100.0	100.0	99.9	85.6	1.5	87.1	-
7.1mm	47.9			99.9	99.9	99.0	76.8	1.5	78.3	-
5mm	3.9			92.8	92.0	95.9	53.6	1.5	55.1	45-68
2.5mm	1.2			59.8	53.9	84.9	34.9	1.5	36.4	25-55
1.25mm	1.0			39.5	31.0	66.8	23.0	1.5	24.5	-
630µm	0.9			27.9	18.5	39.4	14.7	1.5	16.2	-
315µm	0.8			21.0	11.6	17.1	9.2	1.5	10.7	5-20
160µm	0.8			15.9	6.6	6.7	5.9	1.5	7.4	-
80µm	0.7			12.0	3.8	3.7	4.1	1.5	5.6	2-6.5

Notes:

Total Asphalt Cement (AC) Target =	5.50%	Binder Grade :	PG 64-28P
Specific Gravity of AC =	1.014	Mix Type :	NSTIR C-HF
Condition Temperature from Temp/Visc Charts =	See PG worksheet	Analysis Performed By:	Sina Varamini, B.Eng. E.I.T
Compaction blows per face =	75 blows/sid		

Hot-Mix Asphalt Concrete Mix Design (Marshall)

Binder Grade :	PG 64-28P
Mix Type:	NSTIR C-HF
Analysis Performed By:	Sina Varamini, B.Eng. E.I.T

HMA Volumetric Properties							
	Individual Mix Data					D	
PbV	4.50	4.20	4.50	4.80	5.10		
Pb	4.50	5.00	5.50	6.00	6.50	5.50	
Gmm	2.531	2.511	2.492	2.473	2.454	2.492	
Gmb	2.361	2.382	2.400	2.416	2.430	2.400	
Gse	2.723						
Pba	0.69						
Pbe	3.84	4.34	4.85	5.35	5.85	4.85	Specification
VMA	15.7	15.4	15.2	15.0	15.0	15.2	Min 14.0
AV	6.72	5.15	3.69	2.30	0.98	3.69	3.5 - 4.5
VFA	57.1	66.4	75.6	84.7	93.4	75.6	65-78
STAB	12.0	11.2	12.2	11.8	13.1	12.1	Min 7.5
FLOW	3.4	3.5	3.3	3.4	4.0	3.5	2 - 4
D/Pbe	1.45	1.28	1.14	1.04	0.95	1.14	-
AFT	7.73	8.79	9.86	10.94	12.04	9.86	-

Terminology

- PbV = Virgin AC by weight of Aggregate %
- PbRAP = RAP AC by weight of Mixture %
- Pb = Total AC Content of Mixture %
- Gmm = Mixture Maximum Specific Gravity (g/cm^3)
- Gmb = Compacted Bulk Specific Gravity (g/cm^3)
- Gse = Aggregate Effective Specific Gravity (g/cm^3)
- Pba = Percent Binder Absorbed %
- Pbe = Effect Asphalt Binder%
- VMA = Voids In Mineral Aggregate %
- AV = Air Voids % ASTM D3203
- VFA = Voids Filled with Asphalt %
- STAB = Marshall Stability (kN) ASTM D1559
- FLOW = Marshall Flow (mm) ASTM D1559
- D/Pbe = Dust to Effective Binder Ratio
- AFT = Average Film Thickness

Sample Production Flow-chart

Sample I.D	Sample Name	RPM	VM	Cross linker [A]	Oil Softener [B]
C1	SBS	-	SBS	-	-
A1	PS+[A]	PS	-	YES	-
A2	PS+[A]+[B]	PS	-	YES	YES
A3	PS	PS	-	-	-
A4	PS+[B]	PS	-	-	YES
B1	LDPE+[A]	LDPE	-	YES	-
B2	LDPE+[A]+[B]	LDPE	-	YES	YES
B3	LDPE	LDPE	-	-	-
B4	LDPE+[B]	LDPE	-	-	YES
D1	LDPE+SBS+[A]	LDPE	SBS (Reduced)	YES	-
D2	LDPE+SBS	LDPE	SBS (Reduced)	-	-
D3	PS+SBS+[A]	PS	SBS (Reduced)	YES	-
D4	PS+SBS	PS	SBS (Reduced)	-	-

Analysis Performed By: *Sina Varamini, B.Eng. E.I.T*

Base Asphalt Binder: *PG 58-28 (provided by GLC)*

**Performance Grade Modified Asphalt
Laboratory Analysis Report**

Sample ID/GLC ID: PS+[A] / A1		Date Sampled: Jan-22/2013	
Module: 2	Sample Source: Tank 6-GLC	Date Tested: -	
	Binder Target: PG 64-28	Report Date: -	
PG Specification: AASHTO M 320-10			
Modifiers Composition			
Polymer: PS	Cross-linker: YES	Oil Softener: NO	
Test	Test Method	Specification	Test Result
Unaged Binder			
Solubility in Trichloroethylene	AASHTO T 44	Minimum 99.0%	>99.0
Rotational Viscosity at 135°C	AASHTO T 316	Maximum 3.00 Pa*s Report, Pa*s	0.439
Dynamic Shear Test Temperature: 64 °C [G*/sin(δ), 10 rad/sec]	AASHTO T 315	Minimum 1.00 kPa	1.32
Rolling Thin-Film Oven Residue (AASHTO T 240)			
Mass Change	AASHTO T 240	Maximum ±1.00%	0.2900
Dynamic Shear Test Temperature: 64 °C [G*/sin(δ), 10 rad/sec]	AASHTO T 315	Minimum 2.20 kPa	3.98
Pressurized Aging Vessel (PAV) Residue [AASHTO R 28]			
Dynamic Shear Test Temperature: 22 °C [G*/sin(δ), 10 rad/sec]	AASHTO T 315	Maximum 5000 kPa	3960
Creep Stiffness Test Temperature: -18 & -12 °C [at 60 sec]	AASHTO T 313	Maximum 300 MPa	207 & 101
Slope, m-value Test Temperature: -18 & -12 °C [at 60 sec]	AASHTO T 313	Minimum 0.300	0.303 & 0.3475
PG Plus Tests			
Elastic Recovery (Original Residue) Test Temperature: 10 °C	AASHTO T 301	Report, %	11.25
Penetration (unaged Residue)	AASHTO T 49	Report, dmm	90
Separation test (unaged Residue)	ASTM D 7173	Report, top & bottom difference	1.40
		Final Binder PG	PG 64-28
Analysis Performed By: Sina Varamini, B.Eng. E.I.T			

Sample ID/GLC ID: <u>PS+[A]+[B] / A2</u>		Date Sampled: <u>Feb-18/2013</u>	
Module: <u>2</u>	Sample Source: <u>Tank 6-GLC</u>	Date Tested: <u>-</u>	
	Binder Target: <u>PG 64-28</u>	Report Date: <u>-</u>	
PG Specification: <u>AASHTO M 320-10</u>			
Modifiers Composition			
Polymer: <u>PS</u>	Cross-linker: <u>YES</u>	Oil Softener: <u>YES</u>	
Test	Test Method	Specification	Test Result
Unaged Binder			
Solubility in Trichloroethylene	AASHTO T 44	Minimum 99.0%	>99.0
Rotational Viscosity at 135°C	AASHTO T 316	Maximum 3.00 Pa*s Report, Pa*s	0.416
Dynamic Shear Test Temperature <u>64</u> °C [G*/sin(δ), 10 rad/sec]	AASHTO T 315	Minimum 1.00 kPa	1.16
Rolling Thin-Film Oven Residue (AASHTO T 240)			
Mass Change	AASHTO T 240	Maximum ±1.00%	0.2100
Dynamic Shear Test Temperature <u>64</u> °C [G*/sin(δ), 10 rad/sec]	AASHTO T 315	Minimum 2.20 kPa	3.27
Pressurized Aging Vessel (PAV) Residue [AASHTO R 28]			
Dynamic Shear Test Temperature <u>22</u> °C [G*/sin(δ), 10 rad/sec]	AASHTO T 315	Maximum 5000 kPa	2637
Creep Stiffness Test Temperature <u>-18 & -12</u> °C [at 60 sec]	AASHTO T 313	Maximum 300 MPa	181 & 84.2
Slope, m-value Test Temperature <u>-18 & -12</u> °C [at 60 sec]	AASHTO T 313	Minimum 0.300	0.310 & 0.369
PG Plus Tests			
Elastic Recovery (Original Residue) Test Temperature <u>10</u> °C	AASHTO T 301	Report, %	10.00
Penetration (unaged Residue)	AASHTO T 49	Report, dmm	99
Separation test (unaged Residue)	ASTM D 7173	Report, top & bottom difference	1.60
		Final Binder PG	PG 64-28
Analysis Performed By: <i>Sina Varamini, B.Eng. E.I.T</i>			

Sample ID/GLC ID: PS / A3		Date Sampled: Jan 30/2013	
Module: 2	Sample Source: Tank 6-GLC	Date Tested: -	
	Binder Target: PG 64-28	Report Date: -	
PG Specification: AASHTO M 320-10			
Modifiers Composition			
Polymer: PS	Cross-linker: NO	Oil Softener: NO	
Test	Test Method	Specification	Test Result
Unaged Binder			
Solubility in Trichloroethylene	AASHTO T 44	Minimum 99.0%	>99.0
Rotational Viscosity at 135°C	AASHTO T 316	Maximum 3.00 Pa*s Report, Pa*s	0.397
Dynamic Shear Test Temperature: 64 °C [G*/sin(δ), 10 rad/sec]	AASHTO T 315	Minimum 1.00 kPa	1.11
Rolling Thin-Film Oven Residue (AASHTO T 240)			
Mass Change	AASHTO T 240	Maximum ±1.00%	0.2900
Dynamic Shear Test Temperature: 64 °C [G*/sin(δ), 10 rad/sec]	AASHTO T 315	Minimum 2.20 kPa	3.07
Pressurized Aging Vessel (PAV) Residue [AASHTO R 28]			
Dynamic Shear Test Temperature: 22 °C [G*/sin(δ), 10 rad/sec]	AASHTO T 315	Maximum 5000 kPa	3406
Creep Stiffness Test Temperature: -18 & -12 °C [at 60 sec]	AASHTO T 313	Maximum 300 MPa	209 & 99.2
Slope, m-value Test Temperature: -18 & -12 °C [at 60 sec]	AASHTO T 313	Minimum 0.300	0.317 & 0.351
PG Plus Tests			
Elastic Recovery (Original Residue) Test Temperature: 10 °C	AASHTO T 301	Report, %	10.00
Penetration (unaged Residue)	AASHTO T 49	Report, dmm	102
Separation test (unaged Residue)	ASTM D 7173	Report, top & bottom difference	2.50
		Final Binder PG	PG 64-28
Analysis Performed By: Sina Varamini, B.Eng. E.I.T			

**Performance Grade Modified Asphalt
Laboratory Analysis Report**

Sample ID/GLC ID: PS+[B]/ A4		Date Sampled: Feb-8/2013	
Module: 2	Sample Source: Tank 6-GLC	Date Tested: -	
	Binder Target: PG 64-28	Report Date: -	
PG Specification: AASHTO M 320-10			
Modifiers Composition			
Polymer: PS	Cross-linker: NO	Oil Softener: YES	
Test	Test Method	Specification	Test Result
Unaged Binder			
Solubility in Trichloroethylene	AASHTO T 44	Minimum 99.0%	>99.0
Rotational Viscosity at 135°C	AASHTO T 316	Maximum 3.00 Pa*s Report, Pa*s	0.397
Dynamic Shear Test Temperature: 64 °C [G*/sin(δ), 10 rad/sec]	AASHTO T 315	Minimum 1.00 kPa	1.02
Rolling Thin-Film Oven Residue (AASHTO T 240)			
Mass Change	AASHTO T 240	Maximum ±1.00%	0.3500
Dynamic Shear Test Temperature: 64 °C [G*/sin(δ), 10 rad/sec]	AASHTO T 315	Minimum 2.20 kPa	3.04
Pressurized Aging Vessel (PAV) Residue [AASHTO R 28]			
Dynamic Shear Test Temperature: 22 °C [G*/sin(δ), 10 rad/sec]	AASHTO T 315	Maximum 5000 kPa	2920
Creep Stiffness Test Temperature: -18 & -12 °C [at 60 sec]	AASHTO T 313	Maximum 300 MPa	180 & 89.5
Slope, m-value Test Temperature: -18 & -12 °C [at 60 sec]	AASHTO T 313	Minimum 0.300	0.311 & 0.372
PG Plus Tests			
Elastic Recovery (Original Residue) Test Temperature: 10 °C	AASHTO T 301	Report, %	5.00
Penetration (unaged Residue)	AASHTO T 49	Report, dmm	110
Separation test (unaged Residue)	ASTM D 7173	Report, top & bottom difference	1.80
		Final Binder PG	PG 64-28
Analysis Performed By: Sina Varamini, B.Eng. E.I.T			

Sample ID/GLC ID: <u>LDPE+[A]/ B1</u>		Date Sampled: <u>Jan-22/2013</u>	
Module: <u>2</u>	Sample Source: <u>Tank 6-GLC</u>	Date Tested: <u>-</u>	
	Binder Target: <u>PG 64-28</u>	Report Date: <u>-</u>	
PG Specification: <u>AASHTO M 320-10</u>			
Modifiers Composition			
Polymer: <u>LDPE</u>	Cross-linker: <u>YES</u>	Oil Softener: <u>NO</u>	
Test	Test Method	Specification	Test Result
Unaged Binder			
Solubility in Trichloroethylene	AASHTO T 44	Minimum 99.0%	99.8
Rotational Viscosity at 135°C	AASHTO T 316	Maximum 3.00 Pa*s Report, Pa*s	0.646
Dynamic Shear Test Temperature <u>64</u> °C [G*/sin(δ), 10 rad/sec]	AASHTO T 315	Minimum 1.00 kPa	2.54
Rolling Thin-Film Oven Residue (AASHTO T 240)			
Mass Change	AASHTO T 240	Maximum ±1.00%	0.3100
Dynamic Shear Test Temperature <u>64</u> °C [G*/sin(δ), 10 rad/sec]	AASHTO T 315	Minimum 2.20 kPa	7.29
Pressurized Aging Vessel (PAV) Residue [AASHTO R 28]			
Dynamic Shear Test Temperature <u>22</u> °C [G*/sin(δ), 10 rad/sec]	AASHTO T 315	Maximum 5000 kPa	4720
Creep Stiffness Test Temperature <u>-18 & -12</u> °C [at 60 sec]	AASHTO T 313	Maximum 300 MPa	236.5 & 113
Slope, m-value Test Temperature <u>-18 & -12</u> °C [at 60 sec]	AASHTO T 313	Minimum 0.300	0.291 & 0.332
PG Plus Tests			
Elastic Recovery (Original Residue) Test Temperature <u>10</u> °C	AASHTO T 301	Report, %	13.750
Penetration (unaged Residue)	AASHTO T 49	Report, dmm	63.000
Separation test (unaged Residue)	ASTM D 7173	Report, top & bottom difference	1.200
		Final Binder PG	PG 64-22
Analysis Performed By: <i>Sina Varamini, B.Eng. E.I.T</i>			

Sample ID/GLC ID: <u>LDPE+[A]+[B] / B2</u>		Date Sampled: <u>Jan-22/2013</u>	
Module: <u>2</u>	Sample Source: <u>Tank 6-GLC</u>	Date Tested: <u>-</u>	
	Binder Target: <u>PG 64-28</u>	Report Date: <u>-</u>	
PG Specification: <u>AASHTO M 320-10</u>			
Modifiers Composition			
Polymer: <u>LDPE</u>	Cross-linker: <u>YES</u>	Oil Softener: <u>YES</u>	
Test	Test Method	Specification	Test Result
Unaged Binder			
Solubility in Trichloroethylene	AASHTO T 44	Minimum 99.0%	99.9
Rotational Viscosity at 135°C	AASHTO T 316	Maximum 3.00 Pa*s Report, Pa*s	0.543
Dynamic Shear Test Temperature <u>64</u> °C [G*/sin(δ), 10 rad/sec]	AASHTO T 315	Minimum 1.00 kPa	1.77
Rolling Thin-Film Oven Residue (AASHTO T 240)			
Mass Change	AASHTO T 240	Maximum ±1.00%	0.2900
Dynamic Shear Test Temperature <u>64</u> °C [G*/sin(δ), 10 rad/sec]	AASHTO T 315	Minimum 2.20 kPa	4.92
Pressurized Aging Vessel (PAV) Residue [AASHTO R 28]			
Dynamic Shear Test Temperature <u>22</u> °C [G*/sin(δ), 10 rad/sec]	AASHTO T 315	Maximum 5000 kPa	3660
Creep Stiffness Test Temperature <u>-18 & -12</u> °C [at 60 sec]	AASHTO T 313	Maximum 300 MPa	184 & 98.9
Slope, m-value Test Temperature <u>-18 & -12</u> °C [at 60 sec]	AASHTO T 313	Minimum 0.300	0.303 & 0.347
PG Plus Tests			
Elastic Recovery (Original Residue) Test Temperature <u>10</u> °C	AASHTO T 301	Report, %	11.250
Penetration (unaged Residue)	AASHTO T 49	Report, dmm	76.000
Separation test (unaged Residue)	ASTM D 7173	Report, top & bottom difference	1.700
		Final Binder PG	PG 64-28
Analysis Performed By: <i>Sina Varamini, B.Eng. E.I.T</i>			

Sample ID/GLC ID: <u>LDPE / B3</u>		Date Sampled: <u>Jan-22/2013</u>	
Module: <u>2</u>	Sample Source: <u>Tank 6-GLC</u>	Date Tested: <u>-</u>	
	Binder Target: <u>PG 64-28</u>	Report Date: <u>-</u>	
PG Specification: <u>AASHTO M 320-10</u>			
Modifiers Composition			
Polymer: <u>LDPE</u>	Cross-linker: <u>NO</u>	Oil Softener: <u>NO</u>	
Test	Test Method	Specification	Test Result
Unaged Binder			
Solubility in Trichloroethylene	AASHTO T 44	Minimum 99.0%	99.4
Rotational Viscosity at 135°C	AASHTO T 316	Maximum 3.00 Pa*s Report, Pa*s	0.415
Dynamic Shear Test Temperature <u>64</u> °C [G*/sin(δ), 10 rad/sec]	AASHTO T 315	Minimum 1.00 kPa	1.53
Rolling Thin-Film Oven Residue (AASHTO T 240)			
Mass Change	AASHTO T 240	Maximum ±1.00%	0.0300
Dynamic Shear Test Temperature <u>64</u> °C [G*/sin(δ), 10 rad/sec]	AASHTO T 315	Minimum 2.20 kPa	4.30
Pressurized Aging Vessel (PAV) Residue [AASHTO R 28]			
Dynamic Shear Test Temperature <u>22</u> °C [G*/sin(δ), 10 rad/sec]	AASHTO T 315	Maximum 5000 kPa	3780
Creep Stiffness Test Temperature <u>-18 & -12</u> °C [at 60 sec]	AASHTO T 313	Maximum 300 MPa	193 & 94.4
Slope, m-value Test Temperature <u>-18 & -12</u> °C [at 60 sec]	AASHTO T 313	Minimum 0.300	0.311 & 0.350
PG Plus Tests			
Elastic Recovery (Original Residue) Test Temperature <u>10</u> °C	AASHTO T 301	Report, %	13.500
Penetration (unaged Residue)	AASHTO T 49	Report, dmm	71.000
Separation test (unaged Residue)	ASTM D 7173	Report, top & bottom difference	2.300
		Final Binder PG	PG 64-28
Analysis Performed By: <i>Sina Varamini, B.Eng. E.I.T</i>			

Sample ID/GLC ID: <u>LDPE + [B] / B4</u>		Date Sampled: <u>Jan-30/2013</u>	
Module: <u>2</u>	Sample Source: <u>Tank 6-GLC</u>	Date Tested: <u>-</u>	
	Binder Target: <u>PG 64-28</u>	Report Date: <u>-</u>	
PG Specification: <u>AASHTO M 320-10</u>			
Modifiers Composition			
Polymer: <u>LDPE</u>	Cross-linker: <u>NO</u>	Oil Softener: <u>YES</u>	
Test	Test Method	Specification	Test Result
Unaged Binder			
Solubility in Trichloroethylene	AASHTO T 44	Minimum 99.0%	>99.0
Rotational Viscosity at 135°C	AASHTO T 316	Maximum 3.00 Pa*s Report, Pa*s	0.511
Dynamic Shear Test Temperature <u>64</u> °C [G*/sin(δ), 10 rad/sec]	AASHTO T 315	Minimum 1.00 kPa	1.66
Rolling Thin-Film Oven Residue (AASHTO T 240)			
Mass Change	AASHTO T 240	Maximum ±1.00%	0.3500
Dynamic Shear Test Temperature <u>64</u> °C [G*/sin(δ), 10 rad/sec]	AASHTO T 315	Minimum 2.20 kPa	4.75
Pressurized Aging Vessel (PAV) Residue [AASHTO R 28]			
Dynamic Shear Test Temperature <u>22</u> °C [G*/sin(δ), 10 rad/sec]	AASHTO T 315	Maximum 5000 kPa	
Creep Stiffness Test Temperature <u>-18 & -12</u> °C [at 60 sec]	AASHTO T 313	Maximum 300 MPa	198 & 102
Slope, m-value Test Temperature <u>-18 & -12</u> °C [at 60 sec]	AASHTO T 313	Minimum 0.300	0.301 & 0.356
PG Plus Tests			
Elastic Recovery (Original Residue) Test Temperature <u>10</u> °C	AASHTO T 301	Report, %	12.50
Penetration (unaged Residue)	AASHTO T 49	Report, dmm	82
Separation test (unaged Residue)	ASTM D 7173	Report, top & bottom difference	2.10
		Final Binder PG	PG 64-28
Analysis Performed By: <i>Sina Varamini, B.Eng. E.I.T</i>			

Sample ID/GLC ID: <u>SBS (Cont.) / C1</u>		Date Sampled: <u>Jan 22/2013</u>	
Module: <u>2</u>	Sample Source: <u>Tank 6-GLC</u>	Date Tested: <u>-</u>	
	Binder Target: <u>PG 64-28</u>	Report Date: <u>-</u>	
PG Specification: <u>AASHTO M 320-10</u>			
Modifiers Composition			
Polymer: <u>SBS</u>	Cross-linker: <u>NO</u>	Oil Softener: <u>NO</u>	
Test	Test Method	Specification	Test Result
Unaged Binder			
Solubility in Trichloroethylene	AASHTO T 44	Minimum 99.0%	>99.0
Rotational Viscosity at 135°C	AASHTO T 316	Maximum 3.00 Pa*s Report, Pa*s	0.686
Dynamic Shear Test Temperature <u>64</u> °C [G*/sin(δ), 10 rad/sec]	AASHTO T 315	Minimum 1.00 kPa	2.73
Rolling Thin-Film Oven Residue (AASHTO T 240)			
Mass Change	AASHTO T 240	Maximum ±1.00%	0.3100
Dynamic Shear Test Temperature <u>64</u> °C [G*/sin(δ), 10 rad/sec]	AASHTO T 315	Minimum 2.20 kPa	7.39
Pressurized Aging Vessel (PAV) Residue [AASHTO R 28]			
Dynamic Shear Test Temperature <u>22</u> °C [G*/sin(δ), 10 rad/sec]	AASHTO T 315	Maximum 5000 kPa	4140
Creep Stiffness Test Temperature <u>-18 & -12</u> °C [at 60 sec]	AASHTO T 313	Maximum 300 MPa	213 & 99
Slope, m-value Test Temperature <u>-18 & -12</u> °C [at 60 sec]	AASHTO T 313	Minimum 0.300	0.338 & 0.295
PG Plus Tests			
Elastic Recovery (Original Residue) Test Temperature <u>10</u> °C	AASHTO T 301	Report, %	55.00
Penetration (unaged Residue)	AASHTO T 49	Report, dmm	73
Separation test (unaged Residue)	ASTM D 7173	Report, top & bottom difference	0.60
		Final Binder PG	PG 64-28
Analysis Performed By: <i>Sina Varamini, B.Eng. E.I.T</i>			

**Performance Grade Modified Asphalt
Laboratory Analysis Report**

Sample ID/GLC ID: <u>LDPE+SBS+[A] / D1</u>		Date Sampled: <u>Feb-25/13</u>	
Module: <u>2</u>	Sample Source: <u>Tank 6-GLC</u>	Date Tested: <u>-</u>	
	Binder Target: <u>PG 64-28</u>	Report Date: <u>-</u>	
PG Specification: <u>AASHTO M 320-10</u>			
Modifiers Composition			
Polymer: <u>LDPE/SBS</u>	Cross-linker: <u>YES</u>	Oil Softener: <u>NO</u>	
Test	Test Method	Specification	Test Result
Unaged Binder			
Solubility in Trichloroethylene	AASHTO T 44	Minimum 99.0%	>99.0
Rotational Viscosity at 135°C	AASHTO T 316	Maximum 3.00 Pa*s Report, Pa*s	0.519
Dynamic Shear Test Temperature <u>64</u> °C [G*/sin(δ), 10 rad/sec]	AASHTO T 315	Minimum 1.00 kPa	1.45
Rolling Thin-Film Oven Residue (AASHTO T 240)			
Mass Change	AASHTO T 240	Maximum ±1.00%	0.3100
Dynamic Shear Test Temperature <u>64</u> °C [G*/sin(δ), 10 rad/sec]	AASHTO T 315	Minimum 2.20 kPa	4.03
Pressurized Aging Vessel (PAV) Residue [AASHTO R 28]			
Dynamic Shear Test Temperature <u>22</u> °C [G*/sin(δ), 10 rad/sec]	AASHTO T 315	Maximum 5000 kPa	4140
Creep Stiffness Test Temperature <u>-18 & -12</u> °C [at 60 sec]	AASHTO T 313	Maximum 300 MPa	198 & -
Slope, m-value Test Temperature <u>-18 & -12</u> °C [at 60 sec]	AASHTO T 313	Minimum 0.300	0.327 & -
PG Plus Tests			
Elastic Recovery (Original Residue) Test Temperature <u>10</u> °C	AASHTO T 301	Report, %	58.00
Penetration (unaged Residue)	AASHTO T 49	Report, dmm	97
Separation test (unaged Residue)	ASTM D 7173	Report, top & bottom difference	0.70
		Final Binder PG	PG 64-28
Analysis Performed By: <i>Sina Varamini, B.Eng. E.I.T</i>			

Sample ID/GLC ID: <u>LDPE+SBS / D2</u>		Date Sampled: <u>March-5/13</u>	
Module: <u>2</u>	Sample Source: <u>Tank 6-GLC</u>	Date Tested: <u>-</u>	
	Binder Target: <u>PG 64-28</u>	Report Date: <u>-</u>	
PG Specification: <u>AASHTO M 320-10</u>			
Modifiers Composition			
Polymer: <u>LDPE/SBS</u>	Cross-linker: <u>NO</u>	Oil Softener: <u>NO</u>	
Test	Test Method	Specification	Test Result
Unaged Binder			
Solubility in Trichloroethylene	AASHTO T 44	Minimum 99.0%	>99.0
Rotational Viscosity at 135°C	AASHTO T 316	Maximum 3.00 Pa*s Report, Pa*s	0.468
Dynamic Shear Test Temperature <u>64</u> °C [G*/sin(δ), 10 rad/sec]	AASHTO T 315	Minimum 1.00 kPa	1.30
Rolling Thin-Film Oven Residue (AASHTO T 240)			
Mass Change	AASHTO T 240	Maximum ±1.00%	0.3100
Dynamic Shear Test Temperature <u>64</u> °C [G*/sin(δ), 10 rad/sec]	AASHTO T 315	Minimum 2.20 kPa	3.62
Pressurized Aging Vessel (PAV) Residue [AASHTO R 28]			
Dynamic Shear Test Temperature <u>22</u> °C [G*/sin(δ), 10 rad/sec]	AASHTO T 315	Maximum 5000 kPa	3157
Creep Stiffness Test Temperature <u>-18 & -12</u> °C [at 60 sec]	AASHTO T 313	Maximum 300 MPa	218 & -
Slope, m-value Test Temperature <u>-18 & -12</u> °C [at 60 sec]	AASHTO T 313	Minimum 0.300	0.314 & -
PG Plus Tests			
Elastic Recovery (Original Residue) Test Temperature <u>10</u> °C	AASHTO T 301	Report, %	53.00
Penetration (unaged Residue)	AASHTO T 49	Report, dmm	102
Separation test (unaged Residue)	ASTM D 7173	Report, top & bottom difference	1.50
		Final Binder PG	PG 64-28
Analysis Performed By: <i>Sina Varamini, B.Eng. E.I.T</i>			

**Performance Grade Modified Asphalt
Laboratory Analysis Report**

Sample ID/GLC ID: <u>SBS+PS+[A] / D3</u>		Date Sampled: <u>March-19/13</u>	
Module: <u>2</u>	Sample Source: <u>Tank 6-GLC</u>	Date Tested: <u>-</u>	
	Binder Target: <u>PG 64-28</u>	Report Date: <u>-</u>	
PG Specification: <u>AASHTO M 320-10</u>			
Modifiers Composition			
Polymer: <u>PS/SBS</u>	Cross-linker: <u>YES</u>	Oil Softener: <u>NO</u>	
Test	Test Method	Specification	Test Result
Unaged Binder			
Solubility in Trichloroethylene	AASHTO T 44	Minimum 99.0%	>99.0
Rotational Viscosity at 135°C	AASHTO T 316	Maximum 3.00 Pa*s Report, Pa*s	0.518
Dynamic Shear Test Temperature <u>64</u> °C [G*/sin(δ), 10 rad/sec]	AASHTO T 315	Minimum 1.00 kPa	1.42
Rolling Thin-Film Oven Residue (AASHTO T 240)			
Mass Change	AASHTO T 240	Maximum ±1.00%	0.2300
Dynamic Shear Test Temperature <u>64</u> °C [G*/sin(δ), 10 rad/sec]	AASHTO T 315	Minimum 2.20 kPa	3.71
Pressurized Aging Vessel (PAV) Residue [AASHTO R 28]			
Dynamic Shear Test Temperature <u>22</u> °C [G*/sin(δ), 10 rad/sec]	AASHTO T 315	Maximum 5000 kPa	3060
Creep Stiffness Test Temperature <u>-18 & -12</u> °C [at 60 sec]	AASHTO T 313	Maximum 300 MPa	202 & 94.7
Slope, m-value Test Temperature <u>-18 & -12</u> °C [at 60 sec]	AASHTO T 313	Minimum 0.300	0.322 & 0.377
PG Plus Tests			
Elastic Recovery (Original Residue) Test Temperature <u>10</u> °C	AASHTO T 301	Report, %	54.00
Penetration (unaged Residue)	AASHTO T 49	Report, dmm	95
Separation test (unaged Residue)	ASTM D 7173	Report, top & bottom difference	0.90
		Final Binder PG	PG 64-28
Analysis Performed By: <i>Sina Varamini, B.Eng. E.I.T</i>			

Sample ID/GLC ID: <u>SBS+PS / D4</u>		Date Sampled: <u>April-19/13</u>	
Module: <u>2</u>	Sample Source: <u>Tank 6-GLC</u>	Date Tested: <u>-</u>	
	Binder Target: <u>PG 64-28</u>	Report Date: <u>-</u>	
PG Specification: <u>AASHTO M 320-10</u>			
Modifiers Composition			
Polymer: <u>PS/SBS</u>	Cross-linker: <u>NO</u>	Oil Softener: <u>NO</u>	
Test	Test Method	Specification	Test Result
Unaged Binder			
Solubility in Trichloroethylene	AASHTO T 44	Minimum 99.0%	>99.0
Rotational Viscosity at 135°C	AASHTO T 316	Maximum 3.00 Pa*s Report, Pa*s	0.430
Dynamic Shear Test Temperature <u>64</u> °C [G*/sin(δ), 10 rad/sec]	AASHTO T 315	Minimum 1.00 kPa	2.49
Rolling Thin-Film Oven Residue (AASHTO T 240)			
Mass Change	AASHTO T 240	Maximum ±1.00%	0.2300
Dynamic Shear Test Temperature <u>64</u> °C [G*/sin(δ), 10 rad/sec]	AASHTO T 315	Minimum 2.20 kPa	3.24
Pressurized Aging Vessel (PAV) Residue [AASHTO R 28]			
Dynamic Shear Test Temperature <u>22</u> °C [G*/sin(δ), 10 rad/sec]	AASHTO T 315	Maximum 5000 kPa	3110
Creep Stiffness Test Temperature <u>-18 & -12</u> °C [at 60 sec]	AASHTO T 313	Maximum 300 MPa	206 & 96.2
Slope, m-value Test Temperature <u>-18 & -12</u> °C [at 60 sec]	AASHTO T 313	Minimum 0.300	0.309 & 0.367
PG Plus Tests			
Elastic Recovery (Original Residue) Test Temperature <u>10</u> °C	AASHTO T 301	Report, %	51.00
Penetration (unaged Residue)	AASHTO T 49	Report, dmm	103
Separation test (unaged Residue)	ASTM D 7173	Report, top & bottom difference	1.70
		Final Binder PG	PG 64-28
Analysis Performed By: <i>Sina Varamini, B.Eng. E.I.T</i>			